



**US Army Corps
of Engineers**
Waterways Experiment
Station

Technical Report CERC-96-10
June 1996

Geologic Effects on Behavior of Beach Fill and Shoreline Stability for Southeast Lake Michigan

*by Larry E. Parson, Andrew Morang, WES
Robert B. Nairn, Baird & Associates*

19960719 021

Approved For Public Release; Distribution Is Unlimited

19960719 021

DTIC QUALITY INSPECTED 4

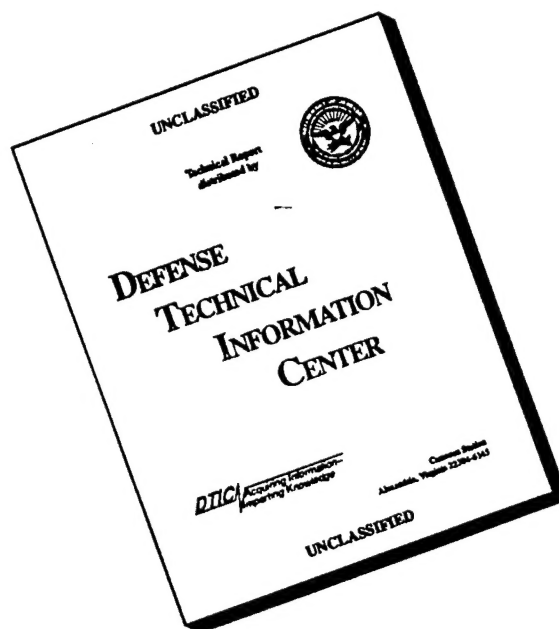
Prepared for Headquarters, U.S. Army Corps of Engineers

The contents of this report are not to be used for advertising, publication, or promotional purposes. Citation of trade names does not constitute an official endorsement or approval of the use of such commercial products.



PRINTED ON RECYCLED PAPER

DISCLAIMER NOTICE



THIS DOCUMENT IS BEST QUALITY AVAILABLE. THE COPY FURNISHED TO DTIC CONTAINED A SIGNIFICANT NUMBER OF PAGES WHICH DO NOT REPRODUCE LEGIBLY.

Geologic Effects on Behavior of Beach Fill and Shoreline Stability for Southeast Lake Michigan

by Larry E. Parson, Andrew Morang

U.S. Army Corps of Engineers
Waterways Experiment Station
3909 Halls Ferry Road
Vicksburg, MS 39180-6199

Robert B. Nairn

Baird & Associates
221 Lakeshore Road East
Oakville, Ontario, Canada L6J 1H7

Final report

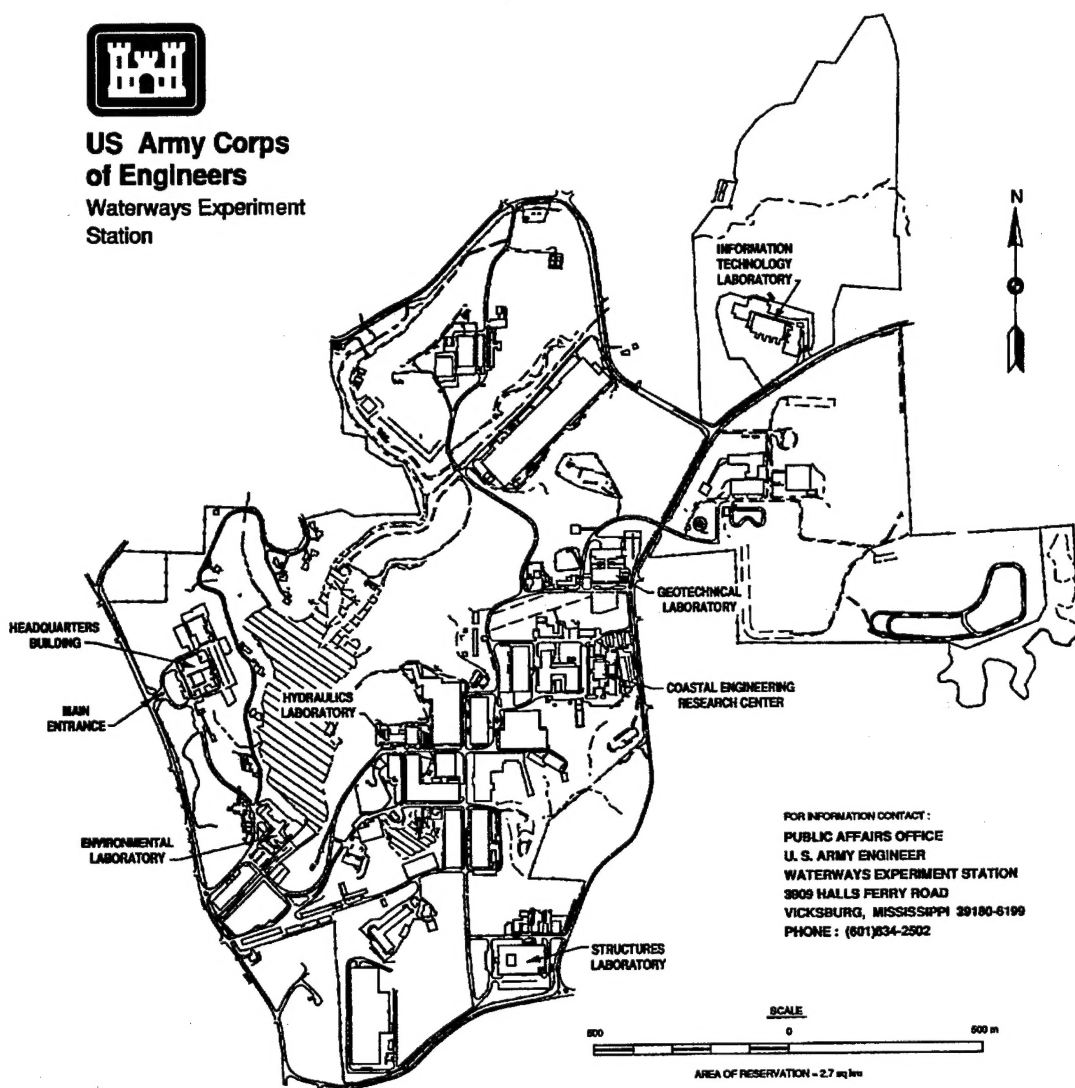
Approved for public release; distribution is unlimited

DTIC QUALITY INSPECTED 4

Prepared for U.S. Army Corps of Engineers
Washington, DC 20314-1000



**US Army Corps
of Engineers**
Waterways Experiment
Station



Waterways Experiment Station Cataloging-in-Publication Data

Parson, Larry E.

Geologic effects on behavior of beach fill and shoreline stability for southeast Lake Michigan / by Larry E. Parson, Andrew Morang, Robert B. Nairn ; prepared for U.S. Army Corps of Engineers.

104 p. : ill. ; 28 cm. — (Technical report ; CERC-96-10)

Includes bibliographic references.

1. Beach nourishment — Michigan, Lake. 2. Shore protection — Michigan, Lake. 3. Shorelines — Michigan, Lake — Mathematical models. I. Morang, Andrew 1953- II. Nairn, Robert B. III. United States. Army. Corps of Engineers. IV. U.S. Army Engineer Waterways Experiment Station. V. Coastal Engineering Research Center (U.S. Army Engineer Waterways Experiment Station) VI. Title. VII. Series: Technical report (U.S. Army Engineer Waterways Experiment Station) ; CERC-96-10.

TA7 W34 no.CERC-96-10

Contents

Preface	vi
1—Introduction	1
Purpose	1
Scope	1
Project History and Description	2
2—Geological Setting	7
Shoreline Characteristics	7
Shoreline Recession	9
Wave Climate	9
3—Cohesive Processes	10
4—Monitoring Program	12
Data Collection	12
Data Analysis	18
5—Till Downcutting Investigation	23
Description of Samples	23
Test Methodology	24
Test Results for Clear Water	27
Test Results with Sand in Flow	27
Test Results Summary	31
Interpretation of Downcutting Investigation Results	32
Comparison to Other Studies	33
6—Cross-Shore Sediment Transport and Profile Response Model	36
Description of Model Input	38
Model Results	40
Summary of the Model Results	46
7—Summary and Conclusions	48
References	50
Appendix A: Geotechnical Analysis of Glacial Till	A1
Appendix B: Calculation of Shear Stress for Test Sequences Used in the Flume Investigation	B1

Appendix C: Raw Depth Data From Flume Study	C1
Appendix D: Module Flow Chart of COSMOS-2D Numerical Model	D1
Appendix E: Storm Events Identified Using Hindcast Wave Data	E1
SF 298	

List of Figures

Figure 1.	Location of St. Joseph, MI, project area	3
Figure 2.	Parallel jetties stabilizing the entrance of St. Joseph Harbor ...	4
Figure 3.	Project fill construction features	6
Figure 4.	Composite grain size distribution of the coarse fill material ...	6
Figure 5.	Cross section of a typical cohesive profile (from Kamphuis (1987))	11
Figure 6.	Location of St. Joseph project data collection sites	13
Figure 7.	Profile survey at St. Joseph line R10 during November 1993. Rod man is wearing a diving dry suit	14
Figure 8.	Location of sediment samples along the profile for the St. Joseph monitoring project	15
Figure 9.	Till samples collected at AR-14. The sample on the right has already been sealed in gypsum cement to preserve the natural moisture content during shipping and storage	16
Figure 10.	Hindcast station location map for the generation of wave data for St. Joseph	17
Figure 11.	Profile data availability at St. Joseph, MI	19
Figure 12.	Pre-fill composite grain size distribution for the St. Joseph feeder beach area	20
Figure 13.	Grain size distribution of the glacial till lake bed material ...	21
Figure 14.	Ground penetrating profile record at R-14 indicating the thickness of the overlying unconsolidated sediments and the position of the cohesive substratum profile	22
Figure 15.	Till sample 1 prior to testing in the flume	24
Figure 16.	Till sample 2 prior to testing in the flume	25
Figure 17.	Tilting flume used for testing the downcutting processes for the glacial till substratum	25
Figure 18.	LDV apparatus used to determine shear stress exerted on the till bed	26
Figure 19.	Results for clear water testing of samples 1 and 2	28

Figure 20.	Condition of sample 1 after breaking apart during clear-water testing	29
Figure 21.	Test results for sand in flow for samples 1 and 2	30
Figure 22.	Erosion condition of sample 1 after using clear water in flume	30
Figure 23.	Erosion condition of sample 2 after sand was included in water flow	31
Figure 24.	Comparison of clear-water erosion rates (mm/hr) from St. Joseph with other cohesive substrates from various other studies	34
Figure 25.	Comparison of sand in flow erosion rates (mm/hr) from St. Joseph with other cohesive substrates from various other studies	35
Figure 26.	Profile change for R9 from the 24 January 1992 storm predicted for the 0.2-mm grain size and actual water level	42
Figure 27.	Profile change for R9 from the 24 January 1992 storm predicted for the 0.2-mm grain size and high water level	42
Figure 28.	Profile change for R9 from the 24 January 1992 storm predicted for 2.0-mm grain size and actual water level	43
Figure 29.	Profile change for R9 from the 24 January 1992 storm predicted for 2.0-mm grain size and high water level	43
Figure 30.	Profile change for R14 from the 24 January 1992 storm predicted for 0.2-mm grain size and actual water level	45
Figure 31.	Profile change for R14 from the 24 January 1992 storm predicted for 0.2-mm grain size and high water level	45
Figure 32.	Profile change for R14 from the 24 January 1992 storm predicted for 2.0-mm grain size and average water level	46
Figure 33.	Profile change for R14 from the 24 January 1992 storm predicted for 2.0-mm grain size and high water level	47

Preface

The investigation summarized in this report was conducted by the U.S. Army Engineer Waterways Experiment Station's (WES's) Coastal Engineering Research Center (CERC) and was selected for study and funded by the Monitoring Completed Coastal Projects (MCCP) program. The MCCP Program Manager is Ms. Carolyn Holmes. This program is sponsored by Headquarters, U.S. Army Corps of Engineers (HQUSACE). The HQUSACE Technical Monitors are Messrs. John H. Lockhart, Jr., Charles Chesnutt, and Barry W. Holliday. The project is under the jurisdiction of the U.S. Army Engineer District, Detroit.

Work was performed under the general supervision of Ms. Joan Pope, Chief, Coastal Structures and Evaluation (CSE) Branch, CERC; Mr. Thomas W. Richardson, Chief, Engineering Development Division, CERC; Mr. Charles C. Calhoun, Jr., Assistant Director, CERC; and Dr. James R. Houston, Director, CERC.

This report was prepared by Mr. Larry E. Parson and Dr. Andrew Morang of the CSE Branch and Dr. Robert Naim of W.F. Baird & Associates, Coastal Engineers, Ltd. Field data collection was performed by many individuals from the Detroit District's Grand Haven Area Office, CERC, the U.S. Geological Survey, Western Michigan University, and the University of Michigan. Technical reviewers of the report were Mr. Ronald Erickson, U.S. Army Engineer District, Detroit, Mr. J. Bailey Smith, CERC, and Mr. Randall Wise, CERC.

At the time of publication of this report, Director of WES was Dr. Robert W. Whalin. Commander was COL Bruce K. Howard, EN.

The contents of this report are not to be used for advertising, publication, or promotional purposes. Citation of trade names does not constitute an official endorsement or approval of the use of such commercial products.

1 Introduction

Purpose

Beach nourishment has become a common engineering solution for beach erosion control and restoration in the Great Lakes and has been recognized as beneficially affecting the stability of downdrift shorelines. A monitoring program to evaluate the effects of beach nourishment material placed on a cohesive shoreline in southeast Lake Michigan was conducted at St. Joseph, Michigan, by the U.S. Army Engineer Waterways Experiment Station's Coastal Engineering Research Center (CERC). The monitoring effort, initiated in 1991, was part of the Monitoring Completed Coastal Projects program. A major element of the study was to investigate the geologic controls on near-shore morphology and confirm the existence of a shallow glacial till lake bed foundation. Information derived from the field monitoring program was used in conjunction with two-dimensional (2-D) numerical model simulations of the coastal erosion processes to develop an understanding of shoreline and lakebed evolution. An important consideration is the exposure of the glacial till foundation, which is believed to result in irreversible erosion or downcutting of the lakebed.

Techniques commonly used for U.S. Army Corps of Engineers (USACE) coastal projects were employed in placing the nourishment material at the St. Joseph project area. However, these techniques were developed for sandy shores and may not provide the protection required by the cohesive shorelines that exist at St. Joseph and throughout many areas of the Great Lakes. Understanding the coastal geologic processes that govern the morphology of the Great Lakes and other cohesive environments will aid in reevaluating beach nourishment design for these areas.

Scope

In addition to evaluating the overall effectiveness of the performance of the beach nourishment program, this study was directed toward investigating some of the geologic variables that affect cohesive shores. These unique geologic controls must be considered when planning and designing beach nourishment for the Great Lakes. Such information will be beneficial for issues

including: quantity of fill, frequency of fill, grain size characteristics of the fill and location of the placement (the latter, both in plan and profile). The primary objective of the study was to develop an improved understanding of the relationship between the movement of the cohesionless sediment (both fine and coarse grain components) and the irreversible downcutting of the underlying glacial till at the St. Joseph project site.

Laboratory testing was conducted to investigate the downcutting process using undisturbed glacial till samples extracted from the lake bed offshore from St. Joseph. The samples were placed in a flume to measure downcutting rates at various water flow velocities. The tests were conducted using both clear water and water containing sediments with grain sizes representative of the fill materials used at St. Joseph.

Data collected during the monitoring program were input into a 2-D numerical model to describe the cross-shore sediment process and to predict the profile response to storm conditions with the influence of the underlying glacial till represented as an erosion-resistant sub-layer. The 2-D profile change tests were performed on 10 of the profile locations.

Project History and Description

This study focuses on a 6-km (3.7-mile) section of shore extending southward from the jetties of St. Joseph Harbor. St. Joseph is located in Berrien County, MI, along the southeastern shore of Lake Michigan about 32 km (20 miles) north of the Indiana/Michigan border (Figure 1). In 1903, parallel jetties were constructed to stabilize the entrance of the St. Joseph River (Figure 2). These jetties have been responsible for downdrift shoreline erosion. The U.S. Army Engineer District (USAED), Detroit (1973) determined that the jetties interrupt the southward transport of approximately 84,000 m³ of sediment per year. In 1976, an approved Section 111 erosion mitigation plan authorized annual placement of fill material (~0.2 mm) from maintenance dredging of St. Joseph Harbor to feed the eroding downdrift shoreline. To date, over 1.1 million m³ of dredged material have been placed on the beaches south of the jetties as summarized in Table 1. In addition to the dredged materials, coarser material (~2.0 mm) was hauled by truck from upland sources and placed south of the jetties. The coarse placement was intended to act as a feeder beach to replenish the downdrift shores. The most recent coarse fills occurred in 1991 and 1993.

Beach nourishment at St. Joseph was authorized under Section 111 of the River and Harbor Act of 1968. The project involves placing fill material to provide feeder beaches to mitigate shore damage caused by entrapment or diversion of littoral sediments by the St. Joseph Harbor navigation structures (USAED, Detroit 1977). The feeder beach at Lions Park starts at the centerline of Park Street, 380 m (1,250 ft) south of the St. Joseph jetties, extending southward 1,250 m (4,100 ft) as illustrated in Figure 3. The coarse sediment



Figure 1. Location of St. Joseph, MI, project area

renourishment prompting this study occurred during September, 1991, when $54,500 \text{ m}^3$ ($71,000 \text{ yd}^3$) of coarse material was placed along the feeder beach. The material was brought by truck from an upland commercial site and placed between the ordinary high water mark (elevation 177.1 m or 580.8 ft) and the most landward 4-ft depth contour (elevation 174.6 m or 572.8 ft) to provide a maximum width of 46 m (150 ft). The maximum design height for the placed material was an elevation of 178.3 m (584.8 ft).

The 1991 coarse fill material was a glacial outwash (moraine) sand-gravel composite free of clay, organic soil, sod, roots, brush, wood, rubbish, oil, metal, chemical contaminants, and other waste materials. The material exhibits a poorly sorted, bimodal distribution of gravel and sand with a mean composite grain size of -1.21ϕ (2.31 mm) and standard deviation of 2.69 (Figure 4).

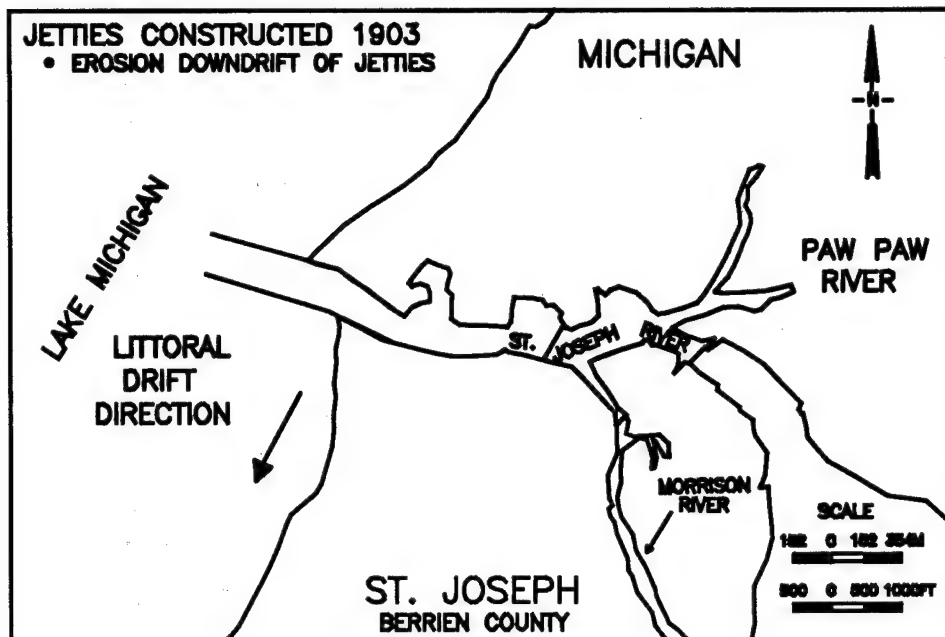


Figure 2. Parallel jetties stabilizing the entrance of St. Joseph Harbor

Table 1
Summary of Beach Fills at the St. Joseph Project Area

Year	Dredged, m ³ (yd ³)	Trucked, m ³ (yd ³)	Type
1970	22,900 (30,000)		Fine
1971	16,300 (21,300)		Fine
1972	32,900 (43,000)		Fine
1973	6,100 (8,000)		Fine
1974	19,600 (25,600)		Fine
1975	38,800 (50,800)		Fine
1976 ¹	72,000 (94,200)	212,600 (278,000)	Fine
1977	123,900 (162,000)		Fine
1978	68,400 (89,500)		Fine
1979	84,700 (110,800)		Fine
1980	71,100 (93,000)		Fine
1981	50,300 (65,800)		Fine
1982	89,900 (117,600)		Fine
1983	169,400 (221,500)		Fine
1984	76,500 (100,000)		Fine
1985	28,800 (37,700)		Fine
1986	11,200 (14,700)	120,400 (157,500)	Fine/coarse
1987	2,500 (3,300)	47,800 (62,500)	Fine/coarse
1988		84,600 (110,700)	Coarse
1989	14,300 (18,700)		Fine
1990	38,200 (50,000)		Fine
1991	40,100 (52,500)	54,300 (71,100)	Fine/coarse
1992	25,700 (33,600)		Fine
1993	1,500 (1,900)	39,300 (51,400)	Fine/coarse
Total	1,105,200 (1,445,500)	559,500 (731,800)	1,625,100 (2,177,300)

¹ Denotes implementation of Section 111 Plan.

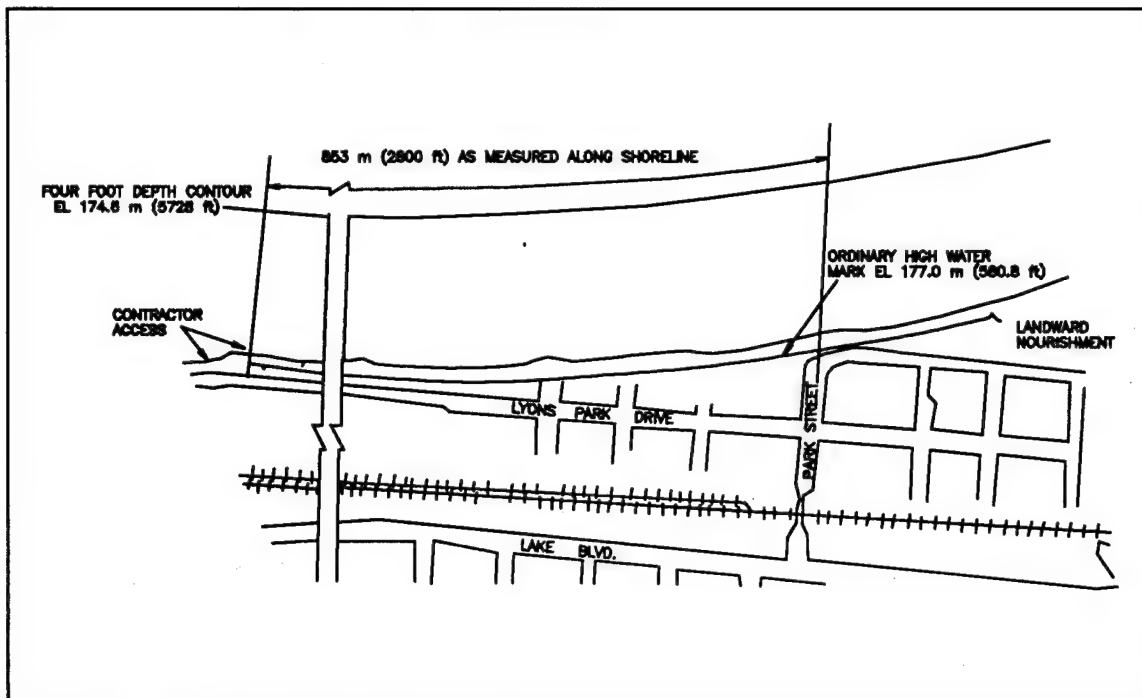


Figure 3. Project fill construction features

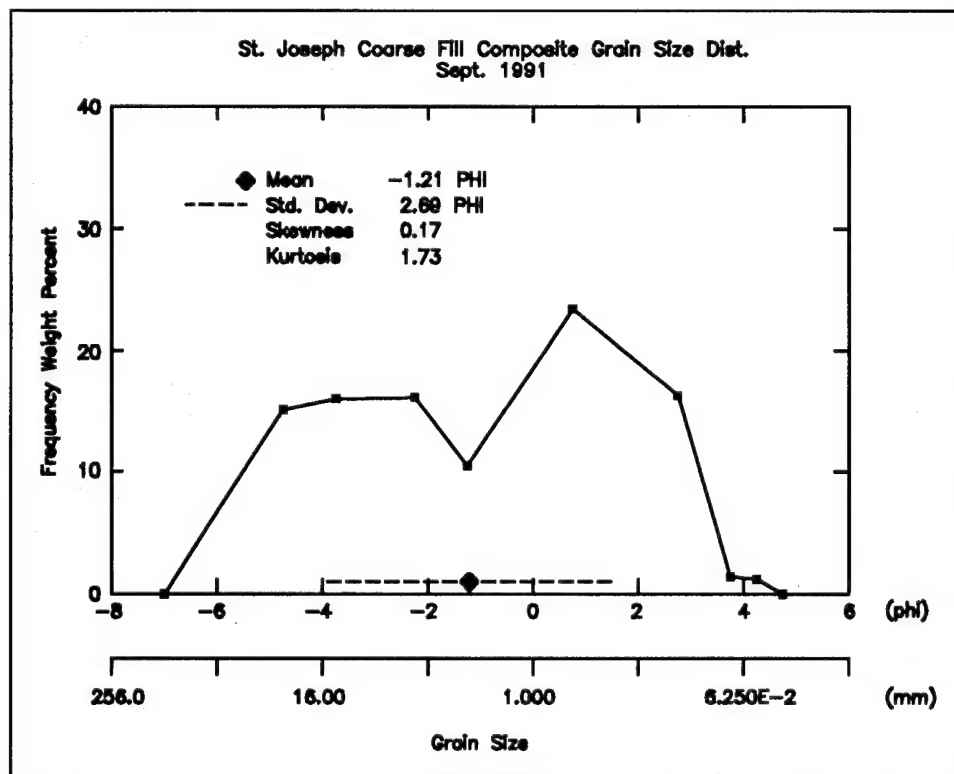


Figure 4. Composite grain size distribution of the coarse fill material

2 Geological Setting

Shoreline Characteristics

The shoreline of Lake Michigan is a product of the last Pleistocene ice age, which commenced approximately 18,000 years ago. Lake Michigan occupies a large depression as a result of multiple Pleistocene continental glaciations (Chrastowski and Thompson 1992). The most recent glaciation occurred during the Wisconsinan time by the Lake Michigan Lobe of the Laurentian ice sheet (Hough 1958). The lobe in part filled the Lake Michigan depression with massive deposits consisting of materials that were carried or dragged along beneath the moving ice. Following the maximum southerly advance of the ice sheets, glacial recession created, exposed, and modified glacial deposits, accompanied by drastic changes in lake levels. These events were responsible for shaping the present shoreline features (Raphael and Kureth 1988). Benton and Passero (1990) classified four types of glacial deposits in the St. Joseph vicinity: moraines, outwash plains, lacustrine, and eolian. *Moraines* form along glacial margins, outlining the position of maximum ice advancement. Morainal sediments are typically complex mixtures of gravel, sand, and clay, a material called *glacial till*. *Outwash plains* are deposits composed primarily of sand and gravel originating from glacial meltwater. *Lacustrine* deposits, mostly clay, are left in lakes where meltwaters carry fine sediment. *Eolian* processes are responsible for coastal sand dunes.

Seismic and coring investigations conducted by Lineback et al. (1971) and Lineback, Gross, and Meyer (1972) recognize four major glacial till units in Lake Michigan. Their studies revealed that the Wadsworth Till Member forms the consolidated lake bed of the southern and southeastern parts of Lake Michigan and underlies the younger non-till sediments. The Wadsworth Till is gray in color and is composed of clayey-silty materials characterized by an illite content of greater than 70 percent. This formation covers the lake bottom at thicknesses of up to 18 m (60 ft) at depths below 30 m. At shallower depths, a veneer of sand and gravel overlies the Wadsworth Till (Lineback and Meyer 1974). In some areas, the veneer may be absent, exposing the underlying till. The till is about 15-30 m thick and overlies bedrock of Devonian and Mississippian shales, siltstones, and dolomite (Chrastowski and Thompson 1992). It is common for the underlying bedrock to become exposed. Lake bed outcrops have been observed by Meisburger, Williams, and Prins (1979) south of the

study site between St. Joseph and the Indiana border. Sauck (1993) identified locations on the lake bed within the project area where glacial till has been exposed.

The shore in the vicinity of St. Joseph consists of high till bluffs and relict dune fields. The subaqueous nearshore sediment is composed of unconsolidated sand/gravel lag overlying consolidated clay sediments (Hands 1970, International Joint Commission 1993). These shores are particularly susceptible to the erosive forces of storm waves approaching from the northwest, especially during periods of higher lake levels. Much of the sand on the beaches and in offshore bars is derived from erosion of the bluffs and dunes. This erosion produces beaches and nearshore zones consisting of a relatively thin layer of sand with scattered lag deposits of gravel which overlie the regional cohesive glacial till (Meisburger, Williams, and Prins 1979). Thus, a highly variable sediment gradation ranging from clay to coarse gravel exists within the beaches in these zones. The beaches in these areas are also characterized by highly irregular sediment zonations as opposed to the more uniform zonations of sandy beaches on the oceanic barrier coasts described by Stauble et al. (1993).

Historically, the nearshore region of southeastern Lake Michigan is characterized by gentle nearshore slopes (approximately 1:80) and the presence of multiple longshore bars. Although Saylor and Hands (1970) have observed the bars to slowly migrate in response to varying lake level conditions, they consider them to be relatively stable features of the profile.

The local shoreline exhibits a small downdrift fillet beach immediately south of the harbor, approximately 400 m (1,300 ft) in length. The 1.1-km (0.7-mile) section of shore between the fillet beach and the Waterworks revetment to the south is partially protected by deteriorated groins. The feeder beach for the nourishment program extends from Park St. (located about 600 m (2,000 ft) south of the south jetty) to just south of the Waterworks revetment. Beginning with the Waterworks revetment and extending about 3.5 km (2.2 miles) to the south, the shoreline is protected by an armor stone revetment constructed for the protection of the CSX Railroad over the first 1.5 km (0.9 mile) and the highway by Michigan Department of Transportation for the next 2 km (1.2 miles). In some places, the revetment is fronted by groins, many of which are in disrepair. Scour and erosion of the lakebed have occurred near many of these structures. The final kilometer (0.6 mile) of shore located south of the end of the revetment consists of various forms of deteriorated wall and sections of entirely unprotected shoreline. Beaches are small or nonexistent in these sediment-starved areas. Where pocket beaches do occur, the sediment is composed of coarse sand and gravel.

Shoreline Recession

The shoreline in the vicinity of St. Joseph is in a state of recession. Birkemeier (1980) determined bluff recession rates for areas south of St. Joseph averaging 4.6 m/year during a period of rising lake levels between 1970 and 1974. Evidence has been presented by Buckler (1981) showing a southward progression of increased erosion rates since at least 1829. Further studies by Buckler and Winters (1983) revealed average bluff recession rates for the area between St. Joseph and Shoreham of approximately 0.6 m/year between 1829 and 1977. Using photogrammetric methods, the Michigan Department of Natural Resources (1978) computed the bluff line recession rate for the St. Joseph region to be approximately 1 m/year over a 50-year period. Preliminary studies by Foster et al. (1992) documented between 3 and 4 m of downcutting of the nearshore lakebed south of the Federal structures near the village of Shoreham.

Wave Climate

Wave hindcasting information (Hubertz, Driver, and Reinhard 1991) representing a 27-year period was used to describe the offshore wave climate for the St. Joseph area. The predominant direction of wave approach is from the southwest, which normally corresponds to periods of low wave energy with mean wave height of 0.8 m (2.6 ft) and mean wave period of 4.0 sec. The maximum wave height from this direction is 4.6 m (15.1 ft). The predominant wave energy, however, approaches from the north and northwest, where the mean wave height is 1.2 m (3.9 ft) with a mean wave period of 4.8 sec. The maximum wave height from these directions, 6.3 m (20.6 ft), occurs during the stormy winter months. The longer fetch distances to the north and northwest across the lake allow larger waves to develop than those that form over the shorter fetches from the south and southwest (USAED, Detroit 1973). This wave climate causes a southward directed net littoral drift as indicated by the accumulation of material and updrift offset to the north of the harbor jetties. Northward transport also occurs and is usually associated with low energy periods, as evident by the lesser accumulation of material against the south jetty (Figure 2).

3 Cohesive Processes

Sandy shores on barrier coasts are generally distinguished by an inexhaustible local supply of beach sediment. In contrast, Naim (1992) defines a shore as cohesive when a cohesive sediment substratum (such as glacial till, glaciolacustrine deposits, soft rock or other consolidated deposits) occupies the dominant role in the change of shoreline shape (i.e., through erosion). In other words, under cohesionless sand and gravel lag deposits, there is an erodible surface which plays the most important role in determining how these shores erode, and ultimately, how they evolve in the long term. Often, the only visual distinction of a cohesive shore (above lake level) is the existence of a backshore bluff. The bluff may be as low as 0.3 m, in the form of a wave-cut terrace, or as high as 50 m or more. Typically, the maturity of the vegetation on the bluff face provides some indication of the rate at which the shore is eroding. Along the study shoreline, the bluff is relatively well-vegetated and stable behind the armor stone revetment. At the base of unprotected sections of the bluff there is often a narrow sand and gravel beach, and offshore, there may be sandbars. Other evidence pointing towards the cohesive shore classification includes the exposure of the cohesive layer beneath the beach during severe storms or the exposure of the cohesive substratum in the troughs between the offshore bar crests. A schematic of a typical cohesive profile as described by Kamphuis (1987) is presented in Figure 5. Both ground-penetrating radar (GPR) and underwater video document considerable exposure of glacial till for the lake bed in the study area.

A cohesive shore erodes and recedes because of the permanent removal and loss of the cohesive material (both from the bluff and the lake bed). The sand cover may come and go (depending on the season, water level, and storm activity), but erosion of the cohesive layer is irreversible. The cohesive layer is often a glacial deposit and derives its strength from the cohesiveness of its clay content and/or through the compression it was subjected to during the period of glaciation. Once this material is eroded by waves, it cannot reconstitute itself, and the cohesive form is lost forever. In a comparison of recent and historic information on bathymetry in the study area, Foster et al. (1992) found that up to 3 to 4 m of lake bed lowering has occurred in less than 25 years. Tests of the till samples extracted from the lake bed revealed that between 70 and 80 percent of the sediment was silt or clay (i.e., smaller than beach sediment sizes). Most cohesive shores are subject to strong alongshore drift, which has the potential to remove large quantities of sand during storms

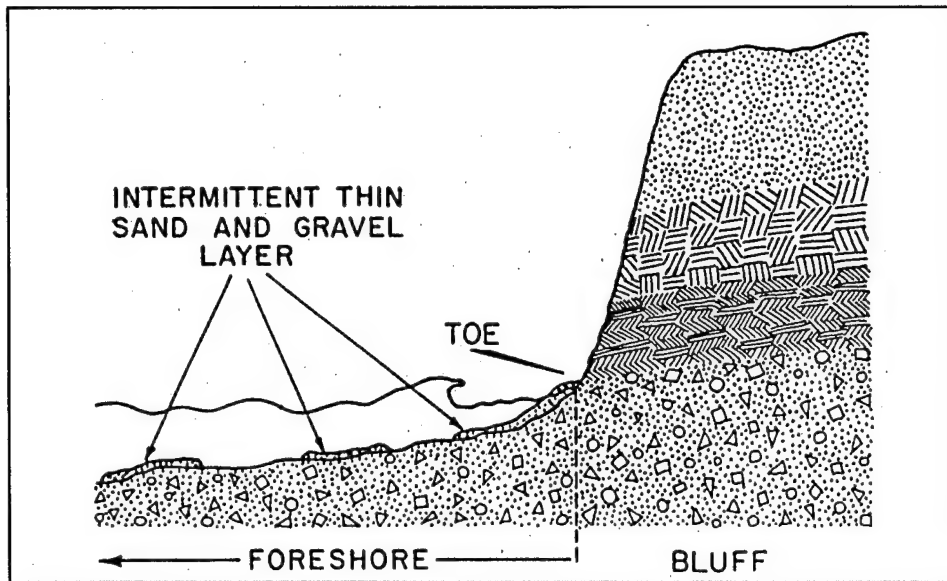


Figure 5. Cross section of a typical cohesive profile (from Kamphuis (1987))

and does not allow stable and protective beaches to build up. Where very large amounts of sand (on the order of $200 \text{ m}^3/\text{m}$) do build up over the cohesive substratum - either at a change in the shoreline orientation or at a large obstruction such as a natural headland or a harbor breakwater, erosion of the cohesive shore and the backshore bluff will be arrested. Where this occurs, the shoreline reverts to a sandy shore classification since the presence of the underlying cohesive material is no longer an important factor in the evolution of the shore. This phenomenon, where bluff erosion is arrested behind a fillet beach, is not evident at St. Joseph because the updrift fillet beach has developed over an old river valley (i.e., there is no backshore bluff immediately south of the jetties).

The critical point to understanding the evolution of cohesive shores is that the shoreline recession (or the associated problems of undermining of shore-based structures) could not continue without the ongoing downcutting of the nearshore lake bed. The long term average rate at which the bluff or shoreline recedes on a cohesive shore is governed by the rate at which the nearshore profile is eroded or downcut.

Where there are downdrift erosion problems related to the interception of sand at an updrift barrier on a cohesive shore, downdrift mitigation efforts such as beach nourishment must be carefully assessed because the sand can act as protective cover or as an abrasive agent (contributing to erosion), depending on the quantity and type of sediment.

4 Monitoring Program

Data Collection

Stauble (1988, 1991) presents comprehensive monitoring procedures for beach nourishment projects. Although developed for sandy shores, these procedures provide the foundation for monitoring the behavior of the St. Joseph beach nourishment. Five data collection profile lines (R-9, R-9a, R-10, R10a, and R-11) spaced approximately 152 m (500 ft) apart (Figure 6) were selected to characterize the behavior of the feeder beach area. Two additional lines, R-8 and R-12, were located immediately north and south of the feeder beach. Additional profiles south of the fill area were selected to assess the downdrift benefits of the fill. These lines, R-14, R-17, R-20, R-22, and R-23, are spaced roughly 0.8 km (0.5 mile) apart. All profiles extend from a stable location on the beach not affected by coastal processes (behind dune, seawall, or bluff line) on a line normal to the shoreline, extending lakeward to a depth of approximately 7.6 m (25 ft) to capture the assumed active profile.

Profile data collection

Profiles at St. Joseph were surveyed by the USAED, Detroit, and by the Department of Ocean Engineering, University of Michigan, under contract to CERC. The USAED, Detroit, established temporary benchmarks at the upper landward end of each survey line from which all elevations and distances during this program were referenced.

Beach profiles were surveyed using level rod and theodolite. The surveyors recorded horizontal distance from and vertical elevation with respect to the benchmark every 3 m across the beach and through the wading zone (Figure 7) on each line. In addition, they recorded coordinates of prominent morphological features along the survey line, such as cusps or ridges.

From wading depth offshore to at least -6 m, surveys were conducted from small boats using a Raytheon survey Fathometer. The echo sounder was calibrated with rod measurement. At each line, buoys were placed at -3-m, -6-m, and -10-m water depths. The positions of the buoys were measured with an electronic distance meter and theodolite. The survey was run from the -10-m

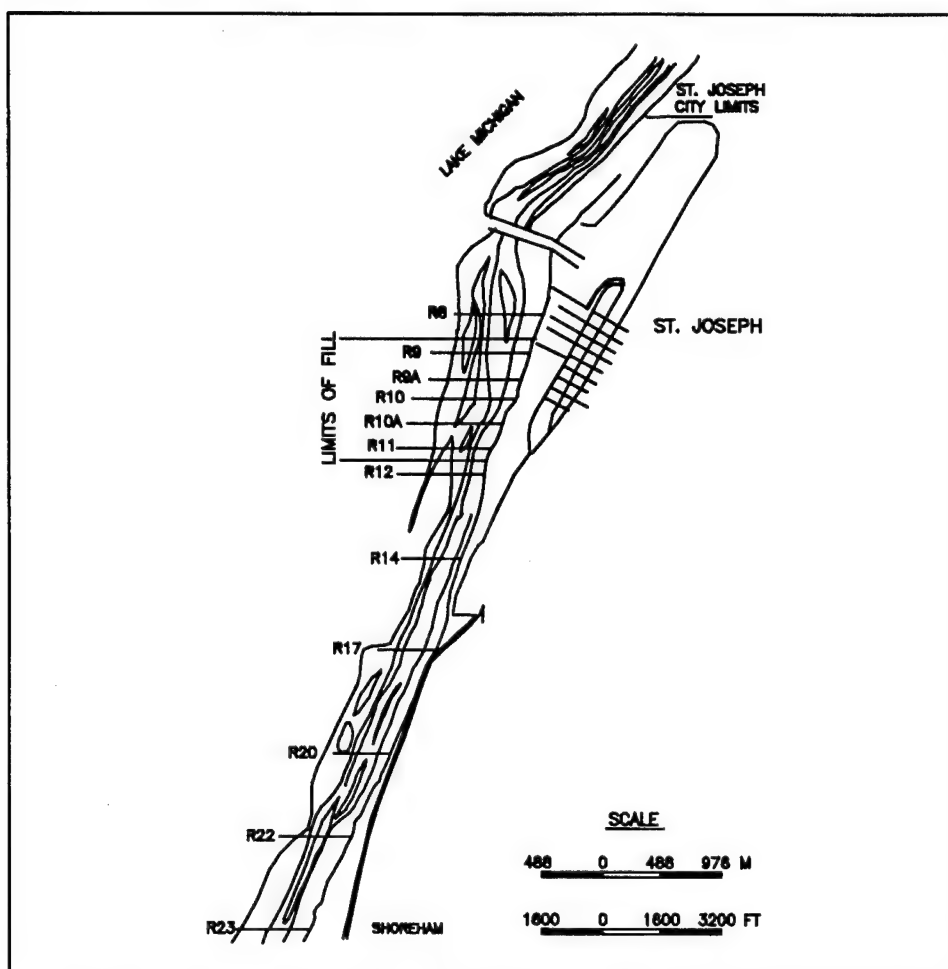


Figure 6. Location of St. Joseph project data collection sites

buoy inshore as shallow as possible to allow overlap with the portion of the beach survey that extended into the wading zone. Analog echo sounder data were recorded on paper charts and had to be digitized in the laboratory before computerized processing was possible. Note that because only the positions of the offshore buoys were actually surveyed, Fathometer data between the buoys are plotted based on linear interpolation.

Vertical control was checked during each survey by measuring the position of the still lake water. The relationship of this level to low water datum was obtained by linear interpretation with measurements at nearby water level stations operated by the National Ocean Survey. Water levels throughout the lakes vary with wind conditions, atmospheric pressure, regional hydrologic factors, local surface runoff, ice cover, seiching, and numerous other factors (Great Lakes Commission 1986). This makes the precise establishment of datum particularly critical for comparative studies of Great Lakes profiles over time; unlike ocean sites, there is no "mean sea level" that can be used as an approximate reference plane.



Figure 7. Profile survey at St. Joseph line R10 during November, 1993. Rod man is wearing a diving dry suit

Sediment sampling

Sediment redistribution across the entire profile was monitored during each survey by collecting surface sediment samples at various morphological locations across the profile consistent with accepted beach sediment sampling techniques described by Stauble (1988, 1992), Byrnes (1989), and the *Shore Protection Manual* (1984). These sampling locations were: toe of dune/bluff; mid-berm; shoreline; bar trough; bar crest; bar seaward slope; and depth of closure, as illustrated in Figure 8. If a bar system was absent or not previously known, samples were taken at approximately 1-m (3-ft) contour intervals to a depth of about 6.4 m (21 ft). The data collection schedule was the same for both the profile surveys and the sediment collection. Survey data and sediment samples were collected just prior to and as soon as possible after fill placement.

Sub-surface imaging was performed under contract by Western Michigan University (Sauck 1993) using GPR, a tool that has proven valuable in examining the shallow stratigraphy of the beach and nearshore in freshwater environments. GPR relies upon the emission, transmission, reflection, and reception of electromagnetic energy and is capable of producing continuous, high-resolution profiles of the subsurface that are similar to those produced by seismic profiling methods. Data obtained from the GPR were used to verify the occurrence of and locate the position of clay (cohesive sediment) which was either exposed or buried under sand and gravel. Till exposure at the time

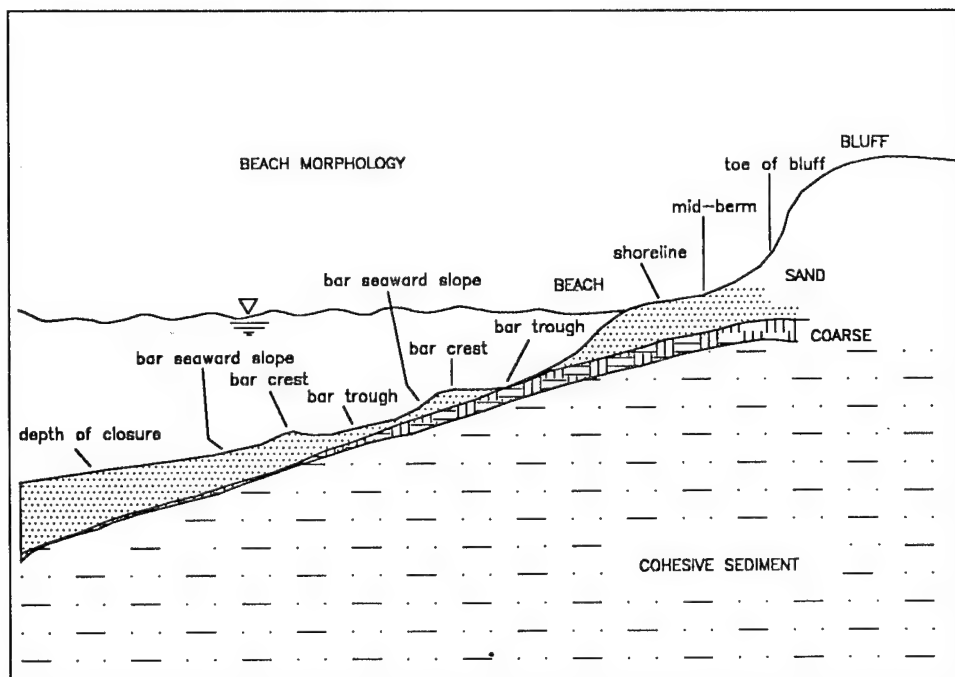


Figure 8. Location of sediment samples along the profile for the St. Joseph monitoring project

of the survey provides only a "snapshot" indication on the position of the clay profile. This was important in providing guidelines for future profiles and estimating the thickness of sand cover (if any). Documenting the position of the underlying till will establish the importance of providing and maintaining an adequate protective sand cover over the cohesive underlayer. GPR surveys were run normal to shore, coinciding mostly on the profile lines south of the feeder beach. Two shore-parallel GPR lines were also run near the shore and towards the outer reaches of the profile survey lines.

An underwater remote operated vehicle known as M-ROVER was used by University of Michigan to visually document glacial till exposures along the survey lines. M-ROVER produced a continuous record of surface features along each line using a combination of a high-resolution color imaging sonar and a high-resolution, low-light color video system. A 35-mm still camera provided photographs of the lake bed.

Samples of the lake bed till were collected along line R-14 in July of 1993. Two blocks of undisturbed till were extracted from the lake bed in about 7.6 m (25 ft) of water using a 6-ton clam bucket operated from a USACE crane barge. The two cube-shaped samples had side dimensions of 0.23 m (9 in.) and 0.30 m (12 in.). Both samples were carefully sealed with gypsum cement and crated with plywood (Figure 9) to preserve natural moisture content during delivery and storage. The larger sample was sent to the USACE Ohio River Division Laboratory for geotechnical testing. After completion of the geotechnical analysis, the remainder of the samples were forwarded to the Hydraulics



Figure 9. Till samples collected at R-14. The sample on the right has been sealed in gypsum cement to preserve the natural moisture content during shipping and storage

Laboratory of the National Research Council of Canada in Ottawa for testing of cohesive abrasion in a unidirectional flow flume.

Wave data generation

Wave information is an essential part of the evaluation of any coastal erosion mitigation project. Ideally, deployment of nearshore directional wave gauges and current meters is desirable to monitor wave transformation and provide data on longshore currents for assessing longshore movement of beach material. However, because instrumentation was unavailable for this project, instead we used wave climate information generated by Hubertz, Driver, and Reinhard (1991) as part of CERC's Wave Information Studies (WIS). On the Great Lakes, hindcast data provide an accurate representation of the deepwater wave climate (Skafel and Bishop 1993). Hubertz, Driver, and Reinhard (1991) also summarize average ice conditions for Lake Michigan. WIS station M59, shown in Figure 10, is the closest hindcast station to St. Joseph. Waves were described on a 3-hr basis for the period from 1956 to the end of 1987. In addition, as part of this investigation, CERC completed a hindcast of hourly wave conditions offshore of St. Joseph for the period from April 1991 to December 1993. The REF/DIF model of Kirby and Dalrymple (1983) was applied to determine wave transformation coefficients for four inshore locations along the study area.

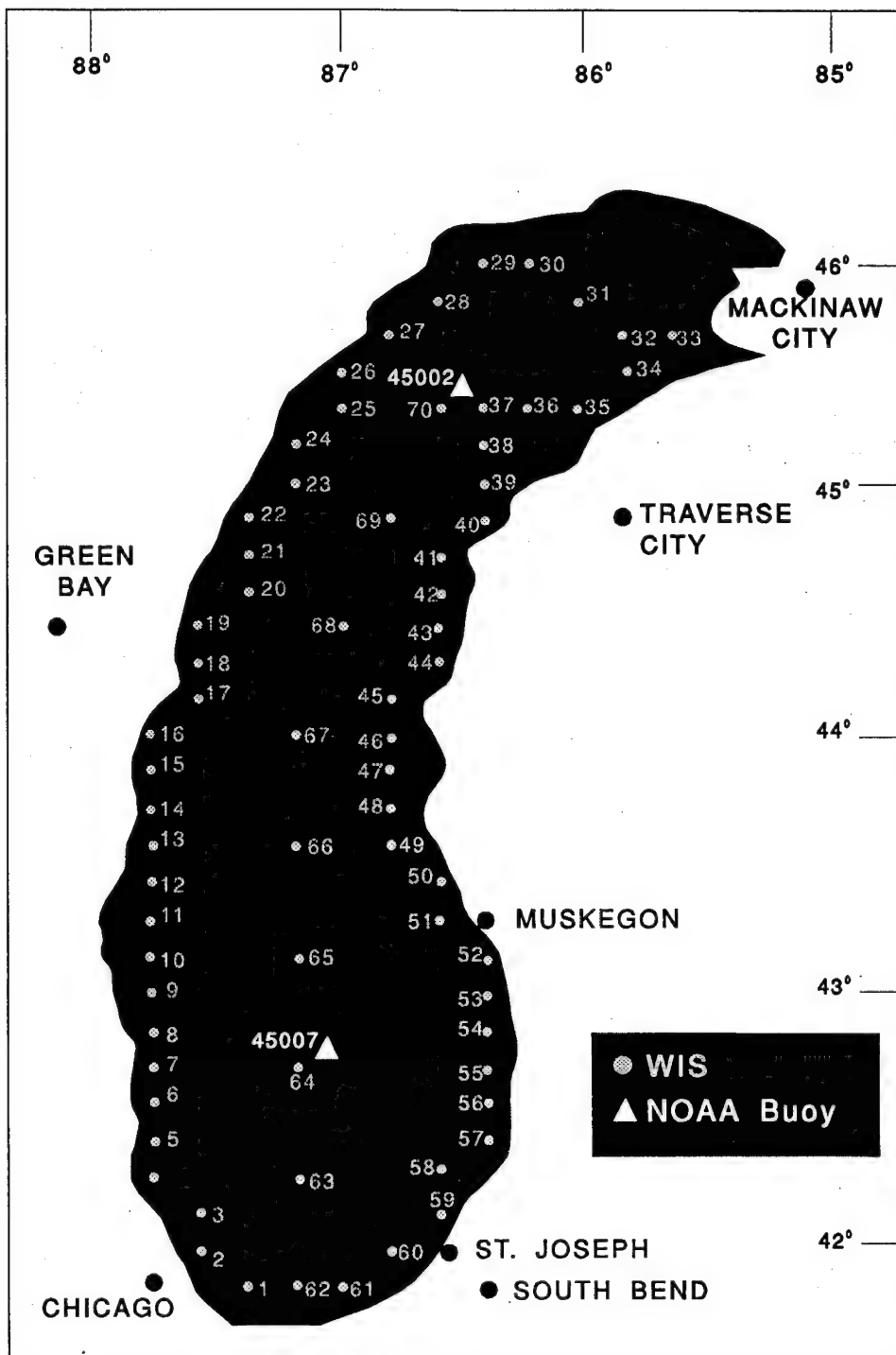


Figure 10. Hindcast station location map for the generation of wave data for St. Joseph. Wave statistics used for St. Joseph were generated for station 59

Aerial photography

Vertical aerial photography overflights of the project area are being performed at least twice a year. The photographs provide a cost-effective method to assess the behavior of the entire project and adjacent shoreline areas. Color photographs, at a scale of 1:6000, will be used to construct a base map and document shoreline change throughout the life of the project.

Data Analysis

Profile data

The Department of Ocean Engineering, University of Michigan, assembled and reduced all beach and offshore profile data. Analog echo sounder records were manually digitized on a digitizing table linked to a personal computer (PC). Using a PC spreadsheet program and custom software, onshore and offshore portions of profiles were joined and converted to CERC's ISRP format (Birkemeier 1984). These ISRP files were sent to CERC via diskette or electronic mail.

Profiles were referenced to either International Great Lakes Datum (IGLD) 1955 or 1985; therefore, elevations were in the range of 540 to 580 ft above sea level. Because most analysts are familiar with profiles that have been plotted with a zero line passing through the upper portion of the shoreface (for ocean sites, typically representing the national geodetic vertical datum or mean low water), the appropriate conversion value was subtracted from the St. Joseph profiles to normalize all profiles to a common zero line:

$$\begin{aligned} Z_{zero} &= Z_{IGLD\ 55} - 576.8 && \text{(for IGLD 1955 data)} \\ Z_{zero} &= Z_{IGLD\ 85} - 577.5 && \text{(for IGLD 1985 data)} \end{aligned} \tag{1}$$

This zero line on the normalized profiles represents the Lake Michigan low water (chart) datum of 577.5 ft (176.0 m) (Coordinating Committee on Great Lakes Basic Hydraulic and Hydrologic Data 1992). Therefore, all profiles can be directly compared with each other. However, note that the zero line does **not** indicate the water level on the day the survey was conducted.

At CERC, all profiles were plotted using the BMAP analysis software that has been developed for display and manipulation of profile data (Sommerfeld et al. 1994). Available profile data extend from 1991 through 1994 (Figure 11).

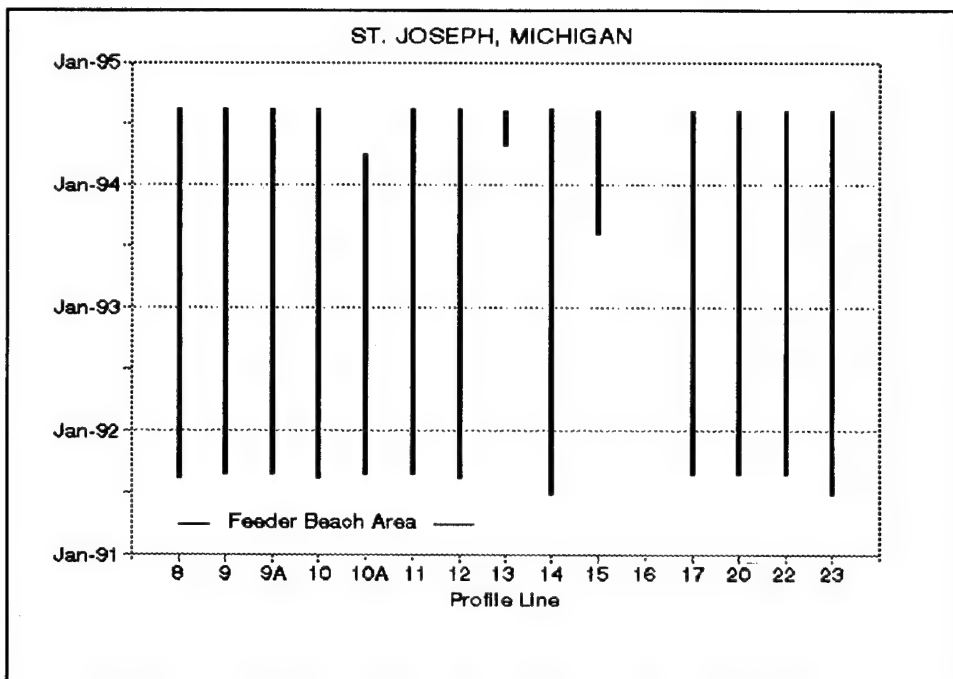


Figure 11. Profile data availability at St. Joseph, MI

Sediment data

Sediment samples collected at the project site were analyzed at CERC's sediment laboratory as described by Parson and Smith (1995). Grain size analyses of the samples were performed using a dry sieving technique outlined by Folk (1980). The methodology employed the sonic sifter described by Underwood (1988), which uses sound waves to enhance the shaking motion of the sediment particles, allowing for faster sieving times and smaller initial samples. Statistical analysis of each sediment sample, performed on CERC's Automated Coastal Engineering System (ACES) software, used the method of moments, a computational method in which all grain size classes are considered in the results. Sediment sizes are expressed in phi (ϕ) units as devised by Krumbein (1934, 1938) and are cross-referenced to millimeters for convenience. Sediment size classifications are described according to the Wentworth size classification (Wentworth 1922).

Native beach sediment characteristics have been described in detail by Parson and Smith (1995) and are summarized in Figure 12. The original native beach at St. Joseph has been obscured by the continuous placement of material from other sources since 1970. The pre-fill (1991) composite mean grain size for the feeder beach area is 1.63ϕ (0.32 mm), with a standard deviation of 1.27, indicating a moderately to poorly sorted distribution. A skewness value of -1.14 indicates a distribution skewed toward the coarser end of the distribution or an excess of coarse material.

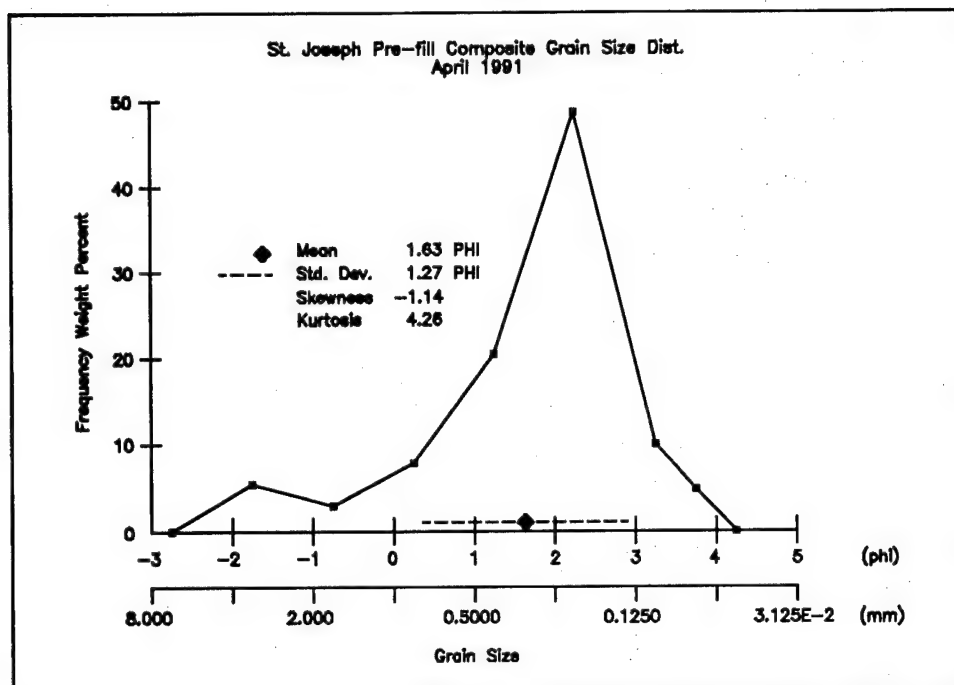


Figure 12. Pre-fill composite grain size distribution for the St. Joseph feeder beach area

Geotechnical tests on the lake bed till were performed by the USACE Ohio River Division Laboratory on two small samples taken from the top and bottom of the larger sample. The averaged results of a grain size analysis revealed that the till sample consisted of: 1 percent gravel, 25 percent sand, and 74 percent fines (i.e., silt and clay). The grain size analysis for the till material is summarized in Figure 13. The clay mineralogy was determined by X-ray diffraction analysis to have a major component of illite, with moderate levels of chlorite (high iron variety). The two samples were classified as: sandy clay with low plasticity and medium consistency and sandy clayey silt with very low plasticity and medium consistency. The samples had shear strengths in the range of 70-100 kPa (0.7-1 tsf). Results of the geotechnical analyses are included in Appendix A.

Subsurface data (GPR)

GPR records were used to measure the thickness of the unconsolidated material overlying glacial till as well as identifying the till profile for input into the numerical model. A GPR record from line R-14 is shown in Figure 14. GPR records were matched with their corresponding profile location, which allowed for the identification of the till surface. Points along the till profile derived from the GPR were selected every 5 to 10 m or less depending upon the relief of the till profile. Measurements for each point were made relating the thickness of the overlying unconsolidated sediment and the position of the till material in relation to the surficial profiles. These

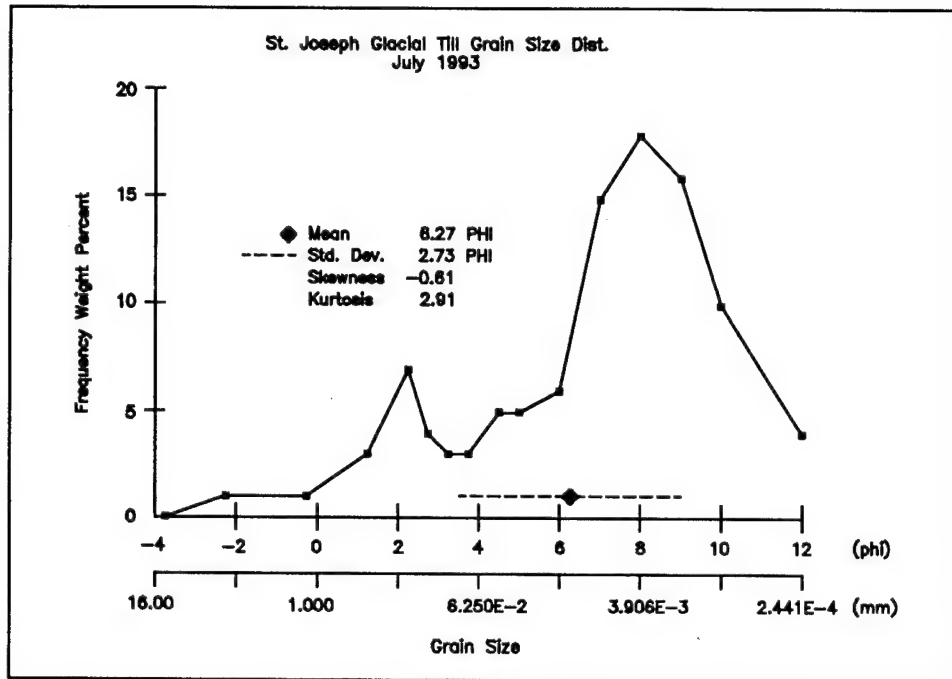


Figure 13. Grain size distribution of the glacial till lake bed material

measurements were input into a 2-D numerical model that simulates coastal processes and defines the profile corresponding to the cohesive substratum. The numerical model used for this investigation is the COSMOS-2D model. As with other sub-bottom geophysical methods, a degree of subjectivity is imposed during interpretation of GPR data.

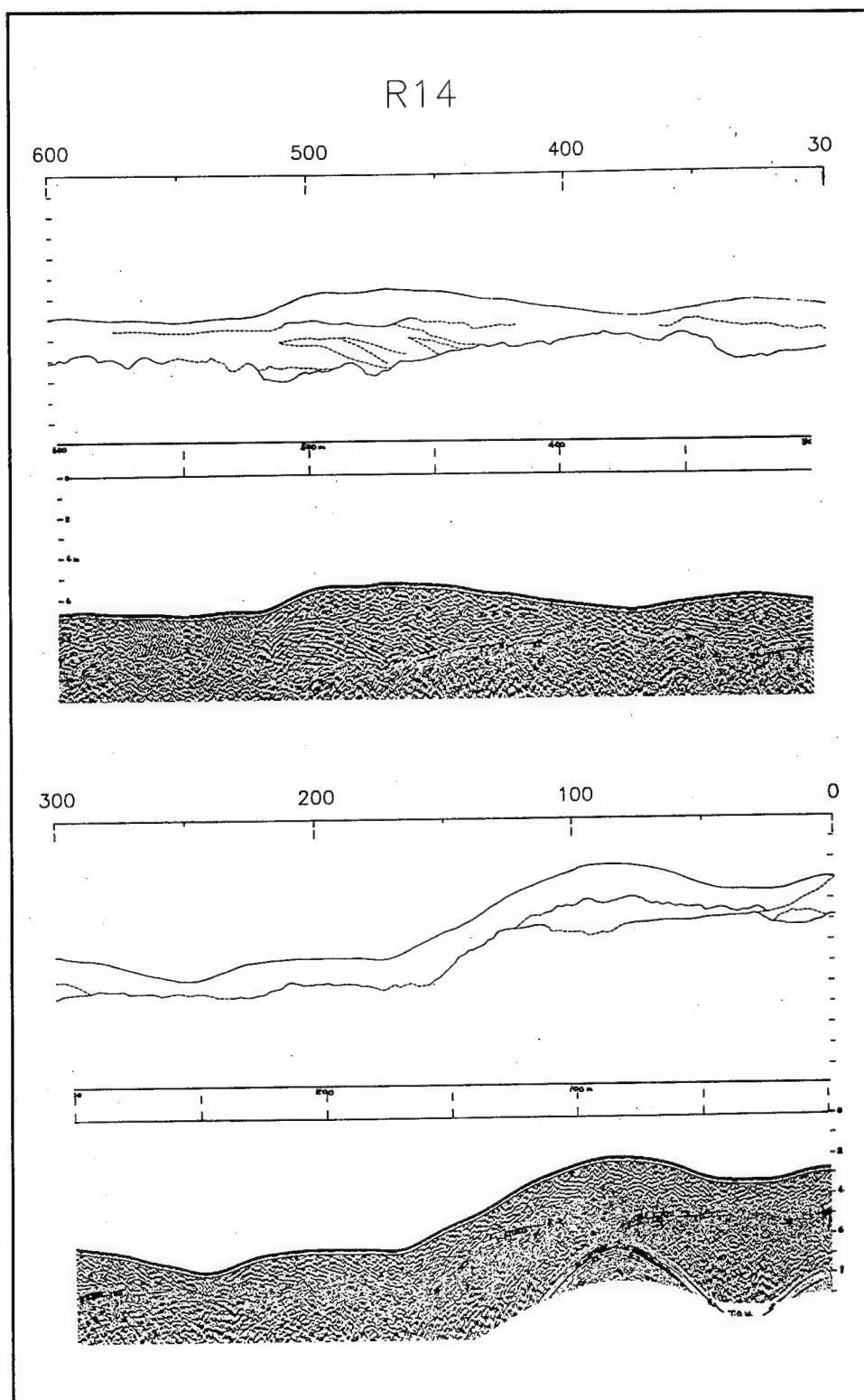


Figure 14. Ground penetrating profile record at R-14 indicating the thickness of the overlying unconsolidated sediments and the position of the cohesive substratum profile

5 Till Downcutting Investigation

This investigation addresses the objective listed in Chapter 1, which was to develop an improved understanding of the relationship between the movement of the cohesionless sediment (both fine- and coarse-grain components) and the irreversible downcutting of the underlying glacial till at the St. Joseph project site. Downcutting of the till, at a micro-scale, is the least-understood aspect of the lake bed and shoreline erosion problem south of St. Joseph Harbor. This investigation consists of the controlled laboratory testing of the downcutting process for undisturbed till samples taken from the lake bed offshore of the St. Joseph study area. The till samples collected in support of this investigation were described in Chapter 4. The remainder of this section addresses the test methodology, erosive response of the till samples, interpretation of the results with respect to downcutting offshore of St. Joseph, and compares test results with the results of previous studies of this nature.

Description of Samples

Two block samples of undisturbed till were obtained through dredging from the lake bed in about 7.6 m (25 ft) of water along line R14 on July 14, 1993. The two cube-shaped samples had side dimensions of 0.23 m (9 in.) and 0.30 m (12 in.). After completion of the geotechnical tests described in Chapter 4, both samples were forwarded to the Hydraulics Laboratory of the National Research Council of Canada in Ottawa. The samples were trimmed to 61 by 28 by 8 cm (or smaller) for testing in the unidirectional flow flume. Sample 1 is shown prior to testing in Figure 15 and consists of two different-colored sediments: a 1-in.-wide light gray sediment along one side of the sample, with the remainder having a dark gray color. Sample 2 is shown prior to testing in Figure 16 and again consists of different-colored sediments, with one third of the sample being the light material and the remainder having the darker gray coloring. The samples were placed on their sides in the flume so that both of the sediment types could be tested at the same time (i.e., the top surface of the test section corresponded to a vertical section of the lake bed material).



Figure 15. Till sample 1 prior to testing in the flume. Note the narrow band of lighter colored sediment along the top edge of the sample

Test Methodology

The samples were tested in a 12.5-m-long open channel tilting flume with a 40-cm-square cross section and glass side walls. The slope of the flume can be varied between 0 and 5 percent. Water is supplied from the upstream end of the flume through a pump-fed tank. Discharge into the flume can be regulated through a valve on the supply line to the discharge tank. Flow in the flume also can be regulated through gates at the upstream and downstream ends. The flume is illustrated in Figure 17. A false floor was installed for these tests located 7 cm above the base of the flume and a drop section was created in the false floor for insertion of the undisturbed samples. When installed and properly leveled, the surface of the samples lay just above the adjacent false floor level.

The shear stress exerted on the bed by the unidirectional flow of fluid was determined indirectly by measuring the vertical profile of velocity just above the bed. In most situations, velocities were measured at six elevations within 2 cm of the bed. Velocity was measured using a laser doppler velocimeter (LDV) system as shown in Figure 18. In steady turbulent flow over a relatively smooth surface, the vertical distribution of velocity normal to the boundary was found to satisfy a logarithmic profile. Calculations of shear stress for the individual test sequences are given in Appendix B. The depth-averaged flow velocities ranged between 0.5 m/s and 3 m/s in the various test sequences.

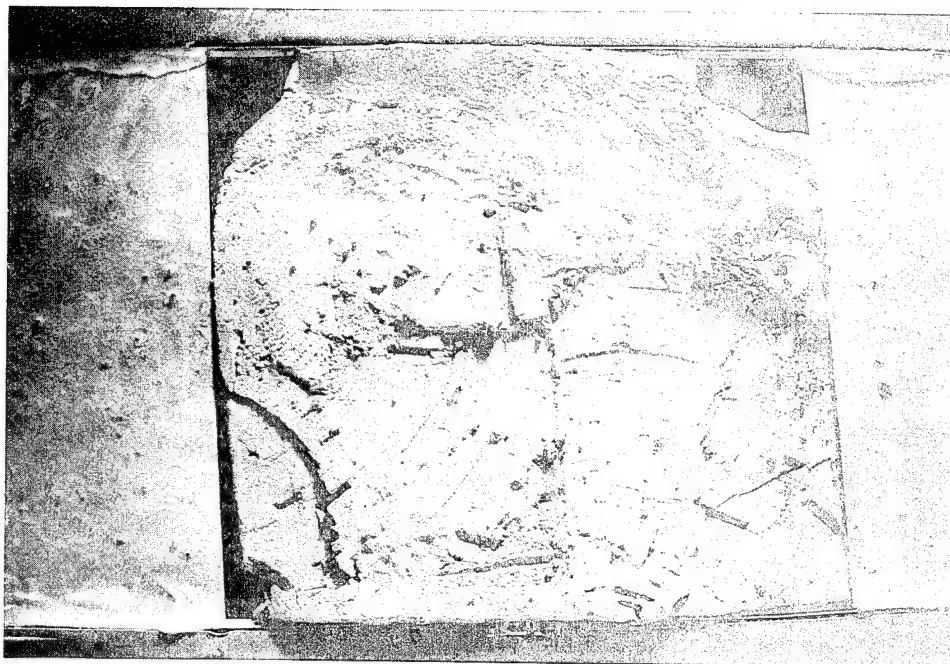


Figure 16. Till sample 2 prior to testing in the flume. The upper one third of the sample consists of the lighter colored sediment

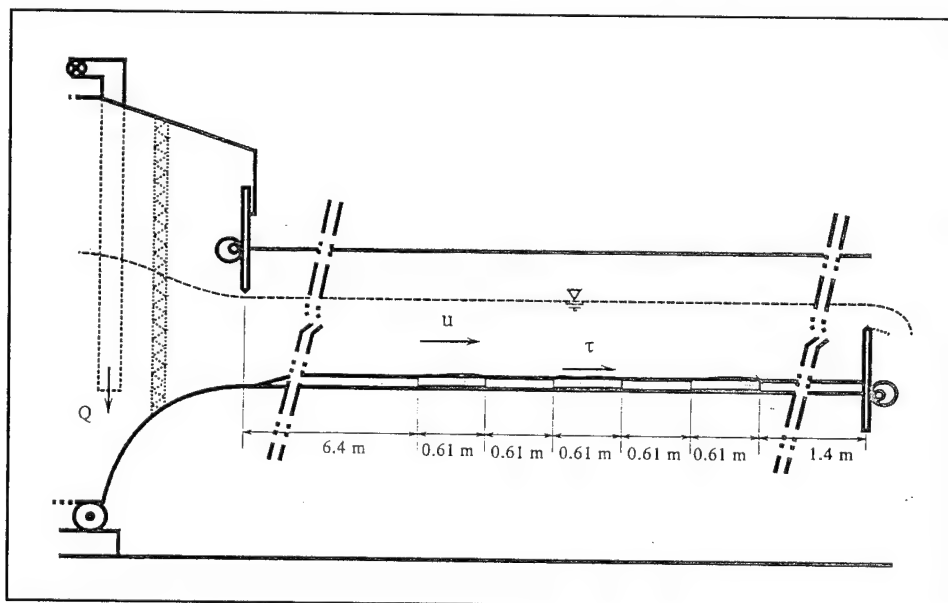


Figure 17. Tilting flume used for testing the downcutting processes for the glacial till substratum (from Cornett et al. (1994))

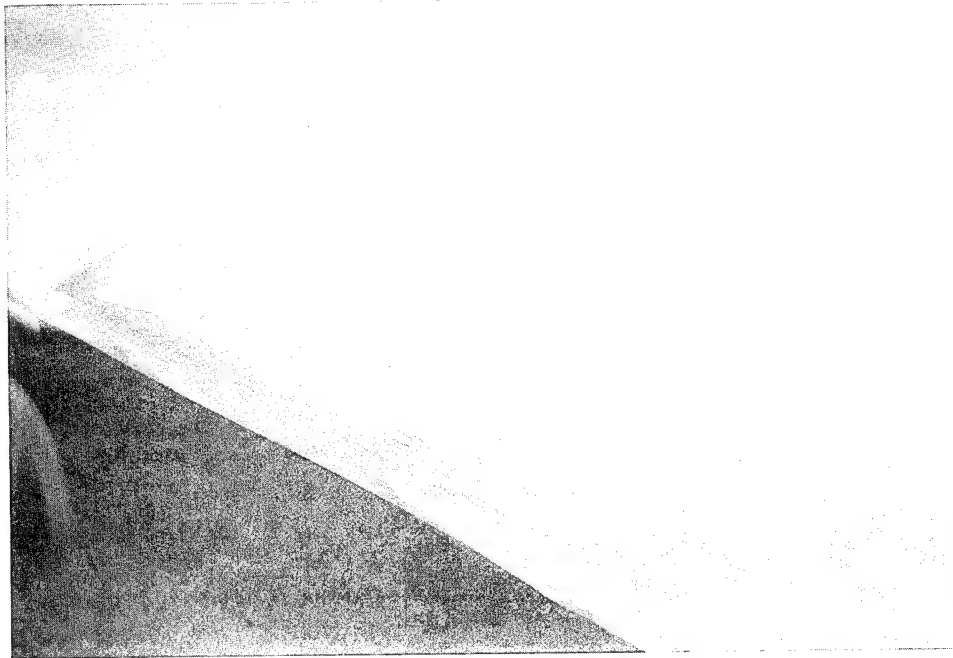


Figure 18. LDV apparatus used to determine shear stress exerted on the till bed

To monitor erosion, the upper surface of the samples was measured at regular intervals using an analog point gauge with an accuracy of 0.025 mm. The gauge was rigidly supported by the flume sidewalls and accurately positioned using a set of calibrated guide marks. About 28 soundings were made across each sample surface to determine average erosion. For both of the samples, the sounding depths for the light and dark gray sediments were segregated prior to determining average erosion or downcutting rates owing to the difference in erosion resistance between the two different-colored sediments. Raw data, consisting of the individual point measurements, are presented in Appendix C.

Sample 1 was tested under clear water conditions only. It was tested through a range of increasing flow conditions to determine the shear stress at the onset of erosion as well as the relationship between erosion rate and shear stress. The maximum shear stress of 14.3 Pa corresponded to an average flow velocity of 3.1 m/s in the open channel. Sample 2 was tested to determine the effects of sand on the erosion rates. Three types of tests were performed consisting of different cohesionless sand cover characteristics as follows: coarse/fine sand mix; coarse sand (with a D_{50} of about 2 mm); and fine sand (with a D_{50} of about 0.2 mm). Depending on the flow velocity, the sand moved across the till samples as dunes, ripples, or as a sparse sand cover, with rolling, saltating, and suspended modes of transport.

Test Results for Clear Water

Testing of both samples revealed that the lighter-color sediment in the samples eroded much faster than the darker sediment. Therefore, separate erosion rates are presented for these two sediment types. In the field, the weaker, light-colored sediment corresponded to the top of the sample as it was extracted from the lake bed. Test results for sample 1 are presented in Table 2 and Figure 19.

Table 2 Erosion Rates (mm/hr) for Clear Water Testing			
Shear Stress (Pa)	Depth Avg. Velocity (m/s)	Dark Sediment (mm/hr)	Light Sediment (mm/hr)
2.3	1.1		Onset of erosion
4.4	1.6	Onset of erosion	2.1
7.7	2.3	0.3	7.8
14.3	3.1	1.0	-

The initiation of erosion for the weaker, light-gray sediment occurred with a shear stress of 2.3 Pa (depth-averaged velocity of 1.1 m/s). For the light sediment, the erosion rates varied between 2.13 and 7.80 mm/hr, whereas the more erosion-resistant dark sediment featured erosion rates between 0.03 and 0.33 mm/hr over the same range of shear stresses.

Light- and dark-colored sediments were distinguished by quite different modes of erosion in the clear-water tests. The surface of the light sediment appeared to dissolve, leading to a general lowering of its surface. In contrast, the dark sediment chipped off around the edges and generally broke off in pieces along fractures. At the maximum velocity of the tilting flume (with a depth-averaged velocity of 3.1 m/s), the back half of the sample washed away entirely after the flow had slowly opened a fracture across the middle of the sample in the dark-colored sediment (see Figure 20).

Test Results with Sand in Flow

Sample 2 test results with cohesionless sediment in the flow are presented in Table 3 and Figure 21. For tests with coarse sand (with a D_{50} of about 2 mm) at a low shear stress of 1.0 Pa (depth-averaged velocity of 0.7 m/s), the grains rolled across the surface of the sample, gouging the weaker, light-colored sediment. The sand was hand-fed to avoid the formation of dunes and burial of the till surface. As the test progressed, the coarse sand stuck to the surface of the light-colored sediment, producing an armor layer. At a higher shear stress of 1.9 Pa (depth-averaged velocity of 1 m/s) with coarse sand in

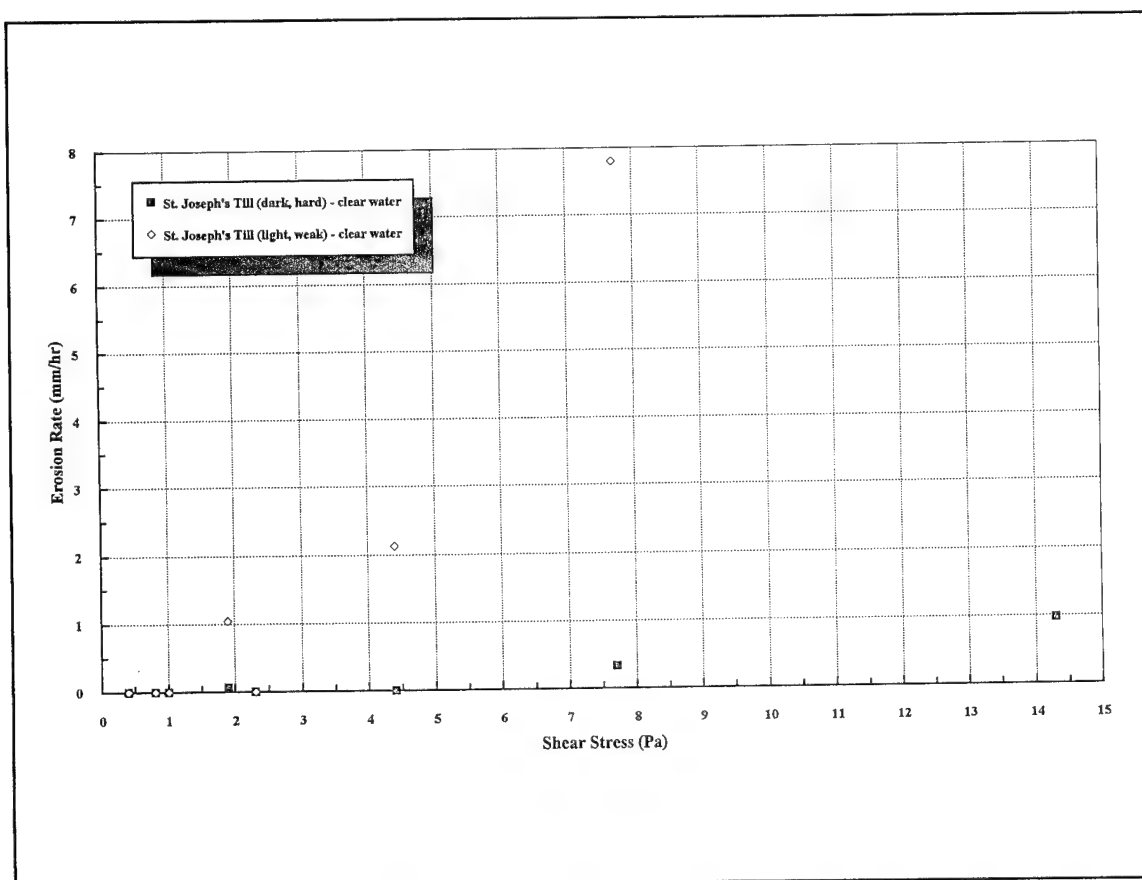


Figure 19. Results for clear-water testing of samples 1 and 2. Erosion rate (mm/hr) versus shear stress (Pa)

the flow, erosion of the dark-colored sediment was more evident. Armoring of the weaker, light-colored sediment persisted. Erosion began for the coarse sand tests at about half the shear stress of that determined in the clear water tests. Erosion rates for the harder, dark sediment were much higher with coarse sand in the flow than for the same shear stress with clear water. Increases in erosion rates were evident but less pronounced for the weaker, light sediment, probably due to the armoring effect that occurred with coarse sand in the flow.

Figures 22 and 23 show eroded samples 1 and 2, respectively. The weaker, light sediment shows much greater erosion than the dark sediment in both cases. The surface of sample 2 reveals the effects of sand abrasion. Figure 20 shows sample 1 breaking in two at the highest shear stress of 14.3 Pa (corresponding to a depth-averaged flow of 3.1 m/s).

The tests with fine sand in the flow were started at a shear stress of 0.8 Pa (depth-averaged velocity of 0.65 m/s). The fine sand grains did not stick to the surface of the weaker, light-colored sediment and effectively removed any of the coarse grains that had been lodged in the surface during previous coarse sand tests. At an increased shear stress of 1.9 Pa, rapid erosion of the light

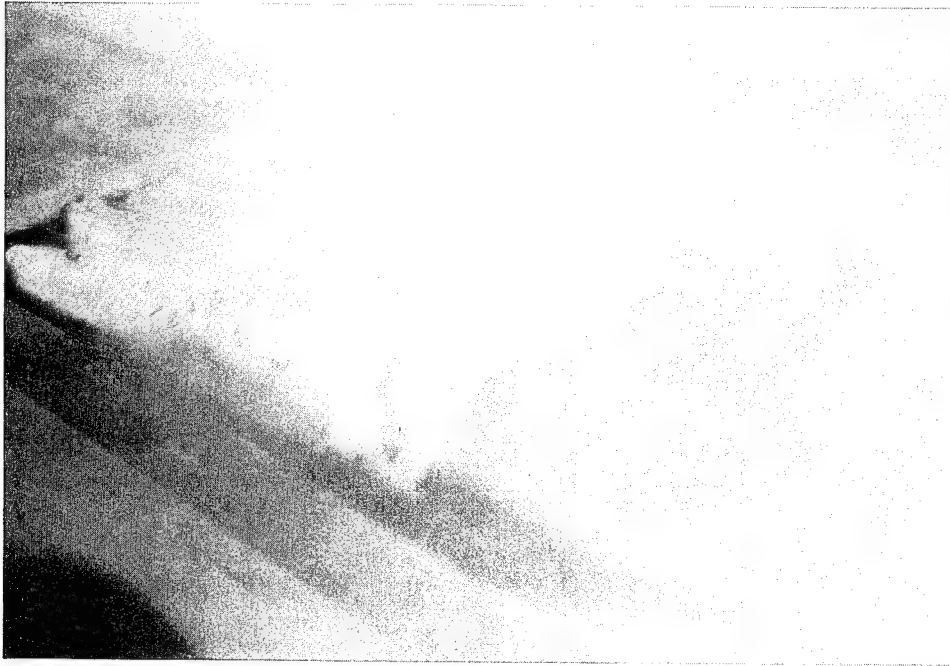


Figure 20. Condition of sample 1 after breaking apart during clear-water testing

Table 3
Erosion Rates (mm/hr) with Sand Added to Flow

Sand Cover	Shear Stress T (Pa)	Depth Avg. Velocity (m/s)	Dark Sediment (mm/hr)	Light Sediment (mm/hr)
Coarse sand	1.0	0.7	0.58	0.77 ¹
	1.9	1.0	2.01	1.73 ¹
Fine sand	0.8	0.65	0.53	1.47
	1.9	1.0	1.85	7.80
Clear water	1.9	1.0	0.07	1.04
Coarse/fine mixture	0.4	0.4	0.24	0.79

¹ Coarse sand partially armored the till surface in these tests.

sediment was observed at a rate comparable to the 7.7-Pa clear-water test result. The erosion rate of the dark sediment at both the low and high flows with fine sand was considerably greater than that in the clear-water test with a similar flow velocity.

Tests with sediment consisting of a mixture of fine and coarse sand were performed with a shear stress of 0.4 Pa (depth-averaged flow velocity of

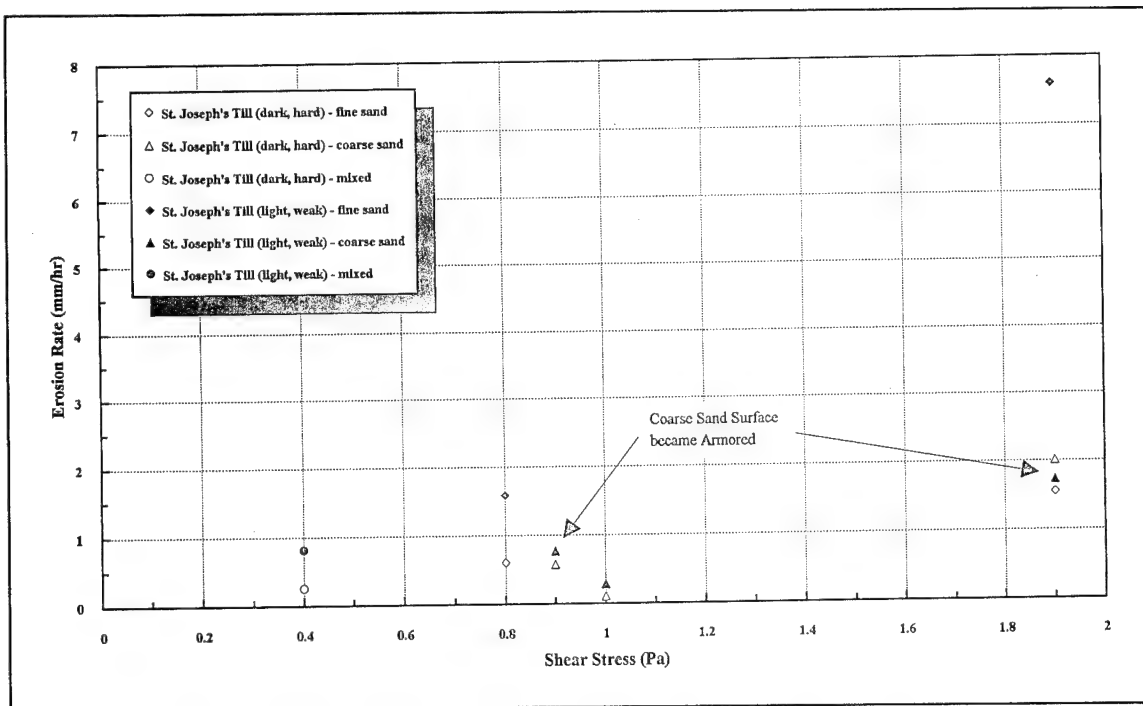


Figure 21. Test results for sand in flow for samples 1 and 2. Erosion rates (mm/hr) versus shear stress (Pa)



Figure 22. Erosion condition of sample 1 after using clear water in flume

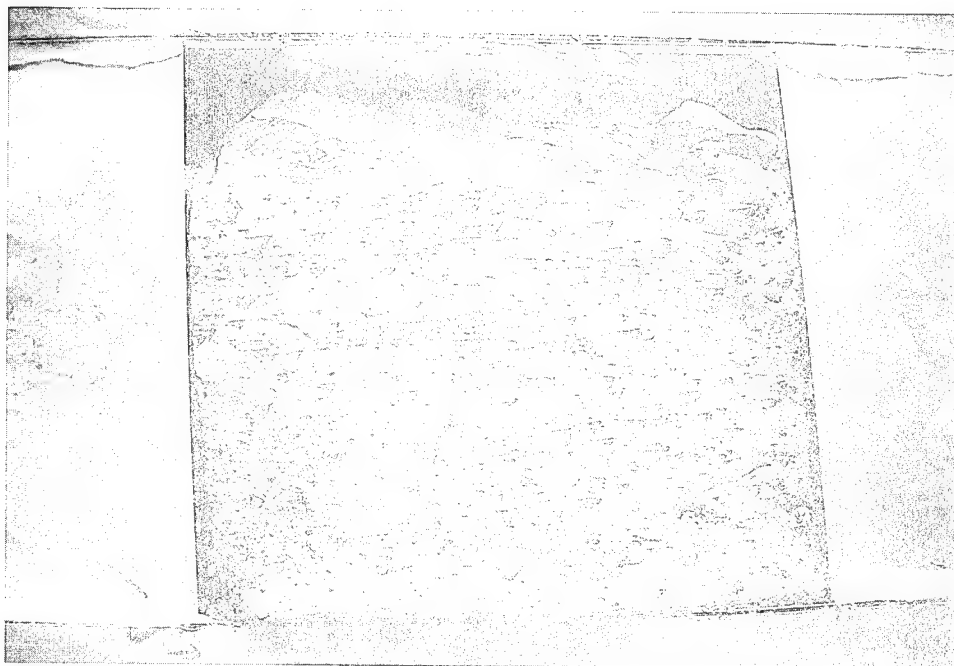


Figure 23. Erosion condition of sample 2 after sand was included in water flow

0.4 m/s). Measured erosion rates were comparable to values observed in clear-water tests with shear stresses that were 10 to 15 times greater. Tests at this shear stress level were also performed with clear water and there was no measurable erosion.

Test Results Summary

In summary, the flume test results indicate that the dark-colored sediment was much more erosion-resistant than the light sediment (erosion rates of the light sediment were between 5 and 20 times greater). Shear stresses to initiate erosion were reduced to less than 1 Pa with sand in the flow (reducing the threshold shear stress by a factor of about 4 for the dark sediment and 2 for the light sediment). The erosion rates with sand in the flow were comparable to rates in the clear-water tests where shear stresses were 5 (for the weaker, light sediment) to 10 (for the harder, dark sediment) times greater. When compared to similar tests with the fine sand, the tests with the coarse sand and the weak, light sediment featured a reduced erosion rate due to armoring (i.e., as some coarse grains were embedded in the sample surface). For the more resistant dark sediment, erosion rates were similar for the fine and coarse sand.

Interpretation of Downcutting Investigation Results

The laboratory findings have some important implications for the process of downcutting at the lake bed in the study area. The difference in erosion resistance between the light- and dark-colored glacial till could explain the dramatic and detailed lake bed relief evident in the profile surveys and underwater video of exposed till. As the till abrades, some additional down-cutting could result from fracturing and separation of large pieces of till from the lake bed (as occurred in one of the laboratory tests). The relative importance of the abrasion process to overall downcutting versus the importance of large-scale fracturing is unclear at this time. However, it should be recognized that the fracturing process could only occur through the creation of irregular lake bed relief, which in turn must be a result of the abrasion process.

There are two possibilities regarding the presence of two different sediment types in the samples. First, they may represent different till units, possibly created through the fracturing of an older unit and infilling with a more recent deposit. The other possibility is that the lighter colored, weak sediment represents a weathered surface caused by long-term exposure to the lake water. A review of the geotechnical test results for the two samples (presumably representing the two sediment types discussed here) tends to refute the latter possibility, as they revealed different characteristics with respect to grain size distribution, porosity, and water content.

It is interesting that there were differences in erosion rates of the weaker light sediment with the fine and coarse sand. However, this finding can be attributed to the armoring effect created when the coarse sediment stuck to the surface of the till. It was noted that when fine sediment was introduced, the embedded coarse grains were dislodged. Therefore, for the mixed sediment that would exist in the field, this armoring phenomenon (at least with coarse sand) probably does not occur. Therefore, there is probably no measurable difference between the downcutting of a section of lake bed that is covered with coarser beach nourishment sediment versus the fine nourishment material.

Laboratory results may be interpreted in terms of potential downcutting in the field by considering the shear stress at the lake bed for some typical wave conditions. Two depths were selected (2 m and 5 m) corresponding to the average position of the two inner troughs between the sandbars (i.e., at locations where the till is exposed or where the sand cover is thin). Six waves were selected to represent all of the wave conditions from the WIS hindcast for the period 1956 to 1988. Calculated shear stresses related to the wave orbital velocity for each of these wave conditions at the two depths are given in Table 4. It should be noted that these are the peak shear stresses, and they are only reached instantaneously once every wave cycle.

Clearly, shear stresses due to wave action are capable of causing erosion of the till with or without the presence of sand for the larger wave conditions.

Table 4
Typical Wave Conditions and Associated Peak Shear Stresses

Wave Characteristics			Shear Stress (Pa)	
Hs (m)	T (s)	Duration (hrs per yr)	d = 2m	d = 5m
0.3	3.0	240.0	0.7	0.1
0.5	4.0	360.0	2.7	0.6
1.0	5.0	190.0	17.4	2.6
1.5	6.0	90.0	39.6 ¹	6.4
2.0	6.5	50.0	39.9 ¹	19.8
3.0	7.0	10.0	40.4 ¹	47.0

¹ Breaking wave conditions.
Note: Bottom roughness of 0.0025 m was assumed.

Laboratory tests revealed that the threshold for erosion varied between a low of less than 0.5 Pa with sand in the flow to a high of 2 to 4 Pa under the clear-water conditions (for the light and dark sediment, respectively). Based on the laboratory results given in Table 3, an average downcutting rate under erosive conditions is about 2 mm/hour. If a section of till on the lake bed was exposed for the entire year, the downcutting could be up to 0.7 m at the 2-m depth and 0.35 m at the 5-m depth (this calculation assumes the average downcutting rate and considers that the peak wave shear stresses are only instantaneous). It is unlikely that this magnitude of downcutting is sustained at any one location over a year, because for a significant amount of time the till will be buried under a sandbar (or a sufficient protective cover layer will exist). Laboratory tests of profile downcutting in a wave flume (reported by Nairn (1992) and Skafel and Bishop (1994)) showed that only a very thin cover would protect the underlying till from erosion (perhaps as little as 2-5 cm, depending on the wave conditions).

For the lake bed in the study area, the preliminary findings of Foster et al. (1992) show that between the 2-m and 5-m contours, up to 3 m of downcutting was experienced over a large area between 1945/6 and 1964/5, which gives an average annual downcutting rate of about 0.16 m/year. The annual drop in the lake bed could occur over a period of 80 hr at a downcutting rate of 2 mm/hr. This 80-hr duration is in the same order of magnitude as the number of hours of storm wave conditions each year.

Comparison to Other Studies

The unidirectional flow flume apparatus has been used at both the National Research Council of Canada Hydraulics Laboratory and at the Queen's University Coastal Engineering Laboratory to test the erosion resistance of cohesive

sediment samples in other studies. These included lake bed samples from Lake Erie (e.g., Port Stanley and Waterlain Till), river bed samples from four rivers in Ontario, and a seabed glacial till sample from the Canadian Atlantic coast (near Prince Edward Island). The results of the St. Joseph tests are compared to the results of these other studies in Figures 24 and 25 for the clear water and sand in flow tests, respectively. The St. Joseph results are separated into two groups corresponding to the weak, light-colored sediment and the harder, dark sediment.

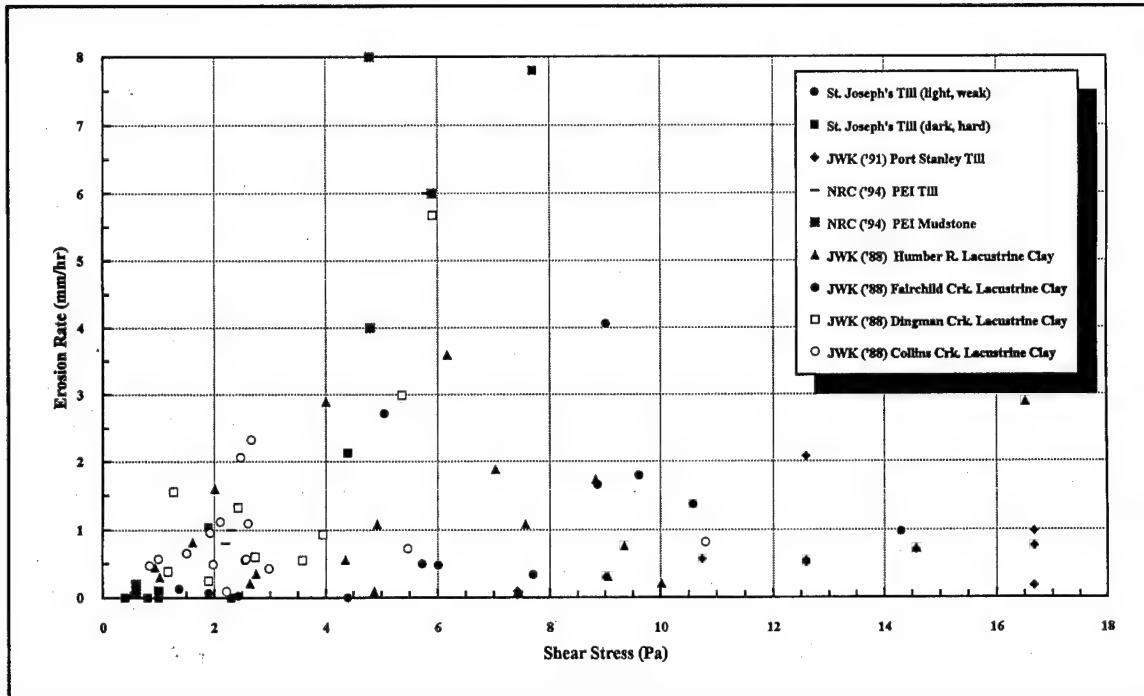


Figure 24. Comparison of clear-water erosion rates (mm/hr) from St. Joseph with other cohesive substrates from various other studies

In the clear-water results of Figure 24, there appear to be two populations relating to high and low erosion resistances. The weaker, light-colored sediment falls in the low erosion-resistance group, which consists of some of the lacustrine clay results from the Ontario rivers along with a very weak mudstone from Prince Edward Island. The dark sediment from the St. Joseph samples falls in the more erosion-resistant group, which includes some of the lacustrine clay samples from Ontario, and in particular, the Port Stanley Till from Lake Erie.

In Figure 25, giving the sand in flow test results, there does not appear to be any grouping of results. However, the results for the darker, more erosion-resistant sediment from the St. Joseph's samples are located in the low erosion range along with the Lake Erie sample test results.

These results appear to indicate that once sand is introduced to the erosion process, the characteristics of the till become a secondary factor to the rate of

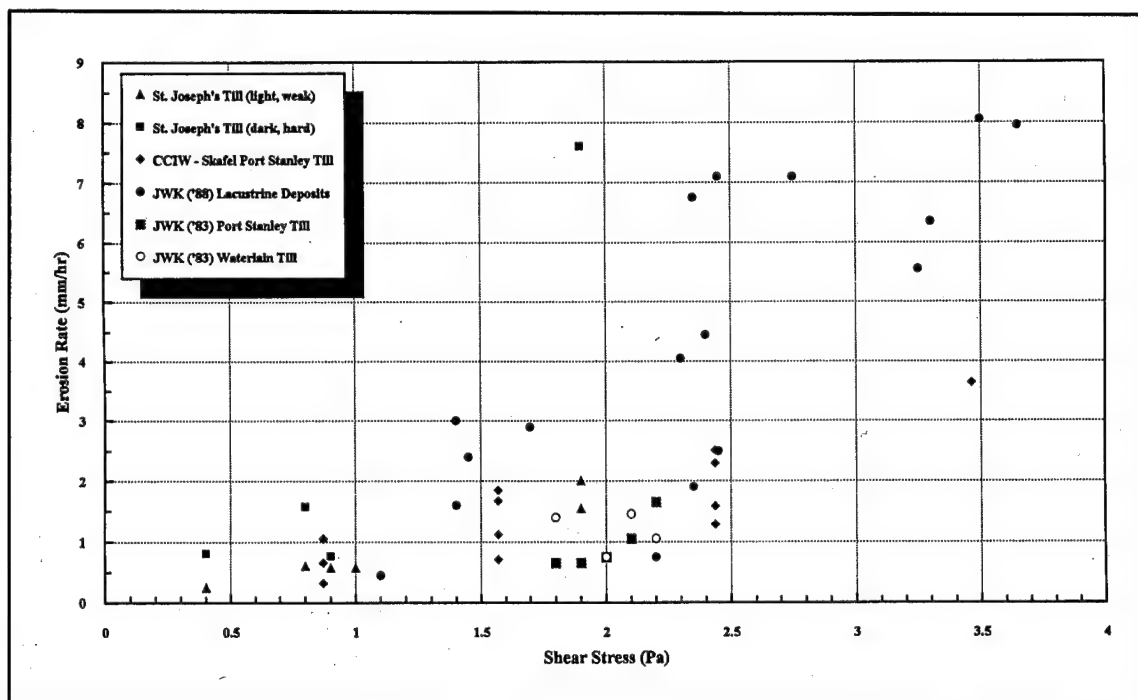


Figure 25. Comparison of sand in flow erosion rates (mm/hr) from St. Joseph with other cohesive substrates from various other studies

erosion. Nevertheless, the remaining scatter in Figure 25 is probably explained by the variation in the physical and chemical properties of the different samples.

6 Cross-Shore Sediment Transport and Profile Response Model

The cross-shore sediment transport calculations were completed with COSMOS, which is a deterministic numerical model for the simulation of coastal processes. The model consists of several predictive phases, including descriptions of the following parameters across a profile:

- a. Random wave transformation, including refraction, bottom friction, shoaling, breaking, wave decay, runup, and overtopping.
- b. Steady currents, including undertow and wave- and tide-induced long-shore currents.
- c. Orbital velocities.
- d. Suspended sediment distribution through the vertical, bed load, and suspended load in cross-shore and alongshore directions.
- e. Profile change related to gradients in cross-shore sediment transport (COSMOS-2D) and both cross-shore and alongshore sediment transport (COSMOIS-3D).

This part of the study addresses only the cross-shore component of sediment transport and profile response to storms. Downdrift effects from the feeder beach in relation to longshore transport rates will be addressed in a later report. Each of the processes listed above is evaluated at approximately 200 finite difference calculation points across the profile. The various individual predictive phases of COSMOS, as well as the integrated model, have been extensively tested against both laboratory and field data (Southgate and Nairn 1993, Nairn and Southgate 1993). Flowcharts showing the various predictive modules of COSMOS-2D are presented in Appendix D.

COSMOS has been applied in over 100 engineering projects throughout the world to determine: average annual alongshore transport rates; beach and dune erosion during storms; the influence of sea level rise and lake level fluctuation

on erosion processes; downcutting of cohesive sediment profiles (short-term and long-term); erosion and scour at the toe of structures; the storm response and longevity of beach fill projects; impacts of structures on coastal processes; stable beach planform alignments; and offshore sediment loss rates. COSMOS has proven to be an accurate and robust predictive tool that can be applied to any site without the need for calibration (except where downcutting must be calculated) (Southgate and Naim 1993, Naim and Southgate 1993).

This process-based numerical model, which has been developed for sandy shores, has been adapted for application to cohesive shores and for shores with seawalls or revetments. Within the input description for the profile characteristics, a second profile shape may be specified corresponding to the cohesive substratum (or on inerodible coastal structures), thus allowing for a description of an overlying sand veneer. The sediment transport and profile change routines pertaining to the overlying cohesionless sediment are modified to address the possibility of supply-limited sediment transport. For example, where the sand cover is very thin, the predicted potential cross-shore transport at a specific location may be unattainable if the gradient in transport between two adjacent calculation points implies more erosion than is possible due to the presence of the cohesive layer (or a coastal structure). In these cases, the potential transport rate is reduced to the supply-limited level.

The downcutting process of the cohesive sediment is more complicated and less understood than the transport of the overlying sand. A conceptual model of downcutting was presented by Naim, Pinchin, and Philpot (1986). It has been postulated by other researchers (Coakley, Rukavina, and Zeman 1986) that shear stress at the bed created by orbital velocities, along with the presence of sand as an abrasive agent, may be responsible for irreversible downcutting of the cohesive surface. However, the shear stress at the bed due to orbital velocity decreases in an onshore direction through the surf zone due to the diminished wave heights in shallower water. This is at odds with the fact that the downcutting must increase closer to shore in order for the profiles to maintain a similar shape as they recede shoreward (as is generally known to occur from a review of historical profile data at numerous sites). Naim, Pinchin, and Philpot (1986) suggested that additional downcutting mechanisms in the surf zone include breaking-induced turbulence, which is able to penetrate to the bed as well as the shear stress attributable to the undertow velocity near the bed. Both the generation of turbulence and the undertow may be quantified by the rate of wave energy decay across the profile for the waves which are broken. Therefore, in COSMOS, the downcutting is attributed to two driving forces: shear stress at the bed caused by orbital velocities (for unbroken waves) and wave energy dissipation in the surf zone (for broken waves). Because of a lack of understanding of the details of the complex erosion process at a microscopic scale, the two erosion mechanisms must be related to downcutting by two empirical coefficients.

Description of Model Input

For this project, the 2-D version of the model has been applied to describe the sediment transport processes for eleven different shore-normal profile locations, as shown in Figure 6. The model input includes: profile shape in x and y coordinates (for both the surface of the sand and the cohesive substratum bottom profile); profile azimuth; a description of the grain size; and wave and water level conditions.

The input profile shape for most of the 2-D tests consisted of the soundings taken on 18 May 1992 for all of the profiles except lines R17, R20, and R22, which were based on the survey of 20 November 1992 (soundings were unavailable for these three lines in the earlier survey). In addition to the sand surface, the COSMOS model requires the input of the underlying glacial till (or cohesive sediment) profile shape. This information was derived from the ground penetrating radar (GPR) tests performed by Sauck (1993) of Western Michigan University. The location of the underlying till surface could be inferred from the GPR data, which were available for lines R10, R12, R13, R14, R15, R17, R20, R22, and R23. The inferred position of the till was confirmed generally by the visible sections of exposed till evident from the underwater video of the lake bed. The COSMOS model also requires the location of any inerodible surfaces, and as such, the revetment along the railroad and the highway were input for lines R12 to R22 (a steel sheet-pile wall also exists at line R23). The profile azimuth for all of the lines was selected to be 290 deg.

The version of COSMOS-2D used in this investigation required a single representative grain size for the entire profile line. The selection of a representative grain size at this site presented a difficult problem. Parson and Smith (1995) present a comprehensive assessment of the native beach characteristics at St. Joseph. One complication relates to the manner in which the numerous fine and coarse sand (poorly sorted) beach nourishments have obscured any native "stationary" grain size characteristics. Furthermore, beaches along eroding Great Lakes shorelines typically consist of a wide range of grain sizes, especially close to shore and on the beach itself. Moreover, the sand and gravel deposits occur in thin patches and ribbons (i.e., also resulting in large gradation variations through the vertical). The size distributions for various beach nourishments are relatively well described. The fine sand component derived from the dredging of the harbor is well-sorted with a D_{50} of 0.2 mm. The coarse fill was trucked to the site from upland sources and consists of poorly sorted material with a bimodal distribution with peaks at 0.6 mm and about 14 mm. The D_{50} of the coarse beach fill is about 2 mm. Prefill grain size characteristics based on a composite of all samples taken in April of 1991 featured a D_{50} of about 0.3 mm. The representative D_{50} for natural conditions (i.e., not altered by beach nourishment) north of the St. Joseph jetties may be on the order of 0.4 mm. This is based on samples from cores taken near the shoreline north of the study area by Patrick Engineering (1995). Their study

also provides a description of 13 boreholes made at the water's edge between South Haven, MI, and Indiana Dunes National Park, IN, in October of 1994.

An important finding of the Parson and Smith (1995) report is that the grain size characteristics are simply not well understood due to the inability of standard sampling techniques to obtain statistically representative samples for Great Lakes beach characteristics. In light of these findings, the COSMOS-2D tests have been performed for different grain sizes to provide a sensitivity assessment of the influence of grain size. For the standard tests of alongshore and cross-shore sediment transport, D_{50} values of 0.2 and 2 mm were adopted. These values are also representative of the two beach fill types (i.e., from harbor dredging and from upland sources).

An important model input relates to wave and lake level conditions. Two sources of wave data were used: the WIS data for station M59, which is located closest to St. Joseph and which covers a period from 1956 to the end of 1987; and deepwater wave hindcast information prepared by CERC for this study covering the period from April 1991 to December 1993. Scatter diagrams for the WIS data are presented in Appendix E. Storms were selected based on any event which featured a peak significant wave height of greater than 2.0 m. The largest storms are ranked by wave height and listed chronologically in Appendix E. While the majority of the largest storms feature waves from the northwest quadrant, there are many storms from the southwest and west (the latter usually consist of an event where the wave direction swings from southwest through to northwest, or the reverse).

Three storms were selected from the recent hindcast period (1991 to 1993) that would be representative of the three types of storms (northwest, southwest, and west). These events, combined with the actual lake levels, were used as input in the cross-shore COSMOS-2D tests. The characteristics of these storms are listed in Appendix E. The 14th of January 1992 storm, when compared on the basis of wave energy to the storm events for the 1956 to 1987 period, ranks the highest for the entire 32-year period. The high wave energy for this storm is a result of the very long duration where waves exceeded 2 m and is not due to the magnitude of the peak wave height (which was only 3.9 m compared to the highest for the long hindcast period of 6.2 m). In addition to tests at the actual lake levels, the storms were also used as input with higher lake levels to represent more extreme conditions than those that existed in the period 1991 to 1993 when the lake levels were low to moderate.

A wave transformation analysis was undertaken by CERC to define the inshore wave conditions at four points along the study area shoreline. This analysis used the REF/DIF model of Kirby and Dalrymple (1983). However, wave directions for the inshore waves derived from this analysis appeared to be unreliable. The REF/DIF model is based on a parabolic solution of the mild slope equations and has a limited range of application with respect to the difference between the approach angle and the angle of the depth contours. This model is most reliably applied by formulating individual grids for each representative wave approach direction. Therefore, the inshore waves required

as input for the 2-D sediment transport modeling were determined by simple linear refraction, which can produce relatively accurate inshore wave directions for the shore-parallel contour conditions in the St. Joseph nearshore area. The wave heights were reduced, where necessary, based on the Texel, Marsen, and Arsløe approach for describing spectral saturation and limiting wave heights (Bouws et al. 1985).

Hourly wave information was obtained for Calumet Harbor for the 1991 to 1993 period, along with historic monthly mean records dating back to 1970. This information was combined with the wave data in either statistical or sequential (i.e., hourly) format as required.

Model Results

COSMOS-2D has been applied to determine the profile change at each of the profiles for several input combinations. The profile change predicted from the 2-D version of the model is based on cross-shore sediment transport gradients only; in other words, the influence of alongshore transport is not considered. Therefore, these results are representative of conditions of normal wave attack (i.e., no oblique waves) where the dominant driving force for profile change is cross-shore sediment transport. Storm wave conditions, particularly at high lake levels, result in the generation of a strong undertow (i.e., offshore-directed steady flow near the lake bed) in the surf zone. The undertow carries large amounts of sediment away from the beach, resulting in erosion. Outside the surf zone, the shoaling of large waves during storms produces onshore transport related to the asymmetry of the waves (i.e., where the onshore-directed orbital velocities are greater than the offshore-directed velocity component). Therefore, at a location in the outer part of the surf zone, there is a convergence of sediment transport which results in bar development. This process of beach erosion and bar development during storms is particularly applicable to medium to fine sand beaches and is described in further detail by Naim (1991).

In the COSMOS-2D tests of profile change, the presence of the underlying glacial till profile has been considered, but only as an erosion-resistant surface. Therefore, supply-limited conditions can arise where the lake bed is swept clean of sediment. Downcutting of the exposed till has not been calculated in these tests, as this process is more complex and requires consideration of three-dimensional sediment transport processes. Till downcutting is considered in the COSMOS-3D tests, to be included in a future report addressing downdrift effects in relation to longshore processes. The erosion-resistant surface in the model input also represents any seawall or revetment structures, where they exist.

The 2-D profile change tests were performed for each of the eleven profile lines. In each case, the input wave conditions represented the storm of 24 January 1992, which featured near-normal wave attack (see Appendix E for

more details). Based on total wave energy, a storm with the intensity of the 24 January 1992 storm is expected to occur about once per year. Four combinations of test runs were completed for each of the eleven profile lines corresponding to average (actual) and high lake level conditions (the latter with a lake level of 1.4 to 1.6 m above low water datum), and grain sizes of 0.2 mm and 2 mm. All of these tests are hypothetical and do not represent changes for any specific storm event. They have been completed to assess the influence of grain size and lake level on profile change characteristics.

The following discussion of the profile response (considering crossshore transport gradients only) provides some of the key observations of the 44 test results. The profile lines fall into two distinct groups: those which are not influenced (or only weakly influenced) by the presence of shore-parallel revetment and seawall structures (lines R8 to R12), and those which are strongly influenced by these structures (lines R14 to R23). The latter profiles do not feature a beach owing to the downcutting of the underlying glacial till that has resulted in deep water at the toe of the revetment or seawall. Examples of COSMOS-2D results are provided for a representative profile from each of the two groups.

The numerical model output for these tests consists of the initial profile shape, intermediate eroded profiles, the final profile, and the underlying fixed profile which represents either the glacial till or the shore protection structure (or both). Only the inner part of the profile is shown (i.e., where profile change is significant). In the beach fill area, the input profile shapes from May 1992 represent prefill conditions (beach nourishment was completed shortly after the May 1992 profiles were surveyed).

The result for line R9 given in Figure 26 is representative of the profile change that was predicted for the northerly group of profiles with the 0.2-mm grain size and an average water level. This grain size is representative of the fine sand conditions associated with beach fill derived from harbor dredging. The storm results in erosion of the upper beach, offshore migration of the inner bar by about 40 m, and a very slight offshore migration of the second bar. These changes result in exposure of the glacial till below the upper beach (where it exists) and possibly some burial of the till in the trough between the two bars. It appears that some till remains exposed in the large trough. The results of the high-water-level tests (Figure 27) show greater beach erosion, but otherwise similar patterns of change. A smaller section of the underlying glacial till is uncovered below the beach because the erosion has occurred in an area where the beach was initially quite thick.

The corresponding 2-mm test results for line R9 under average and high lake conditions are shown in Figures 28 and 29, respectively. This grain size is representative of the coarse sand and gravel beach nourishment that is imported from upland sources. As expected, there is much less profile change compared to the 0.2-mm results. The large bar is predicted to migrate inshore very slightly. For the average lake level test (Figure 28), an inshore bar becomes more pronounced through the convergence of offshore transport from

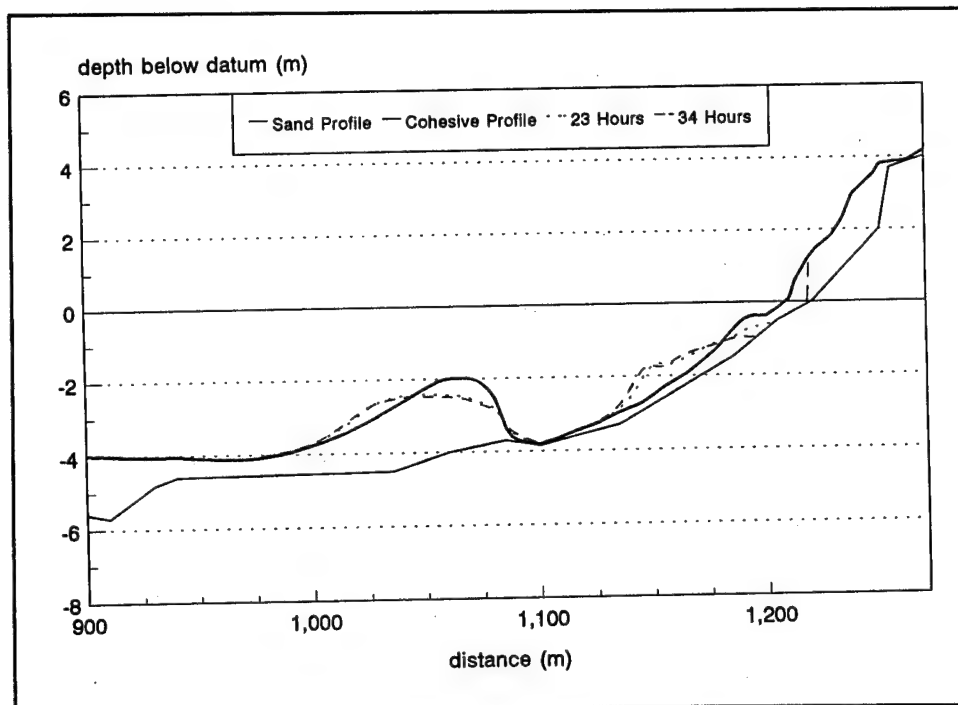


Figure 26. Profile change for R9 from the 24 January 1992 storm predicted for the 0.2-mm grain size and actual water level

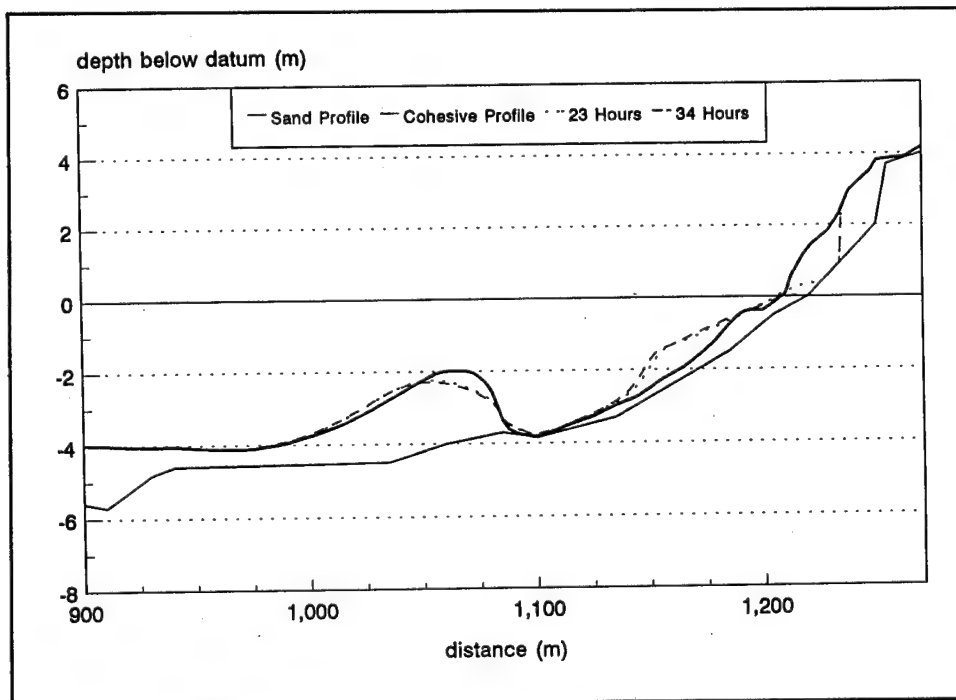


Figure 27. Profile change for R9 from the 24 January 1992 storm predicted for the 0.2-mm grain size and high water level. Shows greater beach erosion with similar change patterns

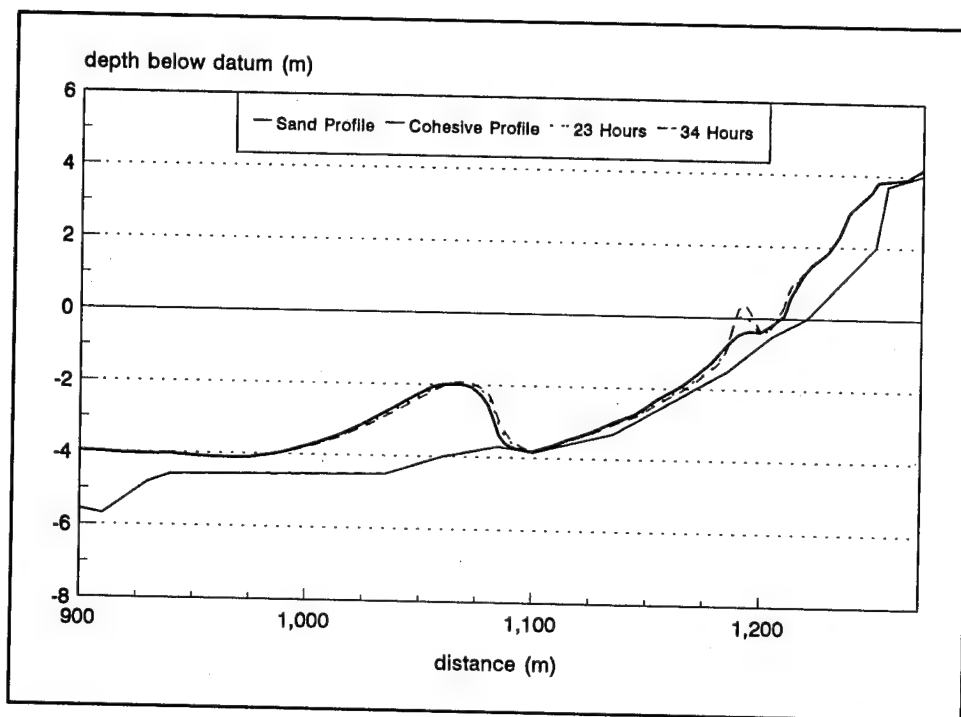


Figure 28. Profile change for R9 from the 24 January 1992 storm predicted for 2.0-mm grain size and actual water level

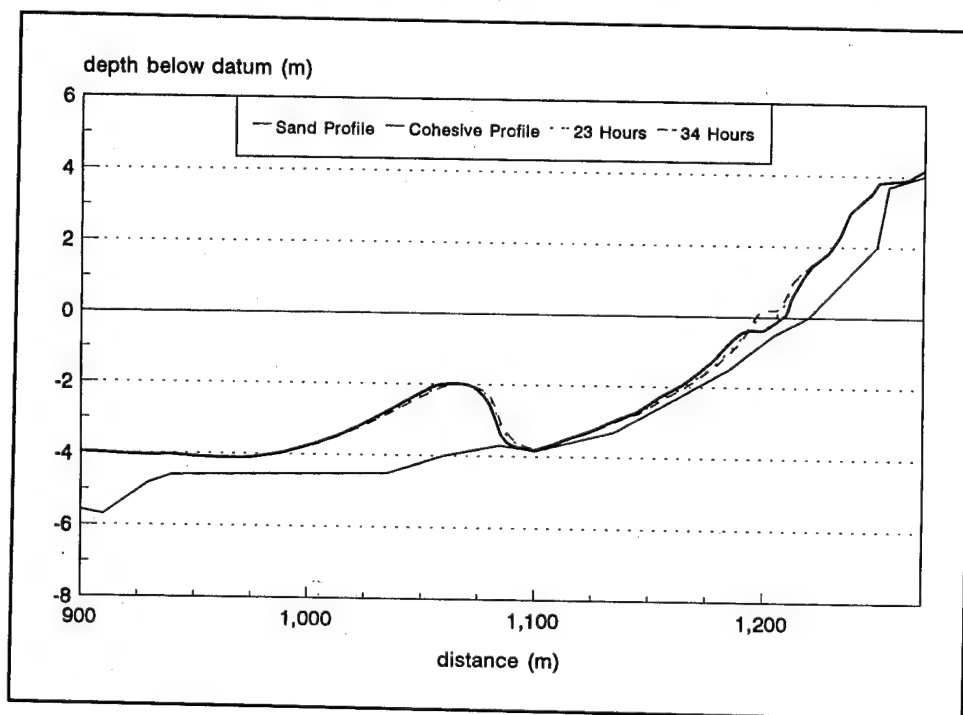


Figure 29. Profile change for R9 from the 24 January 1992 storm predicted for 2.0-mm grain size and high water level

the upper beach and onshore transport across the large trough. During the high lake level test, the small inner bar shifts inshore. With this coarse sediment, the underlying glacial till is not exposed (other than in the bottom of the main trough where the till was exposed at the beginning of the test).

Clearly, the 2-mm sediment is predicted to be more stable in the beach area during storm conditions, and therefore offers better protection to the underlying glacial till. Changes to the area of exposed till in the main trough were minimal in these 2-D cross-shore transport model tests. It is likely that changes in the large bar position (and the exposure of till in this area) are related to alongshore sediment transport gradients or to long-term adjustment of bar position in response to changing lake levels. Evidence of the latter possibility existed in each of the four test results discussed above, as there were small offshore or onshore shifts of the large bar. Over several storm events, these small changes may amount to significant changes in the position of the large bar (and the associated change in exposure of glacial till for this part of the profile).

The COSMOS-2D results for line R14 are representative of the group of profiles influenced by the seawall or revetment. The profile responses for the 0.2-mm sediment at average and high lake levels are given in Figures 30 and 31. The input profile features a small deposit at the base of the revetment with a crest height of just under 2 m and a very large bar deposit, also with a crest height of about 2 m below low water datum. It has been inferred from the GPR survey results that the till may be exposed in the trough between these two deposits as well as in the trough offshore of the large bar. For the average lake level tests, the numerical model predicted that the inner deposit would move away from the toe of the revetment. It is possible that this could lead to additional scour of the glacial till in the immediate vicinity of the revetment toe (if there is no scour protection pad in place). In contrast, the results of the average lake level test show some infilling of the trough between the two deposits which may be sufficient to form a protective cover over the till. The large bar migrates slightly offshore for both the average and high lake level tests, possibly burying (at least partly) a till exposure in the trough offshore of the large bar. The high lake level test features a similar response. This is due to the fact that a change in lake level has less influence on hydrodynamic conditions near the bed (and the associated sediment transport) in the deeper water offshore of the revetment than it does on a natural beach.

The findings of the 0.2-mm tests at line R14 (representing the revetment section of shoreline) indicate that cross-shore changes in lake bed morphology during storm events are probably not responsible for significant changes in the nature of glacial till exposures (with the possible exception of very local toe scour during extreme events - see Figures 30 and 31). Instead, the nature of the till exposures (i.e., location and extent) will vary with the cumulative impact of small cross-shore profile responses to changing lake levels, and to changes related to gradients in alongshore sediment transport.

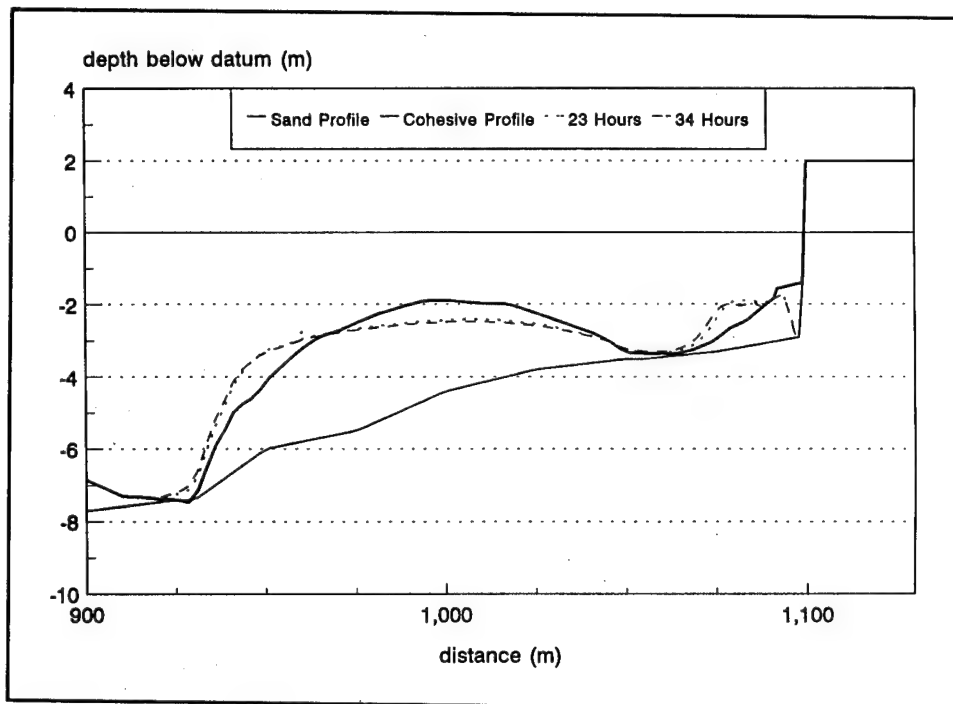


Figure 30. Profile change for R14 from the 24 January 1992 storm predicted for 0.2-mm grain size and actual water level

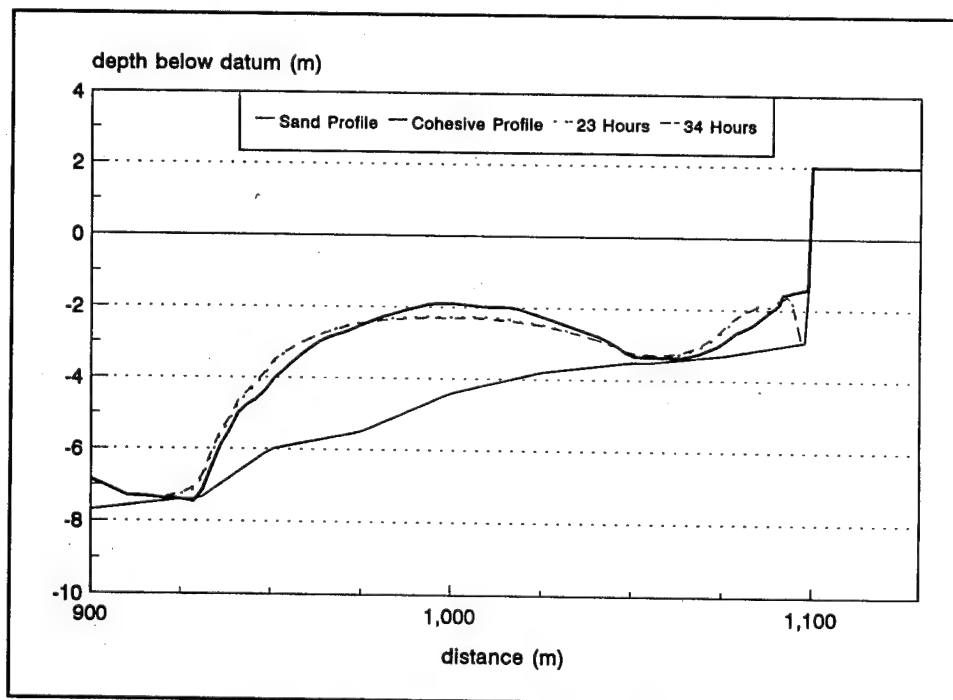


Figure 31. Profile change for R14 from the 24 January 1992 storm predicted for 0.2-mm grain size and high water level

The corresponding 2-mm test results for line R14 under average and high lake conditions are given in Figures 32 and 33, respectively. The profile responses for these two tests are very similar; the only significant change is at the toe of the revetment, where the 2-mm sediment is predicted to migrate onshore and form a small but pronounced bar. There are no significant changes in till exposure.

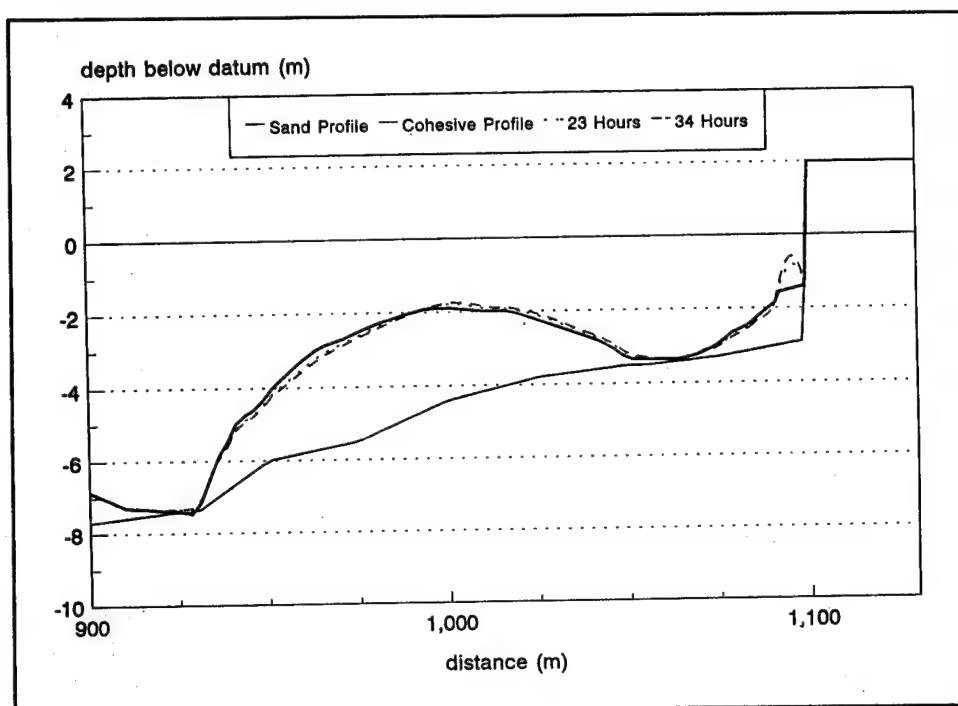


Figure 32. Profile change for R14 from the 24 January 1992 storm predicted for 2.0-mm grain size and actual water level

Therefore, for the deep profiles associated with the section of shoreline protection from lines R14 to R23, there is very little difference in the cross-shore profile response between the 0.2-mm and 2-mm grain sizes. As such, the 2-mm sediment does not provide substantially superior protection to the underlying till as found for the northerly group of more natural profiles (i.e., without shore protection). A possible exception to this finding is the local scour in the immediate vicinity of the toe of the revetment, which only occurred in the 0.2-mm tests. However, the presence of a toe scour pad would render this predicted exposure meaningless.

Summary of the Model Results

When compared to the 0.2-mm sediment, the 2-mm sediment provides much superior protection to the underlying till in the inner surf zone and beach area (i.e., above a depth of about 1 to 2 m). The corollary to this finding is that the 2-mm sediment does not appear to provide superior protection to the

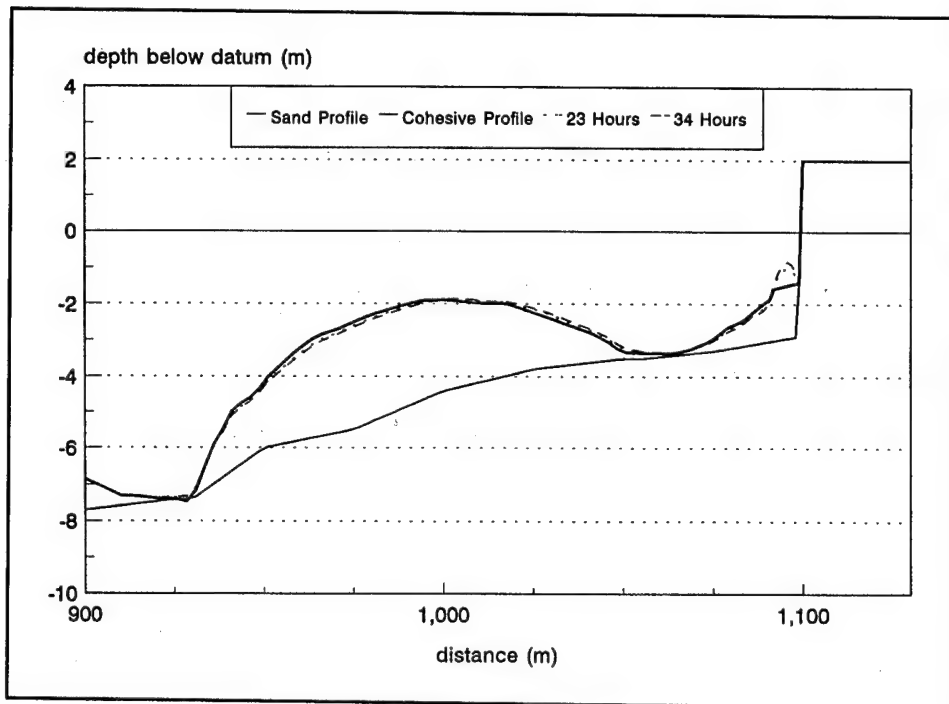


Figure 33. Profile change for R14 from the 24 January 1992 storm predicted for 2.0-mm grain size and high water level

section of the study shoreline where there is no beach (i.e., from lines R14 to R23, where the shoreline is protected by seawall and revetment). Changes in lake levels result in different parts of the glacial till under the upper beach being exposed. Changes to the location and extent of till exposures offshore of the inner surf zone (i.e., for depths greater than 1 to 2 m) must be a result of the cumulative impact of small changes related to storm and lake level cross-shore influences and/or due to changes to lake bed morphology related to alongshore sediment transport processes.

7 Summary and Conclusions

A cohesive sediment substratum such as that exhibited at St. Joseph plays a dominant role in the change of the shoreline shape. Underneath the mobile cohesionless beach deposits there exists a more erosion-resistant (yet erodible) surface which plays a deterministic role in how the shoreline responds to storms. Data obtained using GPR have verified the presence of the cohesive sub-bottom within the active nearshore at the St. Joseph project area. The data have also confirmed areas where the cohesive sub-bottom has become exposed to the erosive effects of waves. Further confirmation of this condition has been provided by visual inspection and actual sampling of the cohesive lake bed material.

Flume testing of the glacial till samples revealed that the material is erodible under certain conditions, with the darker-colored material being more resistant than the lighter-colored material. The tests indicate that there is very little difference between downcutting rates for sections of lake bed that are covered with coarse nourishment material versus fine sand material. The tests also showed that shear stresses due to wave action are capable of causing erosion of exposed till with or without the presence of sand for most wave conditions. Downcutting of this nature would only occur when the till is exposed or only thinly covered.

Cross-shore modeling using COSMOS-2D indicates that, when compared to 0.2-mm sediment, the 2-mm sediment provides much superior protection to the underlying till in the inner surf zone and beach area (i.e., above a depth of about 1 to 2 m). The corollary to this finding is that the 2-mm sediment does not appear to provide superior protection to the section of the study shoreline where there is no beach, with the possible exception of protecting against local scouring in the immediate vicinity of the toe of the large revetments. Local scouring was predicted in the model tests with the 0.2-mm sediment.

The underlying cohesive glacial till is not a completely erosion-resistant foundation. Where the material is exposed or covered by only a very thin layer of sand, downcutting is likely to occur during most wave conditions. Unlike unconsolidated sand and gravel, which may come and go under different energy regimes, fine-grained cohesive material, once eroded, cannot reconstitute itself and is removed from the beach system. The profile erosion that occurs during this process is permanent.

Cross-shore modeling of the St. Joseph study area has provided evidence that the till does become exposed during storms, and the till downcutting laboratory investigation confirmed that the till will erode when subjected to wave shear stresses, with or without the presence of sand or gravel. Changes in lake levels result in different parts of the glacial till under the upper beach being exposed. Changes to the location and extent of till exposures offshore of the inner surf zone must be a result of the cumulative impact of small changes related to storm and lake level cross-shore influences and/or due to changes to lake bed morphology related to alongshore sediment transport processes. Previous findings by Naim (1992) and Skafel and Bishop (1994) revealed that a covering of sand and/or gravel of only 2 to 5 cm would be enough to protect the till from erosion.

Erosion characteristics of cohesive shores are distinctively different when compared to sandy shores, a finding which has an impact on downdrift nourishment requirements. The analyses performed under this study suggest that the beach nourishment program at St. Joseph may provide at least partial protection to the underlying glacial till along and offshore of the feeder beach and the waterworks revetment section of shore. It is unclear whether the beach nourishment is having any negative or positive impact along the 3.5-km revetment section of shoreline south of the waterworks. Whether the beach nourishment is having any positive impact further south will be investigated in the next phase of this project.

Supplying downdrift areas with fill from a feeder beach is a complex process consisting of both cross-shore and longshore components. Because the longshore processes responsible for moving the fill from the feeder beach to locations downdrift of St. Joseph are not yet well understood, the longshore components will be addressed in a subsequent study. A comprehensive understanding of the amount of material being transported to the southern project limits is necessary for designing an effective nourishment program to provide protection to the vulnerable cohesive lake bed.

References

- Benton, S. E., and Passero, R. N. (1990). "Geology and aquifers in Berrien County, Michigan," Technical Report, Western Michigan University, Kalamazoo, MI.
- Birkemeier, W. A. (1980). "The effect of structures and lake level on bluff and shore erosion in Berrien County, Michigan 1970 - 1974," Miscellaneous Paper CERC-80-2, U.S. Army Engineer Waterways Experiment Station, Vicksburg, MS.
- _____. (1984). "A user's guide to ISRP: The interactive survey reduction program," Instruction Report CERC-84-1, U.S. Army Engineer Waterways Experiment Station, Vicksburg, MS.
- Bouws, E., Gunther, H., Rosenthal, W., and Vincent, C. L. (1985). "Similarity of wind wave spectrum in finite depth water; 1, Spectral form," *J. of Geophys. Res.* 90(C1), 975-986.
- Buckler, W. R. (1981). "Rates and implications of bluff recession along the Lake Michigan shore zone of Michigan and Wisconsin," unpublished Ph.D. diss., Michigan State University.
- Buckler, W. R., and Winters, H. A. (1983). "Lake Michigan bluff recession," *Annals American Association of Geographers* 73(1), 89-110.
- Byrnes, M. R. (1989). "SUPERDUCK Beach Sediment Sampling Experiment; Report 1, Data summary and initial results," Miscellaneous Paper CERC-89-18, U.S. Army Engineer Waterways Experiment Station, Vicksburg, MS.
- Chrzastowski, M. J., and Thompson, T. A. (1992). "Late Wisconsinan and Holocene coastal evolution of the southern shore of Lake Michigan," *Quaternary Coasts of the United States: Marine and Lacustrine Systems*, SEPM Special Publication No. 48, 397-413.
- Coakley, J. P., Rukavina, N. A., and Zeman, A. J. (1986). "Wave-induced subaqueous erosion of cohesive tills: Preliminary results," *Proc. of Cohesive Shores '86*. NRC Canada, 120-136.

- Coordinating Committee on Great Lakes Basic Hydraulic and Hydrologic Data. (1992). "IGLD 1985," brochure on the International Great Lakes Datum 1985, U.S. Government Printing Office, Washington, DC.
- Cornett, A., Sigouin, N., and Davies, M. (1994). "Erosive response of Northumberland Strait till and sedimentary rock to fluid flow," TR-1994-22, National Research Council Canada, Institute for Marine Dynamics.
- Folk, R. L. (1980). *Petrology of sedimentary rocks*. Hemphill Publishing Company, Austin, TX.
- Foster, D. S., Brill, A. L., Folger, D. W., Andrensen, C., Carroll, D. G., Fromm, G. L., and Seidel, D. R. (1992). "Preliminary results of a pilot study conducted between St. Joseph, Michigan and Michigan City, Indiana," Open File Report 92-348, U.S. Geologic Survey.
- Great Lakes Commission. (1986). "Water level changes: Factors influencing the Great Lakes," report prepared by Great Lakes Commission, Ann Arbor, MI.
- Hands, E. B. (1970). "A geomorphic map of Lake Michigan." *Proc. 13th Conf. on Great Lakes Res.*, Internat. Assoc. of Great Lakes Res.
- Hough, J. L. (1958). *Geology of the Great Lakes*. University of Illinois Press, Urbana, IL.
- Hubertz, J. M., Driver, D. B., and Reinhard, R. D. (1991). "Wave information studies of U.S. coastlines, hindcast wave information for the Great Lakes," WIS Report 22, U.S. Army Engineer Waterways Experiment Station, Vicksburg, MS.
- International Joint Commission. (1993). "Detailed study site Berrien County, Michigan," Working Committee 2, Potential Damages Task Group, Great Lakes Levels Reference Study Board.
- Kamphuis, J. W. (1987). "Recession rate of glacial till bluffs," *Journal of Waterway, Port, Coastal and Ocean Engineering*. American Society of Civil Engineers 113, 60-73.
- Kirby, J. T., and Dalrymple, R. A. (1983). "A parabolic equation for the combined refraction-diffraction of Stokes Waves by mildly varying topography," *Journal of Fluid Mechanics* 136, 57-96.
- Krumbein, W. C. (1934). "Size frequency distribution of sediments," *Journal of Sedimentary Petrology* 4, 65-77.
- _____. (1938). "Size frequency distribution of sediments and the normal phi curve," *Journal of Sedimentary Petrology* 18, 84-90.

- Lineback, J. A., and Meyer, R. P. (1974). "Glacial tills under Lake Michigan," Environmental Technical Notes 69, Illinois State Geological Survey, Urbana, IL.
- Lineback, J. A., Gross, D. L., and Meyer, R. P. (1972). "Geologic cross sections derived from seismic profiles and sediment cores from southern Lake Michigan," Environmental Geology Note 54, Illinois State Geological Survey, Urbana, IL.
- Lineback, J. A., Gross, D. L., Meyer, R. P., and Unger, W. L. (1971). "High-resolution seismic profiles and gravity cores from southern Lake Michigan," Environmental Geology Note 47, Illinois State Geological Survey, Urbana, IL.
- Meisburger, E. P., Williams, S. J., and Prins, D. A. (1979). "Sand resources of southeastern Lake Michigan," Miscellaneous Report No. 79-3, Coastal Engineering Research Center, U.S. Army Engineer Waterways Experiment Station, Vicksburg, MS.
- Michigan Department of Natural Resources, Division of Land Resource Programs. (1978). "Bluff recession rate study for Berrien County, Michigan."
- Nairn, R. B. (1991). "Problems associated with deterministic modelling of extreme beach erosion events." *Proc. of Coastal Sediments '91*, American Society of Civil Engineers, 588-602.
- _____. (1992). "Designing for cohesive shores." *Coastal Engineering in Canada*. Queens University, Kingston, Ontario.
- Nairn, R. B., and Southgate, H. N. (1993). "Deterministic profile modelling of nearshore processes; Part 2, Sediment transport and beach profile development," *Coastal Engineering* 19 Elsevier, Amsterdam, 57-96.
- Nairn, R. B., Pinchin, B. M., and Philpott, K. L. (1986). "A cohesive coast development model," *Proc. Symposium on Cohesive Shores*. National Research Council Canada, 246-261.
- Parson, L. E., and Smith, J. B. (1995). "Assessment of native beach characteristics for St. Joseph, Michigan-southeastern Lake Michigan," Miscellaneous Paper CERC-95-2, U.S. Army Engineer Waterways Experiment Station, Vicksburg, MS.
- Patrick Engineering. (1995). "Southwest Michigan - geotechnical investigation at eight sites," Contract Report for the U.S. Army Engineer District, Detroit.
- Raphael, C. N., and Kureth, J. C. (1988). "Bluff line recession and economic loss in coastal Berrien County, Michigan," Department of Geography and Geology, Eastern Michigan University, Ypsilanti, MI.

- Saylor, J. H., and Hands, E. B. (1970). "Properties of longshore bars in the Great Lakes." *Proceedings, 12th Conference on Great Lakes Research*. International Association of Great Lakes Research.
- Shore Protection Manual*. (1984). 4th ed., 2 Vol, U.S. Army Engineer Waterways Experiment Station, U.S. Government Printing Office, Washington, DC.
- Skafel, M. G., and Bishop, C. T. (1993). "Validity of wave predictions." *Canadian Coastal Conference, Vancouver*. Vol 1, 81-94.
- _____. (1994). "Flume experiments on the erosion of till shores by waves," *Coastal Engineering* 23, 329-348.
- Sommerfeld, B. G., Mason, J. M., Kraus, N. C., and Larson, M. (1994). "BFM: Beach Fill Module; Report 1, Beach morphology analysis package (BMAP) - user's guide," Instruction Report CERC-94-1, U.S. Army Engineer Waterways Experiment Station, Vicksburg, MS.
- Southgate, H. N., and Naim, R. B. (1993). "Deterministic profile modelling of nearshore processes; Part 1, waves and currents," *Coastal Engineering* 19, 27-56.
- Stauble, D. K. (1988). "Beach nourishment monitoring, a necessity to project design," *Proceedings: Beach Preservation Technology* 88. Florida Shore and Beach Preservation Association.
- _____. (1991). "Recommended physical data collection program for beach nourishment projects," Coastal Engineering Technical Note CETN II-26, U.S. Army Engineer Waterways Experiment Station, Vicksburg, MS.
- _____. (1992). "Long-term profile and sediment morphodynamics: Field Research Facility case history," Technical Report CERC-92-7, U.S. Army Engineer Waterways Experiment Station, Vicksburg, MS.
- Stauble, D. K., Holem, G. W., Byrnes, M. R., Anders, F. J., and Meisburger, E. (1993). "SUPERDUCK beach sediment sample experiment: Beach profile change and foreshore sediment dynamics," Technical Report CERC-93-4, U.S. Army Engineer Waterways Experiment Station, Vicksburg, MS.
- Underwood, S. (1988). "Sonicsifting: A fast and efficient method for sand size analysis," Coastal Engineering Technical Note II-14, U.S. Army Engineer Waterways Experiment Station, Vicksburg, MS.
- U.S. Army Engineer District, Detroit. (1973). "Section 111 detailed project report on shore damage at St. Joseph Harbor, Michigan," Detroit, MI.

U.S. Army Engineer District, Detroit. (1977). "Operation and maintenance manual for Section 111 beach nourishment at St. Joseph, Michigan," Detroit, MI.

Wentworth, C. K. (1922). "A scale and class terms for clastic sediments," *Journal of Geology* 30, 377-92.

W. F. Baird & Assoc. (1995). "Effectiveness of beach nourishment on cohesive shores - St. Joseph, MI," Contract Final Report prepared for Coastal Engineering Research Center, U.S. Army Engineer Waterways Experiment Station, Vicksburg, MS.

Appendix A

Geotechnical Analysis of Glacial Till

Appendix A contains a detailed geotechnical analysis of the glacial till cohesive lake bed material. The samples tested were collected at site R-17 in July 1993. The geotechnical analysis was performed by the U.S. Army Engineer Division, Ohio River. The tests performed included:

- a.* Pre-consolidation shear strength.
- b.* Grain size analysis.
- c.* Void ratio.
- d.* Porosity.
- e.* Moisture content.
- f.* Atterberg limit.
- g.* Permeability.
- h.* Pin hole erosion test.
- i.* Detailed x-ray scan.

X-RAY DIFFRACTION ANALYSIS	OHIO RIVER DIVISION LABORATORY 11275 SEBRING DRIVE CINCINNATI, OHIO 45240		
SOURCE: St. Joseph's, MI			
MATERIAL: Sediment		DATE: 10 September 1993	
PROJECT: St. Joseph's, MI		LAB SPL NO. N/A	
DISTRICT: CEWES-CD-SG		LAB JOB NO. 2/9326X.C166	

INTRODUCTION

Two samples of sediment from the St. Joseph's, MI Project were submitted to CEORDL by the Waterways Experiment Station for X-ray Diffraction analysis. Additional testing by the Materials Section was provided under separate cover.

METHODOLOGY

Both samples were ground to approximately 45 microns using a mortar and pestle. The resultant fractions were dispersed in 200 mL of distilled water and placed in an ultrasonic water bath for 12 minutes to disaggregate the particles. Each sample was allowed to settle, from which then an aliquot was suspended on a substrate and dried overnight (approximately 8 hours). X-ray analysis was then performed on these samples.

In order to identify the clay minerals present, further treatments were necessary. These included: 1) placing the samples in an ethylene glycol atmosphere overnight at room temperature and, 2) heating the samples at 550 degrees Centigrade for 2 hours, followed by room temperature cooling. All samples were then X-rayed after each of the above treatments.

The qualitative mineralogy of the <2 micron clay-size fraction as determined by X-ray diffraction analysis is summarized below.

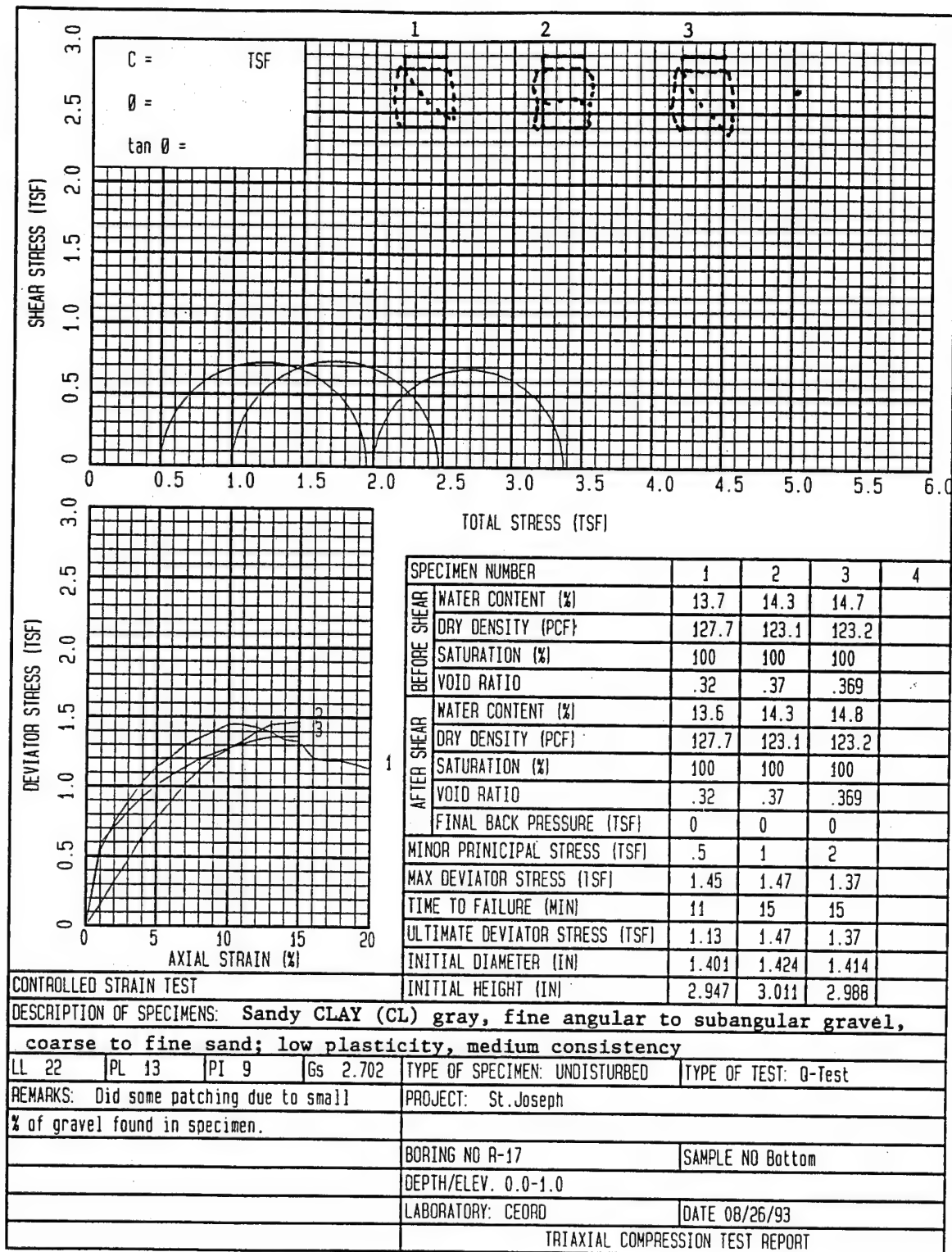
TEST RESULTS

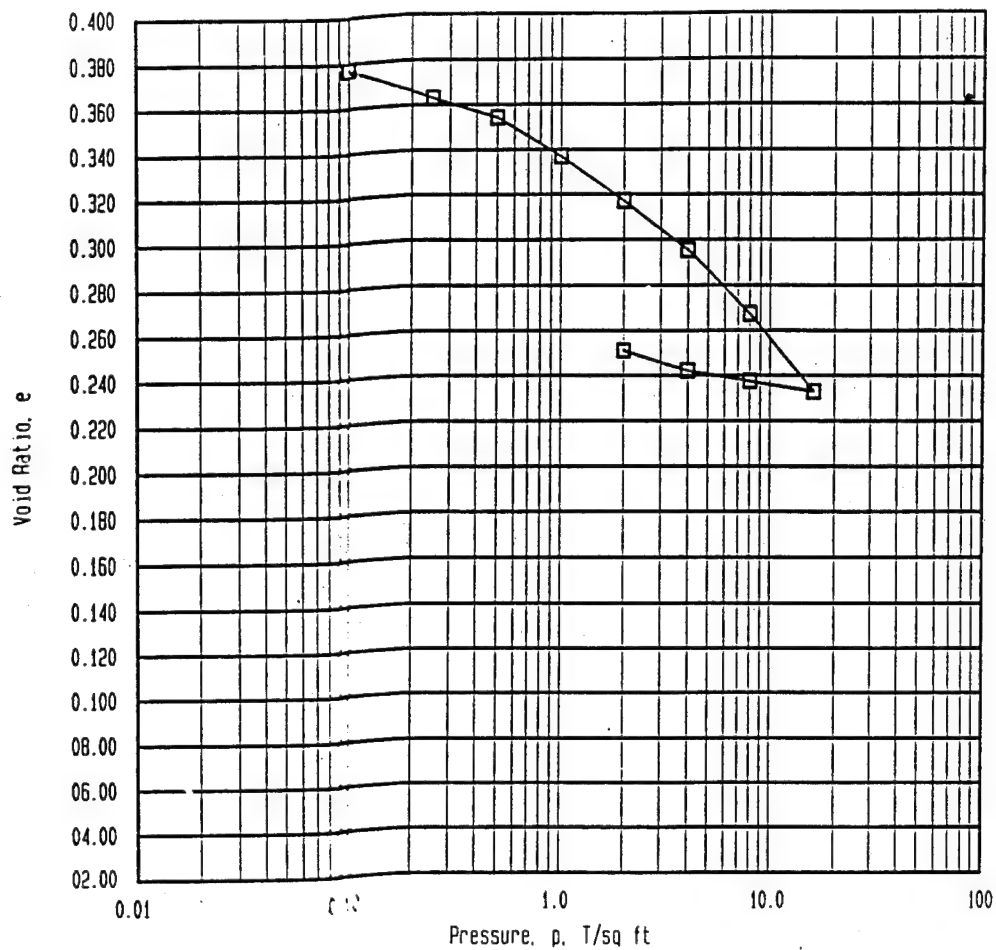
SAMPLE	COMPOSITION			
	MAJOR	MODERATE	MINOR	TRACE
R-17/Top	Illite	Chlorite*		Kaolinite
R-17/Bottom	Illite	Chlorite*	Kaolinite	

*Chlorite is high-iron variety

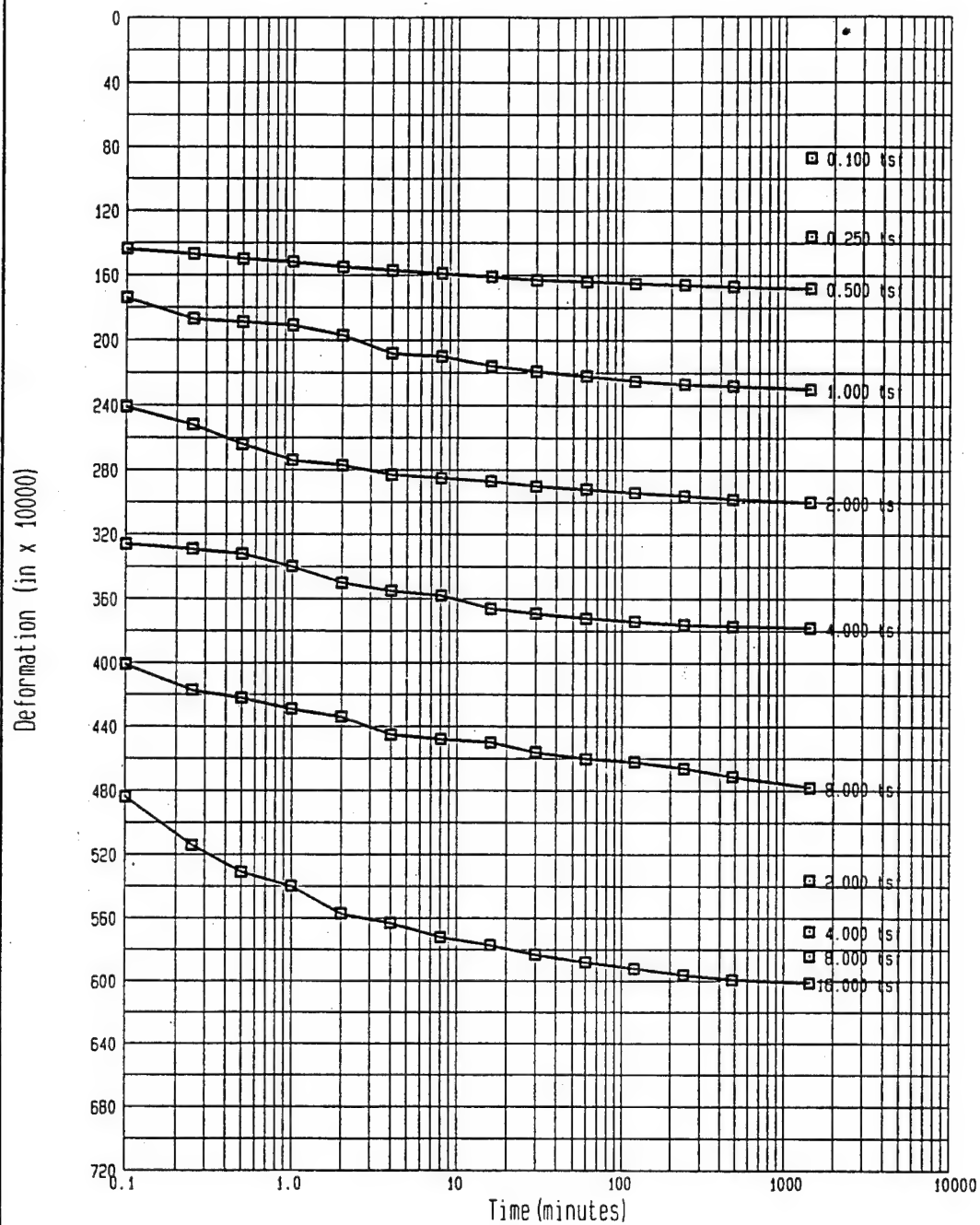


E. Frances Robinson
Chief, Geology Section





Type of Specimen Undisturbed		Before Test		After Test	
Dia. 2.5 in.	ht .5 in.	Water Content, w_0	15.3 %	w_f	12.1 %
Overburden Pressure, P_o T/sq ft		Void Ratio, e_0	.4	e_f	.25
Preconsol. Pressure, P_c T/sq ft		Saturation, S_0	100 %	S_f	100 %
Compression Index, C_c .11		Dry Density	120.3 pcf		134.8 pcf
Classification Sandy CLAY (CL)		k_{20} at e_0			
LL 22	Gs 2.703	Project St. Joseph MI			
PL 13	D ₁₀				
Remarks: Did some patching due to		Area:			
small % of gravel.		Boring No. R-17	Sample No. Bottom		
Page 1 of 2		Depth 0'-1'	Date 09-02-93		
CONSOLIDATION TEST REPORT					



Project St. Joseph MI

Area

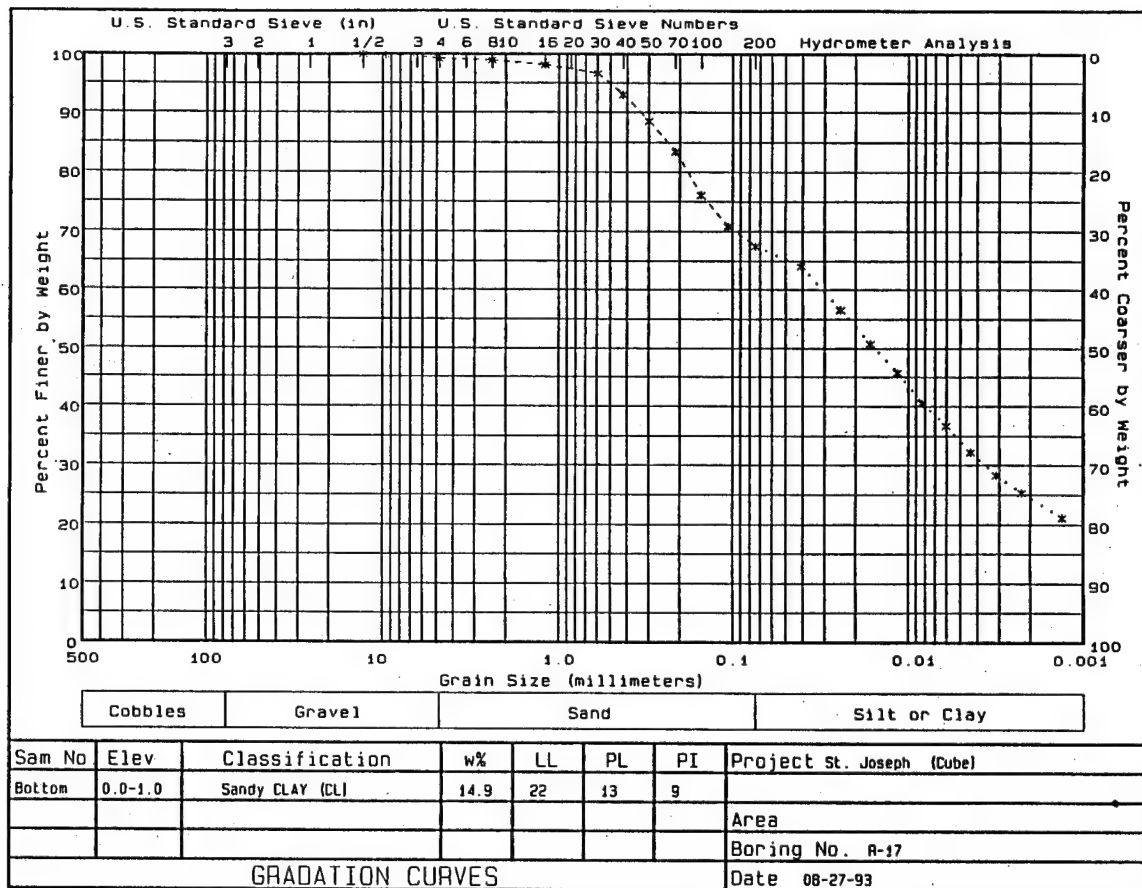
Boring No. R-17

Sample No. Bottom

Depth 0'-1'

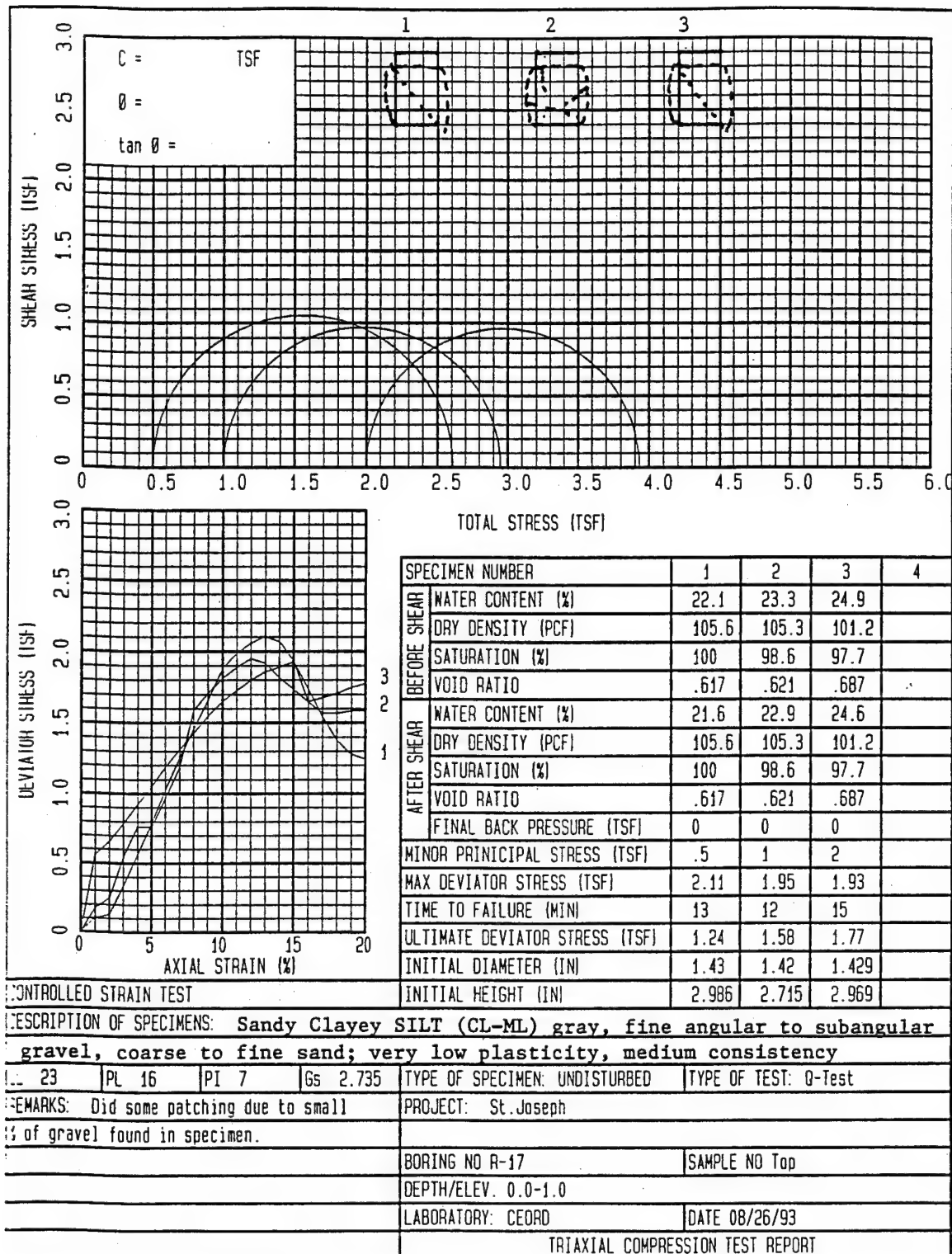
Date 09-02-1993

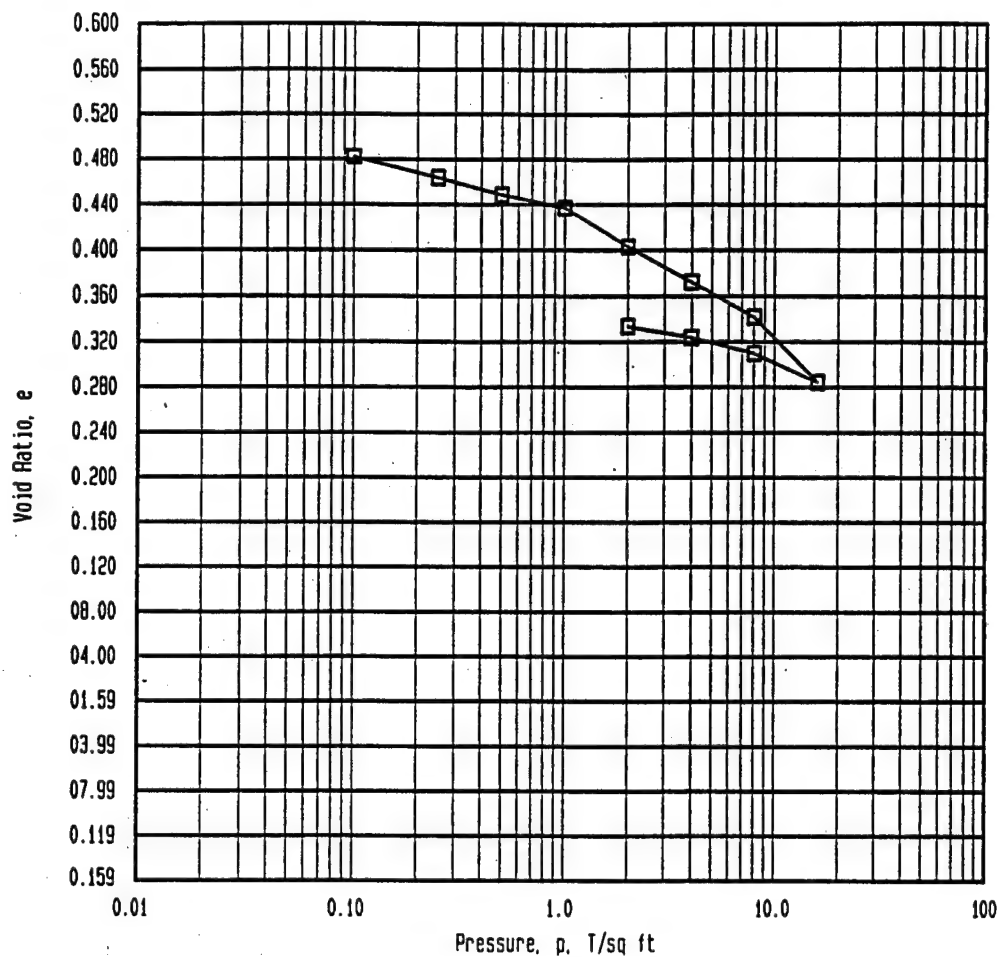
CONSOLIDATION TEST - TIME CURVES



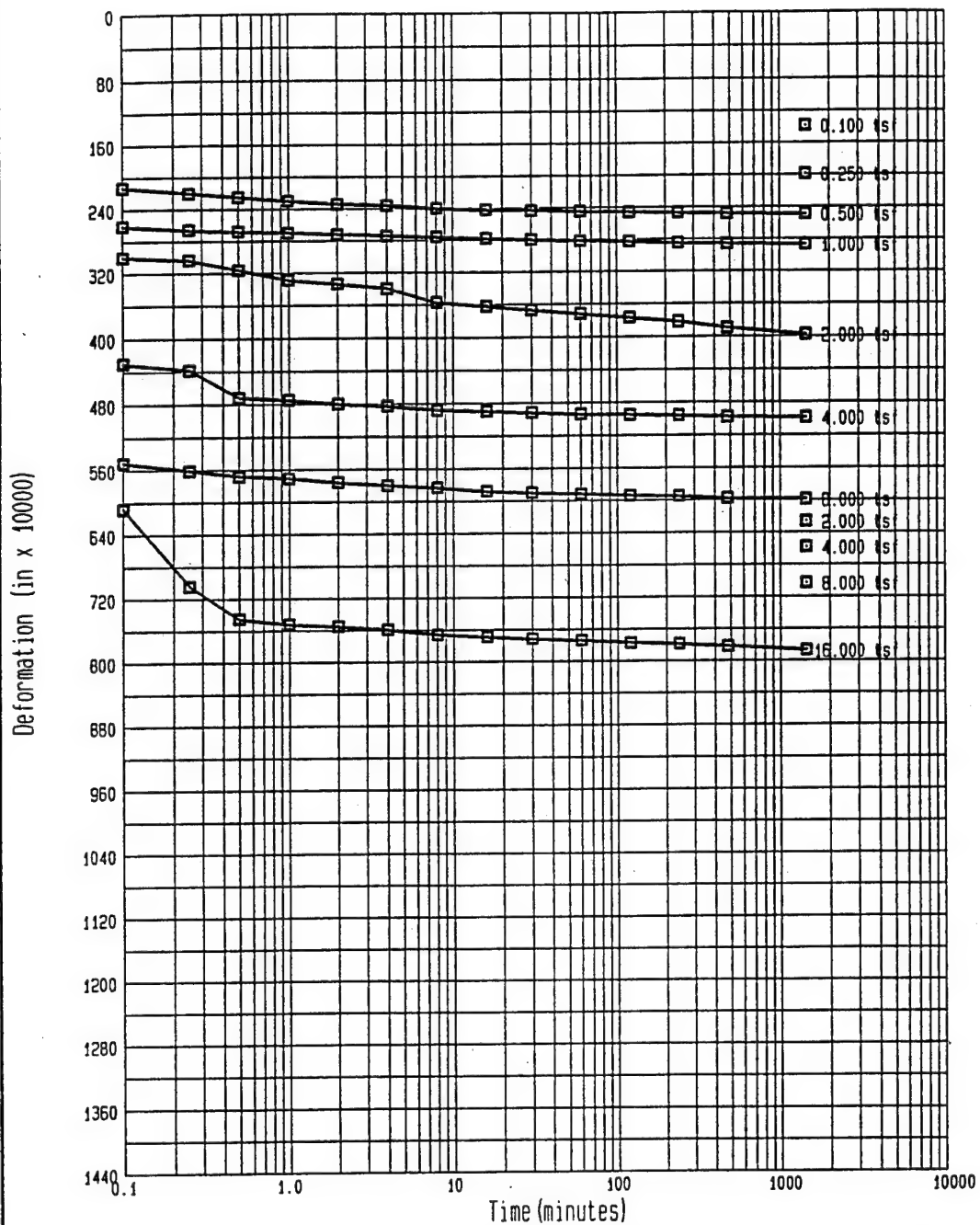
Ohio River Division Laboratories - Soils Laboratory

[illegible]





Type of Specimen Undisturbed		Before Test		After Test	
Dia. 2.5 in.	ht .5 in.	Water Content, w_0	20.3 %	w_f	17.2 %
Overburden Pressure, P_o T/sq ft		Void Ratio, e_0	.523	e_f	.333
Preconsol. Pressure, P_c T/sq ft		Saturation, S_0	100 %	S_f	100 %
Compression Index, C_c .18		Dry Density	111.9 pcf		127.9 pcf
Classification Sandy Clayey SILT		k_{20} at e_0			
LL 23	Gs 2.735	Project St. Joseph MI			
PL 16	D_{10}				
Remarks: Did some patching due to		Area:			
small % of gravel.		Boring No. R-17		Sample No. Top	
Page 1 of 2		Depth 0'-1'		Date 08-31-93	
		CONSOLIDATION TEST REPORT			



Project St. Joseph MI

Area

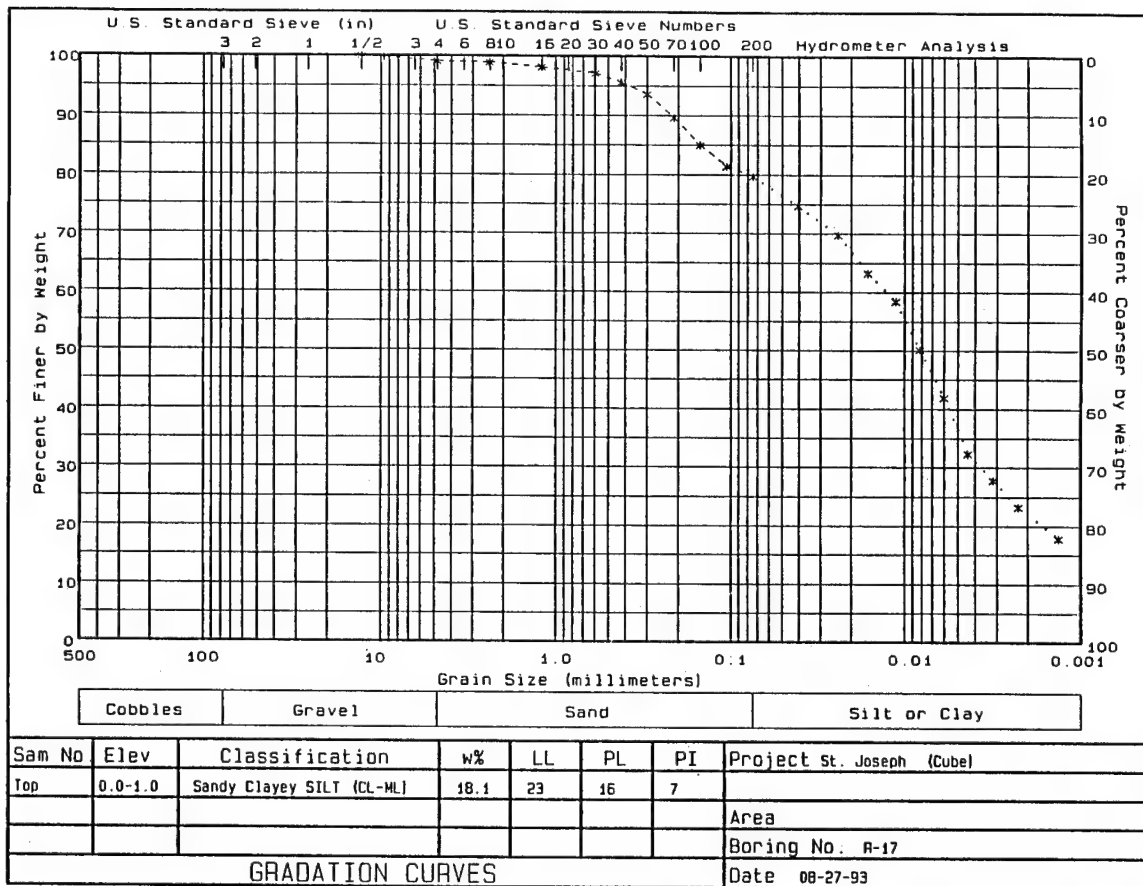
Boring No. R-17

Sample No. Top

Depth 0'-1'

Date 08-31-1993

CONSOLIDATION TEST - TIME CURVES



Appendix B

Calculation of Shear Stress for Test Sequences Used in the Flume Investigation

Appendix B contains the calculations of shear stress for the individual test sequences used in Chapter 5. The shear stress exerted on the bed by the unidirectional flow of fluid was determined indirectly by measuring the vertical profile of velocity just above the bed. In most situations, velocities were measured at six elevations within 2 cm of the bed. Velocity was measured using a laser doppler velocitometer (LDV) system. In steady turbulent flow over a relatively smooth surface, the vertical distribution of velocity normal to the boundary was found to satisfy a logarithmic profile. The depth-averaged flow velocities ranged between 0.5 m/s and 3 m/s in the various test sequences.

Figure 1 is a scatter plot showing the velocity profile of a turbulent flow. The vertical axis is labeled 'velocity (m/s)' and ranges from 0 to 0.8. The horizontal axis is labeled 'ln(y) (m)' and ranges from -10 to -5. The data points are represented by solid squares, and a dashed line indicates a linear fit to the data. The velocity increases linearly with ln(y) in the logarithmic region.

ln(y) (m)	velocity (m/s)
-8.5	0.38
-6.5	0.45
-5.5	0.53
-4.8	0.59
-3.8	0.70
-3.5	0.73
-3.2	0.73

Figure 1 is a scatter plot showing the relationship between velocity (m/s) and $\ln(y)$ (m) for a turbulent flow. The y-axis represents velocity in m/s, ranging from 0 to 1.2 with increments of 0.2. The x-axis represents $\ln(y)$ in meters, ranging from -10 to -5 with increments of 5. There are six data points plotted as solid squares. A dashed line represents a linear fit to these points, showing a positive linear correlation between $\ln(y)$ and velocity in the logarithmic region.

$\ln(y)$ (m)	velocity (m/s)
-7.5	0.62
-6.2	0.82
-5.5	0.88
-4.2	1.08
-3.8	1.12
-3.5	1.15

Figure 1 is a scatter plot showing the relationship between velocity (m/s) and $\ln(y)$ (m). The y-axis is labeled 'velocity (m/s)' and ranges from 0 to 2.0. The x-axis is labeled ' $\ln(y)$ (m)' and ranges from -10 to -5. There are seven data points plotted as solid squares. A dashed line represents a linear fit to these points, showing a positive correlation between $\ln(y)$ and velocity.

$\ln(y)$ (m)	velocity (m/s)
-8.5	0.9
-6.5	1.1
-6.0	1.25
-4.5	1.5
-4.0	1.65
-3.8	1.7
-3.5	1.7

Figure 1 is a scatter plot showing the relationship between velocity (m/s) and $\ln(y)$ (m) for the flow of water over a sand bed. The x-axis is labeled $\ln(y) \text{ (m)}$ and ranges from -10 to -5. The y-axis is labeled velocity (m/s) and ranges from 0 to 2.5. There are six data points plotted as solid squares, and a dashed line represents a linear fit to these points.

$\ln(y) \text{ (m)}$	velocity (m/s)
-8.5	1.25
-6.5	1.55
-5.5	1.75
-4.5	1.95
-3.5	2.25
-3.2	2.35

Date:		1/9/94			
Sample		2 = Coarse sand erosion			
Location of profile		above sample			
Depth		cm			
Slope					
Fluid characteristics:			density:		1000 kg/m ³
			kinematic viscosity:		1.14E-06 m ² /s
			ln(y)	u	u(from a,b)
z	u	y	lny_data	u_data	u_pred
1.228	0.157	0.0005	-7.600902	0.157	0.1687022
1.2315	0.2716	0.004	-5.521461	0.2716	0.2518595
1.2347	0.2909	0.0072	-4.933674	0.2909	0.2753652
1.2425	0.287	0.015	-4.199705	0.287	0.3047167
1.2545	0.3196	0.027	-3.611918	0.3196	0.3282224
1.2682	0.3474	0.0407	-3.201527	0.3474	0.344634
z0 =	1.2275	m			
r^2=	0.7705434				
a=	0.0399902				
b=	0.4726637				
b'=	0.4726636				
u*a=	0.0159961	m/s			
u*b=	0.0160844	m/s			
difference:	8.834E-05	m/s			
u* average	0.0160402	m/s			
Bed Shear	0.2572894	Pa			

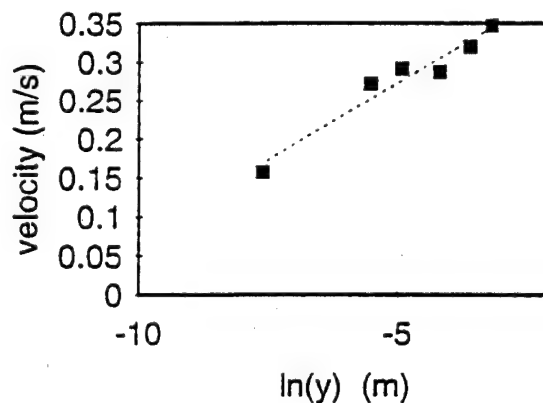


Figure 1 is a scatter plot showing the velocity profile of a turbulent flow. The vertical axis is labeled 'velocity (m/s)' and ranges from 0 to 0.5. The horizontal axis is labeled 'ln(y) (m)' and ranges from -10 to -5. The data points are represented by solid squares, and a dashed line indicates a linear fit to the data. The velocity increases linearly with ln(y) in the logarithmic region.

$\ln(y) \text{ (m)}$	velocity (m/s)
-5.5	0.58
-5.2	0.62
-4.9	0.66
-4.6	0.70
-4.3	0.74
-4.0	0.78
-3.7	0.82

Date:		6/9/94			
Sample		2 =Fine sand erosion (low velocity)			
Location of profile		above sample			
Depth		cm			
Slope					
Fluid characteristics:		density:		1000	kg/m ³
		kinematic viscosity:		1.14E-06	m ² /s
			ln(y)	u	u(from a,b)
z	u	y	lny_data	u_data	u_pred
1.228	0.5006	0.004	-5.521461	0.5006	0.5112787
1.2316	0.5553	0.0076	-4.879607	0.5553	0.5568649
1.2349	0.587	0.0109	-4.518992	0.587	0.5824766
1.2428	0.6461	0.0188	-3.973898	0.6461	0.6211906
1.2544	0.6573	0.0304	-3.493313	0.6573	0.6553231
1.2683	0.6629	0.0443	-3.116771	0.6629	0.6820661
z0 =	1.224	m			
r^2=	0.9196516				
a=	0.0710226				
b=	0.9034272				
b'=	0.9034271				
u*a=	0.028409	m/s			
u*b=	0.0292543	m/s			
difference:	0.0008452	m/s			
u* average	0.0288317	m/s			
Bed Shear	0.8312643	Pa			

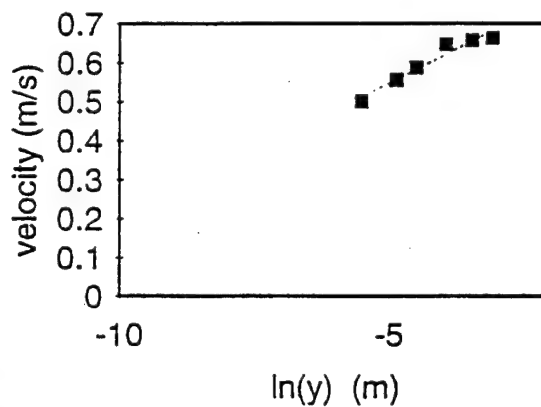


Figure 1 is a scatter plot showing the velocity profile of a turbulent flow. The vertical axis is labeled "velocity (m/s)" and ranges from 0 to 1.2 with major ticks every 0.2. The horizontal axis is labeled "ln(y) (m)" and ranges from -10 to -5 with major ticks at -10 and -5. There are six data points plotted as solid black squares. A dashed line represents a linear fit to these points. The data points are approximately at the following coordinates (ln(y), velocity): (-6.2, 0.78), (-5.8, 0.88), (-5.4, 0.95), (-5.1, 1.02), (-4.8, 1.05), and (-4.5, 1.12).

Appendix C

Raw Depth Data From Flume Study

Raw data, consisting of the individual point measurements, are presented here. To monitor erosion, the upper surface of the samples was measured at regular intervals using an analog point gauge with an accuracy of 0.025 mm. The gauge used to collect the measurements was rigidly supported by the flume side-walls and accurately positioned using a set of calibrated guide marks. About 28 soundings were made across each sample surface to determine average erosion. For both of the samples, the sounding depths for the light and dark gray sediments were segregated prior to determining average erosion or downcutting rates owing to the difference in erosion resistance between the two different-colored sediments.

H. JOSEPH MICRODRILL									
Series Profiles - Sample 2 (compare and find good sample)									
After 10 tests									
	A	B	C	D	E	F	G	H	I
1	1.899	1.854	1.861	1.861	1.873	1.883	1.893	1.903	1.913
2	1.899	1.854	1.861	1.861	1.873	1.883	1.893	1.903	1.913
3	1.899	1.854	1.861	1.861	1.873	1.883	1.893	1.903	1.913
4	1.899	1.854	1.861	1.861	1.873	1.883	1.893	1.903	1.913
5	1.899	1.854	1.861	1.861	1.873	1.883	1.893	1.903	1.913
6	1.899	1.854	1.861	1.861	1.873	1.883	1.893	1.903	1.913
7	1.899	1.854	1.861	1.861	1.873	1.883	1.893	1.903	1.913
8	1.899	1.854	1.861	1.861	1.873	1.883	1.893	1.903	1.913
9	1.899	1.854	1.861	1.861	1.873	1.883	1.893	1.903	1.913
10	1.899	1.854	1.861	1.861	1.873	1.883	1.893	1.903	1.913
11	1.899	1.854	1.861	1.861	1.873	1.883	1.893	1.903	1.913
12	1.899	1.854	1.861	1.861	1.873	1.883	1.893	1.903	1.913
13	1.899	1.854	1.861	1.861	1.873	1.883	1.893	1.903	1.913
14	1.899	1.854	1.861	1.861	1.873	1.883	1.893	1.903	1.913
15	1.899	1.854	1.861	1.861	1.873	1.883	1.893	1.903	1.913
16	1.899	1.854	1.861	1.861	1.873	1.883	1.893	1.903	1.913
17	1.899	1.854	1.861	1.861	1.873	1.883	1.893	1.903	1.913
18	1.899	1.854	1.861	1.861	1.873	1.883	1.893	1.903	1.913
19	1.899	1.854	1.861	1.861	1.873	1.883	1.893	1.903	1.913
20	1.899	1.854	1.861	1.861	1.873	1.883	1.893	1.903	1.913
21	1.899	1.854	1.861	1.861	1.873	1.883	1.893	1.903	1.913
22	1.899	1.854	1.861	1.861	1.873	1.883	1.893	1.903	1.913
23	1.899	1.854	1.861	1.861	1.873	1.883	1.893	1.903	1.913
24	1.899	1.854	1.861	1.861	1.873	1.883	1.893	1.903	1.913
25	1.899	1.854	1.861	1.861	1.873	1.883	1.893	1.903	1.913
26	1.899	1.854	1.861	1.861	1.873	1.883	1.893	1.903	1.913
27	1.899	1.854	1.861	1.861	1.873	1.883	1.893	1.903	1.913
28	1.899	1.854	1.861	1.861	1.873	1.883	1.893	1.903	1.913
29	1.899	1.854	1.861	1.861	1.873	1.883	1.893	1.903	1.913
30	1.899	1.854	1.861	1.861	1.873	1.883	1.893	1.903	1.913
31	1.899	1.854	1.861	1.861	1.873	1.883	1.893	1.903	1.913
32	1.899	1.854	1.861	1.861	1.873	1.883	1.893	1.903	1.913
33	1.899	1.854	1.861	1.861	1.873	1.883	1.893	1.903	1.913
34	1.899	1.854	1.861	1.861	1.873	1.883	1.893	1.903	1.913
35	1.899	1.854	1.861	1.861	1.873	1.883	1.893	1.903	1.913
36	1.899	1.854	1.861	1.861	1.873	1.883	1.893	1.903	1.913
37	1.899	1.854	1.861	1.861	1.873	1.883	1.893	1.903	1.913
38	1.899	1.854	1.861	1.861	1.873	1.883	1.893	1.903	1.913
39	1.899	1.854	1.861	1.861	1.873	1.883	1.893	1.903	1.913
40	1.899	1.854	1.861	1.861	1.873	1.883	1.893	1.903	1.913
41	1.899	1.854	1.861	1.861	1.873	1.883	1.893	1.903	1.913
42	1.899	1.854	1.861	1.861	1.873	1.883	1.893	1.903	1.913
43	1.899	1.854	1.861	1.861	1.873	1.883	1.893	1.903	1.913
44	1.899	1.854	1.861	1.861	1.873	1.883	1.893	1.903	1.913
45	1.899	1.854	1.861	1.861	1.873	1.883	1.893	1.903	1.913
46	1.899	1.854	1.861	1.861	1.873	1.883	1.893	1.903	1.913
47	1.899	1.854	1.861	1.861	1.873	1.883	1.893	1.903	1.913
48	1.899	1.854	1.861	1.861	1.873	1.883	1.893	1.903	1.913
49	1.899	1.854	1.861	1.861	1.873	1.883	1.893	1.903	1.913
50	1.899	1.854	1.861	1.861	1.873	1.883	1.893	1.903	1.913
51	1.899	1.854	1.861	1.861	1.873	1.883	1.893	1.903	1.913
52	1.899	1.854	1.861	1.861	1.873	1.883	1.893	1.903	1.913
53	1.899	1.854	1.861	1.861	1.873	1.883	1.893	1.903	1.913
54	1.899	1.854	1.861	1.861	1.873	1.883	1.893	1.903	1.913
55	1.899	1.854	1.861	1.861	1.873	1.883	1.893	1.903	1.913
56	1.899	1.854	1.861	1.861	1.873	1.883	1.893	1.903	1.913
57	1.899	1.854	1.861	1.861	1.873	1.883	1.893	1.903	1.913
58	1.899	1.854	1.861	1.861	1.873	1.883	1.893	1.903	1.913
59	1.899	1.854	1.861	1.861	1.873	1.883	1.893	1.903	1.913
60	1.899	1.854	1.861	1.861	1.873	1.883	1.893	1.903	1.913
61	1.899	1.854	1.861	1.861	1.873	1.883	1.893	1.903	1.913
62	1.899	1.854	1.861	1.861	1.873	1.883	1.893	1.903	1.913
63	1.899	1.854	1.861	1.861	1.873	1.883	1.893	1.903	1.913
64	1.899	1.854	1.861	1.861	1.873	1.883	1.893	1.903	1.913
65	1.899	1.854	1.861	1.861	1.873	1.883	1.893	1.903	1.913
66	1.899	1.854	1.861	1.861	1.873	1.883	1.893	1.903	1.913
67	1.899	1.854	1.861	1.861	1.873	1.883	1.893	1.903	1.913
68	1.899	1.854	1.861	1.861	1.873	1.883	1.893	1.903	1.913
69	1.899	1.854	1.861	1.861	1.873	1.883	1.893	1.903	1.913
70	1.899	1.854	1.861	1.861	1.873	1.883	1.893	1.903	1.913
71	1.899	1.854	1.861	1.861	1.873	1.883	1.893	1.903	1.913
72	1.899	1.854	1.861	1.861	1.873	1.883	1.893	1.903	1.913
73	1.899	1.854	1.861	1.861	1.873	1.883	1.893	1.903	1.913
74	1.899	1.854	1.861	1.861	1.873	1.883	1.893	1.903	1.913
75	1.899	1.854	1.861	1.861	1.873	1.883	1.893	1.903	1.913
76	1.899	1.854	1.861	1.861	1.873	1.883	1.893	1.903	1.913
77	1.899	1.854	1.861	1.861	1.873	1.883	1.893	1.903	1.913
78	1.899	1.854	1.861	1.861	1.873	1.883	1.893	1.903	1.913
79	1.899	1.854	1.861	1.861	1.873	1.883	1.893	1.903	1.913
80	1.899	1.854	1.861	1.861	1.873	1.883	1.893	1.903	1.913
81	1.899	1.854	1.861	1.861	1.873	1.883	1.893	1.903	1.913
82	1.899	1.854	1.861	1.861	1.873	1.883	1.893	1.903	1.913
83	1.899	1.854	1.861	1.861	1.873	1.883	1.893	1.903	1.913
84	1.899	1.854	1.861	1.861	1.873	1.883	1.893	1.903	1.913
85	1.899	1.854	1.861	1.861	1.873	1.883	1.893	1.903	1.913
86	1.899	1.854	1.861	1.861	1.873	1.883	1.893	1.903	1.913
87	1.899	1.854	1.861	1.861	1.873	1.883	1.893	1.903	1.913
88	1.899	1.854	1.861	1.861	1.873	1.883	1.893	1.903	1.913
89	1.899	1.854	1.861	1.861	1.873	1.883	1.893	1.903	1.913
90	1.899	1.854	1.861	1.861	1.873	1.883	1.893	1.903	1.913
91	1.899	1.854	1.861	1.861	1.873	1.883	1.893	1.903	1.913
92	1.899	1.854	1.861	1.861	1.873	1.883	1.893	1.903	1.913
93	1.899	1.854	1.861	1.861	1.873	1.883	1.893	1.903	1.913
94	1.899	1.854	1.861	1.861	1.873	1.883	1.893	1.903	1.913
95	1.899	1.854	1.861	1.861	1.873	1.883	1.893	1.903	1.913
96	1.899	1.854	1.861	1.861	1.873	1.883	1.893	1.903	1.913
97	1.899	1.854	1.861	1.861	1.873	1.883	1.893	1.903	1.913
98	1.899	1.854	1.861	1.861	1.873	1.883	1.893	1.903	1.913
99	1.899	1.854	1.861	1.861	1.873	1.883	1.893	1.903	1.913
100	1.899	1.854	1.861	1.861	1.873	1.883	1.893	1.903	1.913
101	1.899	1.854	1.861	1.861	1.873	1.883	1.893	1.903	1.913
102	1.899	1.854	1.861	1.861	1.873	1.883	1.893	1.903	1.913
103	1.899	1.854	1.861	1.861	1.873	1.883	1.893	1.903	1.913
104	1.899	1.854	1.861	1.861	1.873	1.883	1.893	1.903	1.913
105	1.899	1.854	1.861	1.861	1.873	1.883	1.893	1.903	1.913
106	1.899	1.854	1.861	1.861	1.873	1.883	1.893	1.903	1.913
107	1.899	1.854	1.861	1.861	1.873	1.883	1.893	1.903	1.913
108	1.899	1.854	1.861	1.861	1.873	1.883	1.893	1.903	1.913
109	1.899	1.854	1.861	1.861	1.873	1.883	1.893	1.903	1.913
110	1.899	1.854	1.861	1.861	1.873	1.883	1.893	1.903	1.913
111	1.899	1.854	1.861	1.861	1.873	1.883	1.893	1.903	1.913
112	1.899	1.854	1.861	1.861	1.873	1.883	1.893	1.903	1.913
113	1.899	1.854	1.861	1.861	1.873	1.883	1.893	1.903	1.913
114	1.899	1.854	1.861	1.861	1.873	1.883	1.893	1.903	1.913
115	1.899	1.854	1.861	1.861	1.873	1.883	1.893	1.903	1.913
116	1.899	1.854	1.861	1.861	1.873	1.883	1.893	1.903	1.913
117	1.899	1.854	1.861	1.861	1.873	1.883	1.893	1.903	1.913
118	1.899	1.854	1.861	1.861	1.873	1.883	1.893	1.903	1.913
119	1.899	1.854	1.861	1.861	1.873	1.883	1.893	1.903	1.913
120	1.899	1.854	1.861	1.861	1.873	1.883	1.893	1.903	1.913
121	1.899	1.854	1.861	1.861	1.873	1.883	1.893	1.903	1.913
122	1.899	1.854							

Flow rate sand erosion test (low velocity)										Flow rate sand erosion test (high velocity)										Flow rate sand erosion test (high velocity)										
	A	B	C	D	E	A'	B'	C'	D'	E'	A	B	C	D	E	A'	B'	C'	D'	E'	A	B	C	D	E	A'	B'	C'	D'	E'
Total	1.889	1.863	1.873	1.875	1.887	1.891	1.892	1.893	1.894	1.895	1.896	1.897	1.898	1.899	1.900	1.901	1.902	1.903	1.904	1.905	1.906	1.907	1.908	1.909	1.910	1.911	1.912	1.913	1.914	1.915
Sample	1.889	1.863	1.873	1.875	1.887	1.891	1.892	1.893	1.894	1.895	1.896	1.897	1.898	1.899	1.900	1.901	1.902	1.903	1.904	1.905	1.906	1.907	1.908	1.909	1.910	1.911	1.912	1.913	1.914	1.915
Angle	2.134	1.874	1.754	1.654	1.554	1.454	1.354	1.254	1.154	1.054	0.954	0.854	0.754	0.654	0.554	0.454	0.354	0.254	0.154	0.054	0.004	0.004	0.004	0.004	0.004	0.004	0.004	0.004	0.004	0.004
Angle	2.134	1.874	1.754	1.654	1.554	1.454	1.354	1.254	1.154	1.054	0.954	0.854	0.754	0.654	0.554	0.454	0.354	0.254	0.154	0.054	0.004	0.004	0.004	0.004	0.004	0.004	0.004	0.004	0.004	0.004
Angle	2.134	1.874	1.754	1.654	1.554	1.454	1.354	1.254	1.154	1.054	0.954	0.854	0.754	0.654	0.554	0.454	0.354	0.254	0.154	0.054	0.004	0.004	0.004	0.004	0.004	0.004	0.004	0.004	0.004	0.004
Angle	2.134	1.874	1.754	1.654	1.554	1.454	1.354	1.254	1.154	1.054	0.954	0.854	0.754	0.654	0.554	0.454	0.354	0.254	0.154	0.054	0.004	0.004	0.004	0.004	0.004	0.004	0.004	0.004	0.004	0.004
Angle	2.134	1.874	1.754	1.654	1.554	1.454	1.354	1.254	1.154	1.054	0.954	0.854	0.754	0.654	0.554	0.454	0.354	0.254	0.154	0.054	0.004	0.004	0.004	0.004	0.004	0.004	0.004	0.004	0.004	0.004
Angle	2.134	1.874	1.754	1.654	1.554	1.454	1.354	1.254	1.154	1.054	0.954	0.854	0.754	0.654	0.554	0.454	0.354	0.254	0.154	0.054	0.004	0.004	0.004	0.004	0.004	0.004	0.004	0.004	0.004	0.004
Angle	2.134	1.874	1.754	1.654	1.554	1.454	1.354	1.254	1.154	1.054	0.954	0.854	0.754	0.654	0.554	0.454	0.354	0.254	0.154	0.054	0.004	0.004	0.004	0.004	0.004	0.004	0.004	0.004	0.004	0.004
Angle	2.134	1.874	1.754	1.654	1.554	1.454	1.354	1.254	1.154	1.054	0.954	0.854	0.754	0.654	0.554	0.454	0.354	0.254	0.154	0.054	0.004	0.004	0.004	0.004	0.004	0.004	0.004	0.004	0.004	0.004
Angle	2.134	1.874	1.754	1.654	1.554	1.454	1.354	1.254	1.154	1.054	0.954	0.854	0.754	0.654	0.554	0.454	0.354	0.254	0.154	0.054	0.004	0.004	0.004	0.004	0.004	0.004	0.004	0.004	0.004	0.004
Angle	2.134	1.874	1.754	1.654	1.554	1.454	1.354	1.254	1.154	1.054	0.954	0.854	0.754	0.654	0.554	0.454	0.354	0.254	0.154	0.054	0.004	0.004	0.004	0.004	0.004	0.004	0.004	0.004	0.004	0.004
Angle	2.134	1.874	1.754	1.654	1.554	1.454	1.354	1.254	1.154	1.054	0.954	0.854	0.754	0.654	0.554	0.454	0.354	0.254	0.154	0.054	0.004	0.004	0.004	0.004	0.004	0.004	0.004	0.004	0.004	0.004
Angle	2.134	1.874	1.754	1.654	1.554	1.454	1.354	1.254	1.154	1.054	0.954	0.854	0.754	0.654	0.554	0.454	0.354	0.254	0.154	0.054	0.004	0.004	0.004	0.004	0.004	0.004	0.004	0.004	0.004	0.004
Angle	2.134	1.874	1.754	1.654	1.554	1.454	1.354	1.254	1.154	1.054	0.954	0.854	0.754	0.654	0.554	0.454	0.354	0.254	0.154	0.054	0.004	0.004	0.004	0.004	0.004	0.004	0.004	0.004	0.004	0.004
Angle	2.134	1.874	1.754	1.654	1.554	1.454	1.354	1.254	1.154	1.054	0.954	0.854	0.754	0.654	0.554	0.454	0.354	0.254	0.154	0.054	0.004	0.004	0.004	0.004	0.004	0.004	0.004	0.004	0.004	0.004
Angle	2.134	1.874	1.754	1.654	1.554	1.454	1.354	1.254	1.154	1.054	0.954	0.854	0.754	0.654	0.554	0.454	0.354	0.254	0.154	0.054	0.004	0.004	0.004	0.004	0.004	0.004	0.004	0.004	0.004	0.004
Angle	2.134	1.874	1.754	1.654	1.554	1.454	1.354	1.254	1.154	1.054	0.954	0.854	0.754	0.654	0.554	0.454	0.354	0.254	0.154	0.054	0.004	0.004	0.004	0.004	0.004	0.004	0.004	0.004	0.004	0.004
Angle	2.134	1.874	1.754	1.654	1.554	1.454	1.354	1.254	1.154	1.054	0.954	0.854	0.754	0.654	0.554	0.454	0.354	0.254	0.154	0.054	0.004	0.004	0.004	0.004	0.004	0.004	0.004	0.004	0.004	0.004
Angle	2.134	1.874	1.754	1.654	1.554	1.454	1.354	1.254	1.154	1.054	0.954	0.854	0.754	0.654	0.554	0.454	0.354	0.254	0.154	0.054	0.004	0.004	0.004	0.004	0.004	0.004	0.004	0.004	0.004	0.004
Angle	2.134	1.874	1.754	1.654	1.554	1.454	1.354	1.254	1.154	1.054	0.954	0.854	0.754	0.654	0.554	0.454	0.354	0.254	0.154	0.054	0.004	0.004	0.004	0.004	0.004	0.004	0.004	0.004	0.004	0.004
Angle	2.134	1.874	1.754	1.654	1.554	1.454	1.354	1.254	1.154	1.054	0.954	0.854	0.754	0.654	0.554	0.454	0.354	0.254	0.154	0.054	0.004	0.004	0.004	0.004	0.004	0.004	0.004	0.004	0.004	0.004
Angle	2.134	1.874	1.754	1.654	1.554	1.454	1.354	1.254	1.154	1.054	0.954	0.854	0.754	0.654	0.554	0.454	0.354	0.254	0.154	0.054	0.004	0.004	0.004	0.004	0.004	0.004	0.004	0.004	0.004	0.004
Angle	2.134	1.874	1.754	1.654	1.554	1.454	1.354	1.254	1.154	1.054	0.954	0.854	0.754	0.654	0.554	0.454	0.354	0.254	0.154	0.054	0.004	0.004	0.004	0.004	0.004	0.004	0.004	0.004	0.004	0.004
Angle	2.134	1.874	1.754	1.654	1.554	1.454	1.354	1.254	1.154	1.054	0.954	0.854	0.754	0.654	0.554	0.454	0.354	0.254	0.154	0.054	0.004	0.004	0.004	0.004	0.004	0.004	0.004	0.004	0.004	0.004
Angle	2.134	1.874	1.754	1.654	1.554	1.454	1.354	1.254	1.154	1.054	0.954	0.854	0.754	0.654	0.554	0.454	0.354	0.254	0.154	0.054	0.004	0.004	0.004	0.004	0.004	0.004	0.004	0.004	0.004	0.004
Angle	2.134	1.874	1.754	1.654	1.554	1.454	1.354	1.254	1.154	1.054	0.954	0.854	0.754	0.654	0.554	0.454	0.354	0.254	0.154	0.054	0.004	0.004	0.004	0.004	0.004	0.004	0.004	0.004	0.004	0.004
Angle	2.134	1.874	1.754	1.654	1.554	1.454	1.354	1.254	1.154	1.054	0.954	0.854	0.754	0.654	0.554	0.454	0.354	0.254	0.154	0.054	0.004	0.004	0.004	0.004	0.004	0.004	0.004	0.004	0.004	0.004
Angle	2.134	1.874	1.754	1.654	1.554	1.454	1.354	1.254	1.154	1.054	0.954	0.854	0.754	0.654	0.554	0.454	0.354	0.254	0.154	0.054	0.004	0.004	0.004	0.004	0.004	0.004	0.004	0.004	0.004	0.004
Angle	2.134	1.874	1.754	1.654	1.554	1.454	1.354	1.254	1.154	1.054	0.954	0.854	0.754	0.654	0.554	0.454	0.354	0.254	0.154	0.054	0.004	0.004	0.004	0.004	0.004	0.004	0.004	0.004	0.004	0.004
Angle	2.134	1.874	1.754	1.654	1.554	1.454	1.354	1.254	1.154	1.054	0.954	0.854	0.754	0.654	0.554	0.454	0.354	0.254	0.154	0.054	0.004	0.004	0.004	0.004	0.004	0.004	0.004	0.004	0.004	0.004
Angle	2.134	1.874	1.754	1.654	1.554	1.454	1.354	1.254	1.154	1.054	0.954	0.854	0.754	0.654	0.554	0.454	0.354	0.254	0.154	0.054	0.004	0.004	0.004	0.004	0.004	0.004	0.004	0.004	0.004	0.004
Angle	2.134	1.874	1.754	1.654	1.554	1.454	1.354	1.254	1.154	1.054	0.954	0.854	0.754	0.654	0.554	0.454	0.354	0.254	0.154	0.054	0.004	0.004	0.004	0.004	0.004	0.004	0.004	0.004	0.004	0.004
Angle	2.134	1.874	1.754	1.654	1.554	1.454	1.354	1.254	1.154	1.054	0.954	0.854	0.754	0.654	0.554	0.454	0.354	0.254	0.154	0.054	0.004	0.004	0.004	0.004	0.004	0.004	0.004	0.004	0.004	0.004
Angle	2.134	1.874	1.754	1.654	1.554	1.454	1.354	1.254	1.154	1.054	0.954	0.854	0.754	0.654	0.554	0.454	0.354	0.254	0.154	0.054	0.004	0.004	0.004	0.004	0.004	0.004	0.004	0.004	0.004	0.004
Angle	2.134	1.874	1.754	1.654	1.554	1.454	1.354	1.254	1.154	1.054	0.954	0.854	0.754	0.654	0.554	0.454	0.354	0.254	0.154	0.054	0.004	0.004	0.004	0.004	0.004	0.004	0.004	0.004	0.004	0.004
Angle	2.134	1.874	1.754	1.654	1.554	1.454	1.354	1.254	1.154	1.054	0.954	0.854	0.754	0.654	0.554	0.454	0.354	0.254	0.154	0.054	0.004	0.004	0.004	0.004	0.004	0.004	0.004	0.004	0.004	0.004
Angle	2.134	1.874	1.754	1.654	1.554	1.454	1.354	1.254	1.154	1.054	0.954	0.854	0.754	0.654	0.554	0.454	0.354	0.254	0.154	0.054	0.004	0.004	0.004	0.004	0.004	0.004	0.004	0.004	0.004	0.004
Angle	2.134	1.874	1.754	1.654	1.554	1.454	1.354	1.254	1.154	1.054	0.954	0.854	0.754	0.654	0.554	0.454	0.354	0.254	0.154	0.054	0.004	0.004	0.004	0.004	0.004	0.004	0.004	0.004	0.004	0.004
Angle	2.134	1.874	1.754	1.654	1.554	1.454	1.354																							

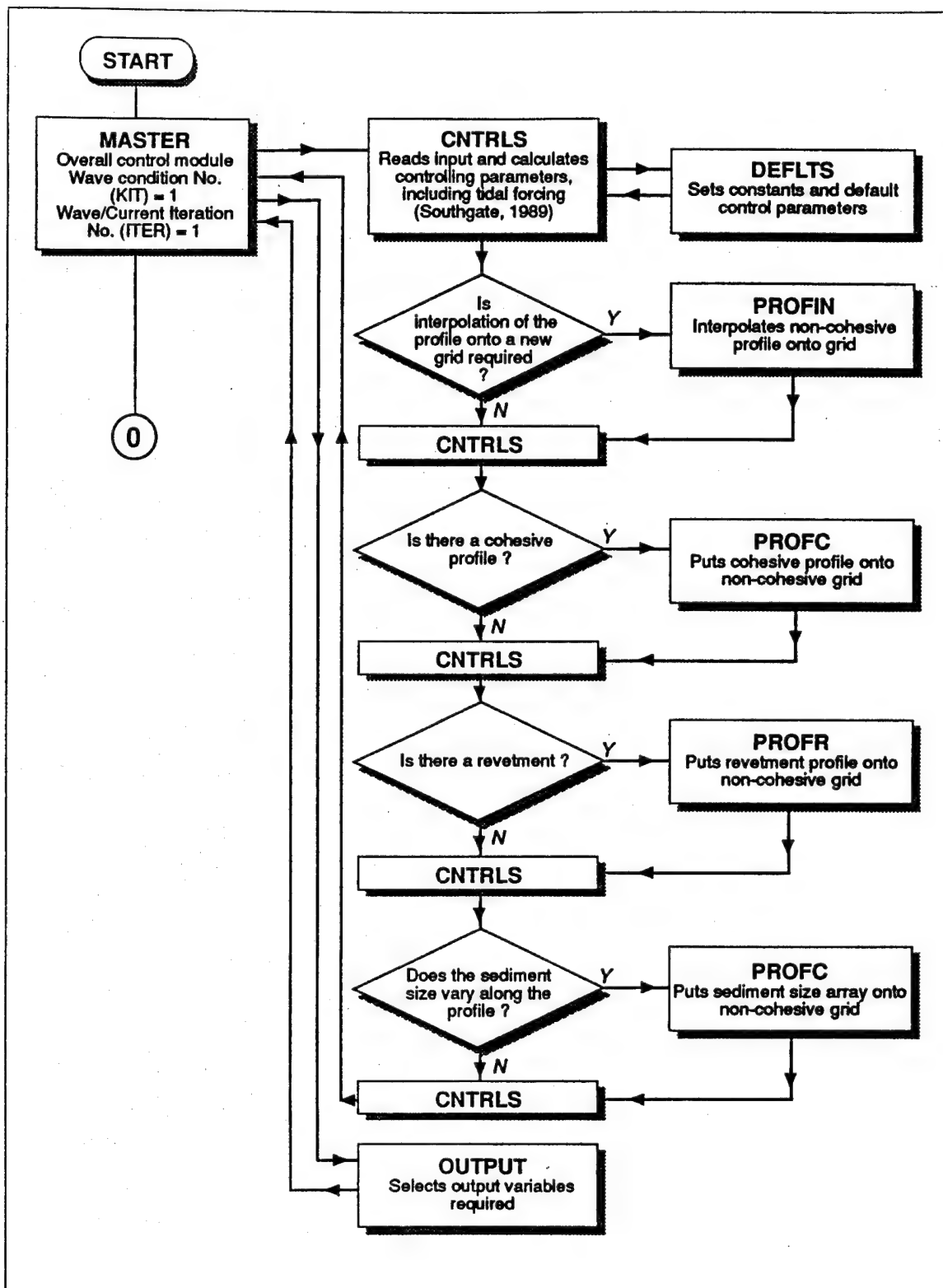
C5

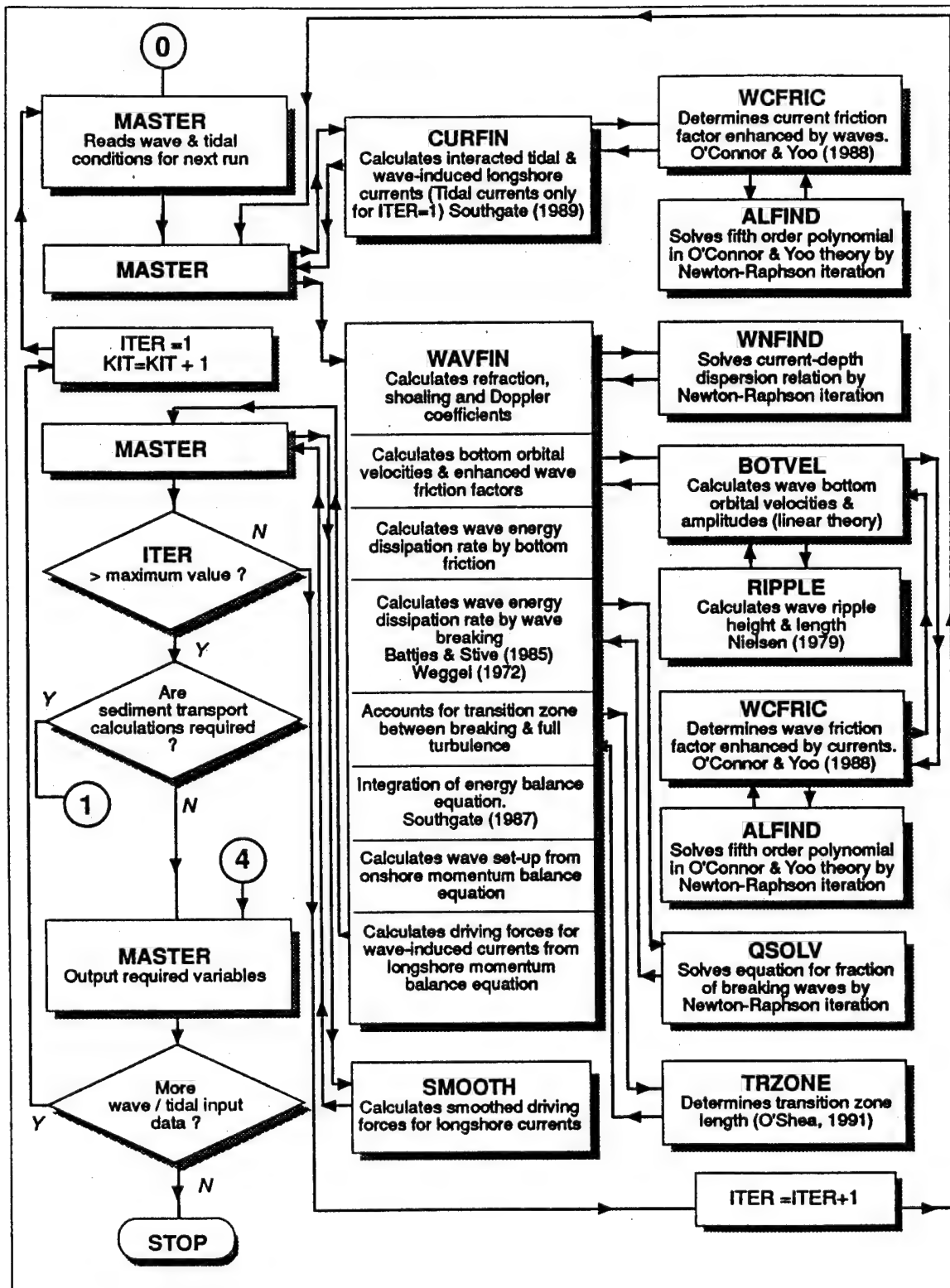
[illegible]

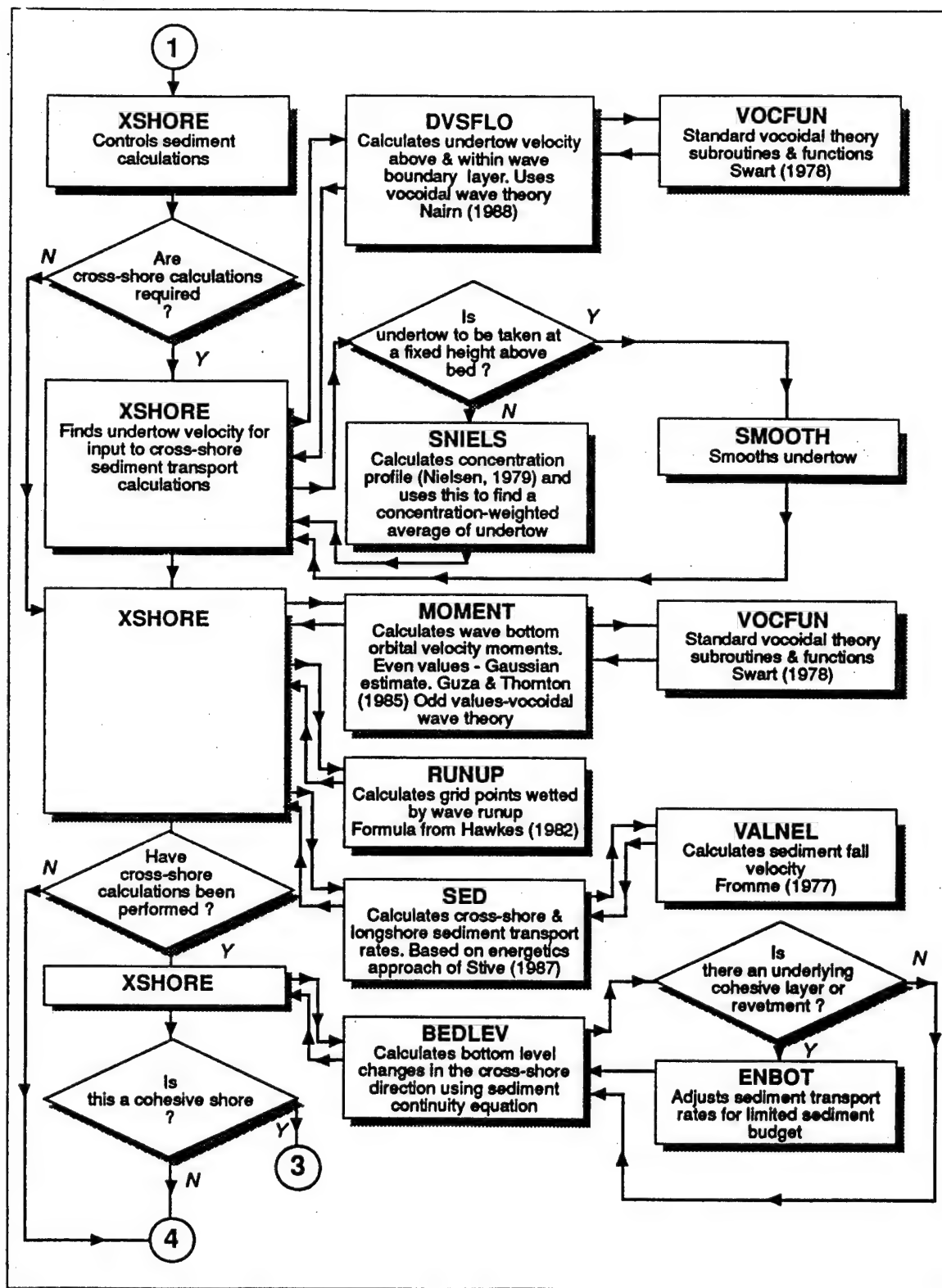
Appendix D

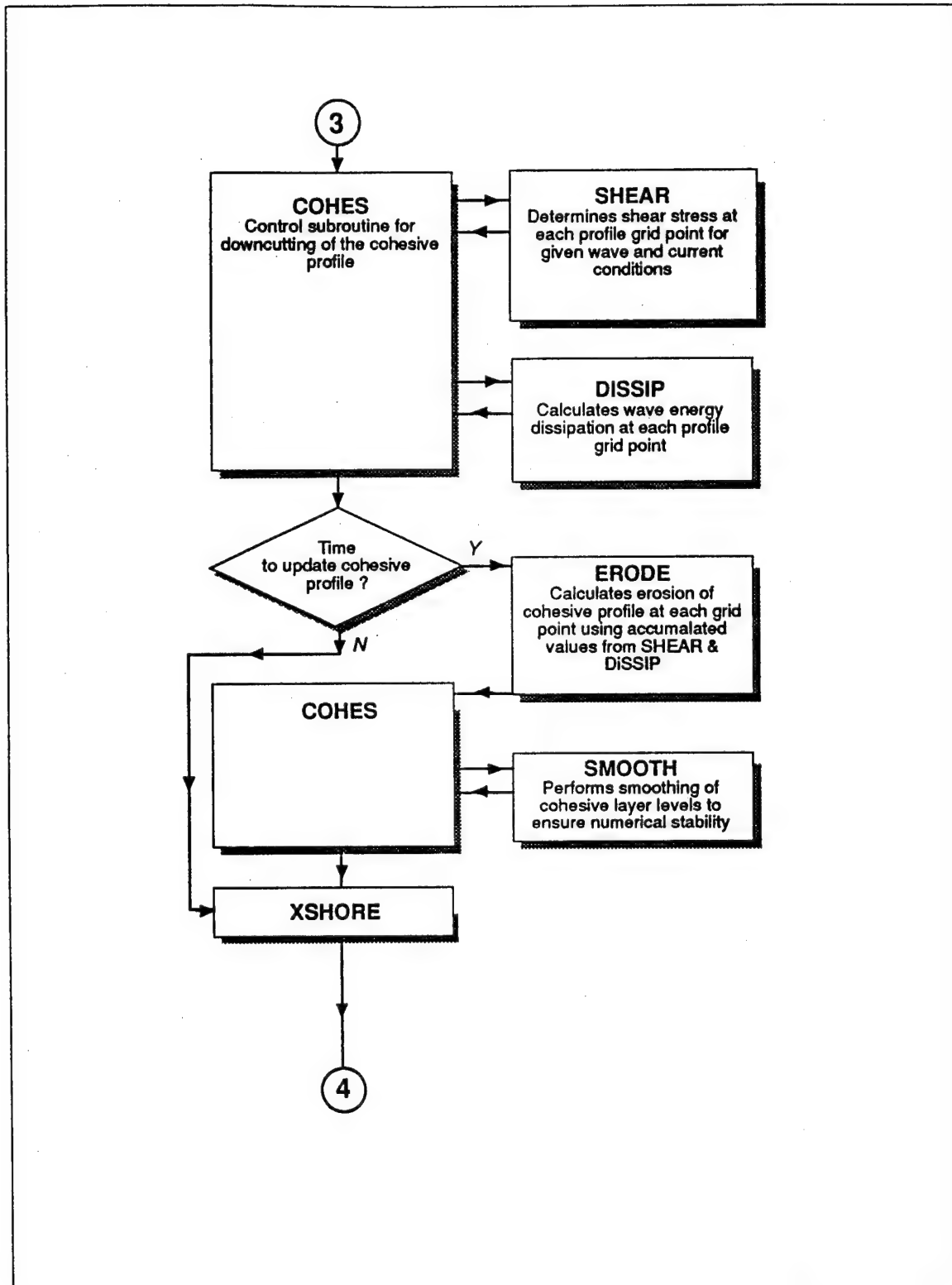
Module Flowchart of COSMOS-2D Numerical Model

Appendix D contains flowcharts showing the various predictive modules of COSMOS-2D. The various individual predictive phases of COSMOS, as well as the integrated model, have been thoroughly tested against both laboratory and field data (Southgate and Naim 1993, Naim and Southgate 1993). COSMOS has been applied in over 100 engineering projects throughout the world to determine: average annual alongshore transport rates; beach and dune erosion during storms; the influence of sea level rise and lake level fluctuation on erosion processes; downcutting of cohesive sediment profiles (short-term and long-term); erosion and scour at the toe of structures; the storm response and longevity of beach fill projects; impacts of structures on coastal processes; stable beach planform alignments; and offshore sediment loss rates. COSMOS has proven to be an accurate and robust predictive tool that can be applied to any site without the need for calibration (except where downcutting must be calculated).









Appendix E

Storm Events Identified Using Hindcast Wave Data

The characteristics of storms from the recent hindcast period (1991 to 1993) are listed in Appendix E. Three storms were selected that would be representative of the three types of storms (northwest, southwest, and west). These events, combined with the actual lake levels, were used as input in the cross-shore COSMOS-2D tests.

Wave Height threshold = 2.00

max Dip Length = 24

min Storm Length = 10

Rank	Storm	Start	End	Peak	Dur	Hs	Ts	Dir	Energy	F>S	P>P
1	381	26JAN78:09	29JAN78:21	26JAN78:24	85	6.2	10	325	3031	506	410
2	158	27NOV66:21	02DEC66:21	28NOV66:21	121	5.9	10	337	2508	362	266
3	324	31JAN76:24	02FEB76:06	01FEB76:21	31	5.4	9.1	344	899	104	80
4	227	26JAN71:09	02FEB71:03	26JAN71:18	163	5.3	9.1	316	3458	236	83
5	509	08FEB87:12	09FEB87:06	08FEB87:21	19	5.3	9.1	349	885	224	215
6	380	08JAN78:18	11JAN78:21	09JAN78:21	76	5.2	9.1	328	2416	239	173
7	487	12FEB85:03	14FEB85:21	13FEB85:06	67	5	9.1	332	2043	488	437
8	322	19JAN76:18	22JAN76:18	21JAN76:18	73	5	8.3	337	1077	149	119
9	303	25FEB75:18	01MAR75:21	25FEB75:24	100	4.9	8.3	282	1880	554	458
10	123	25FEB65:09	26FEB65:21	25FEB65:24	37	4.8	8.3	309	1336	137	98
11	49	21MAR60:24	22MAR60:24	22MAR60:09	25	4.7	8.3	318	809	623	590
12	188	05DEC68:06	6DEC68:09	5DEC68:18	28	4.6	8.3	311	934	404	383
13	81	19MAR63:24	21MAR63:24	20MAR63:21	49	4.6	8.3	314	1652	107	74
14	250	25JAN72:03	25JAN72:21	25JAN72:06	19	4.6	8.3	266	693	203	185
15	368	10NOV77:09	12NOV77:21	11NOV77:12	61	4.5	8.3	315	1336	674	638
16	133	16NOV65:21	17NOV65:21	17NOV65:06	25	4.5	8.3	314	798	113	95
17	407	06APR79:03	6APR79:21	6APR79:09	19	4.4	8.3	313	595	566	539
18	275	17MAR73:09	19MAR73:03	18MAR73:06	43	4.4	7.7	335	1296	173	152
19	311	10NOV75:09	10NOV75:21	10NOV75:15	13	4.3	8.3	267	459	1223	1196
20	228	05FEB71:12	6FEB71:09	5FEB71:18	22	4.2	7.7	250	580	263	239
21	450	23JAN82:12	24JAN82:18	23JAN82:24	31	4.2	8.3	271	674	197	170
22	86	28NOV63:24	30NOV63:03	29NOV63:18	28	4.2	8.3	344	685	161	140
23	284	22FEB74:18	23FEB74:09	22FEB74:24	16	4.1	7.7	321	616	302	287
24	220	04DEC70:03	6DEC70:18	4DEC70:09	64	4.1	7.7	304	1272	116	59
25	350	10JAN77:15	12JAN77:12	10JAN77:24	46	4.1	8.3	312	725	137	83
26	298	11JAN75:09	12JAN75:18	11JAN75:15	34	4.1	7.7	238	942	212	182
27	352	25JAN77:21	1FEB77:21	28JAN77:18	169	4.1	8.3	302	2085	416	287
28	231	27FEB71:06	28FEB71:21	27FEB71:18	40	4.1	8.3	255	1110	380	347
29	167	15FEB67:24	16FEB67:15	16FEB67:06	16	4.1	7.7	282	443	143	119
30	455	03APR82:15	4APR82:18	4APR82:09	28	4.1	8.3	313	866	116	83
31	449	16JAN82:12	17JAN82:06	16JAN82:21	19	4.1	8.3	311	448	176	158
32	464	10NOV83:21	12NOV83:06	11NOV83:21	34	4	8.3	354	909	5489	5480
33	257	22MAR72:06	24MAR72:03	23MAR72:03	46	4	8.3	318	1233	236	209
34	346	20DEC76:12	24DEC76:12	21DEC76:06	97	4	8.3	342	1485	170	83
35	255	07MAR72:18	8MAR72:21	8MAR72:09	28	4	8.3	301	645	95	77
36	314	30NOV75:12	1DEC75:15	30NOV75:24	28	4	7.7	271	717	251	212
37	66	05FEB62:09	06FEB62:21	05FEB62:18	37	4	8.3	314	612	179	149
38	57	09MAR61:06	10MAR61:03	09MAR61:21	22	4	7.7	344	548	296	284
39	263	16DEC72:03	18DEC72:15	16DEC72:18	61	4	8.3	310	1007	515	467
40	399	14JAN79:06	15JAN79:06	14JAN79:12	25	3.9	7.7	338	508	293	251
41	484	12JAN85:24	15JAN85:09	14JAN85:24	58	3.9	8.3	317	827	182	170
42	486	25JAN85:12	26JAN85:03	25JAN85:24	16	3.9	8.3	326	471	155	140
43	448	09JAN82:21	11JAN82:06	10JAN82:06	34	3.9	8.3	301	860	155	128
44	63	06DEC61:24	08DEC61:06	07DEC61:06	31	3.9	7.7	296	687	74	44
45	292	20NOV74:15	21NOV74:21	21NOV74:12	31	3.9	8.3	323	797	170	137
46	94	25JAN64:06	26JAN64:21	25JAN64:21	40	3.9	7.7	253	1029	335	299
47	462	11JAN83:21	12JAN83:09	12JAN83:03	13	3.8	7.7	346	307	353	338
48	419	07JAN80:09	8JAN80:03	7JAN80:12	19	3.8	7.7	256	456	335	314
49	517	15DEC87:18	17DEC87:03	15DEC87:24	34	3.8	7.7	292	636	110	74
50	490	12MAR85:09	12MAR85:24	12MAR85:12	16	3.8	7.7	308	460	188	173
51	232	06MAR71:24	8MAR71:24	7MAR71:09	49	3.8	7.7	311	1098	233	182
52	469	06DEC83:18	7DEC83:09	6DEC83:24	16	3.8	7.7	330	345	197	170
53	427	02DEC80:15	3DEC80:03	2DEC80:24	13	3.8	8.3	345	392	290	275
54	82	03APR63:18	04APR63:15	04APR63:03	22	3.8	7.7	273	570	374	341
55	125	18MAR65:06	19MAR65:21	18MAR65:12	40	3.8	7.7	257	756	239	182
56	122	21FEB65:03	22FEB65:21	21FEB65:21	43	3.8	7.7	318	985	248	215
57	233	15MAR71:18	16MAR71:18	15MAR71:21	28	3.8	7.7	261	610	233	203
58	37	15MAR59:18	17MAR59:09	15MAR59:21	40	3.8	7.1	304	582	251	209
59	372	01DEC77:18	2DEC77:24	2DEC77:03	31	3.7	7.7	268	704	164	134
60	499	12JAN86:15	13JAN86:09	13JAN86:06	19	3.7	7.7	325	375	92	80
61	471	28FEB84:15	29FEB84:24	28FEB84:24	34	3.7	7.7	349	827	1664	1592
62	218	22NOV70:18	24NOV70:18	23NOV70:09	49	3.7	7.7	302	1074	95	56
63	76	02FEB63:18	03FEB63:06	03FEB63:03	13	3.7	9.1	335	386	251	248
64	252	18FEB72:18	20FEB72:09	19FEB72:24	40	3.7	7.7	327	851	395	371
65	470	22DEC83:15	27DEC83:06	24DEC83:15	112	3.7	7.7	311	1532	491	422
66	134	27NOV65:06	29NOV65:06	27NOV65:21	49	3.7	7.1	281	807	296	254
67	266	04JAN73:06	5JAN73:03	4JAN73:09	22	3.7	7.1	251	369	107	74
68	309	19APR75:06	20APR75:12	19APR75:24	31	3.7	7.7	277	560	521	482

Wave Height threshold = 2.00

max Dip Length = 24

min Storm Length = 10

Rank	Storm	Start	End	Peak	Dur	Hs	Ts	Dir	Energy	F->S	P->P
71	100	26MAR64:12	27MAR64:03	26MAR64:18	16	3.6	7.7	303	339	293	212
72	395	12DEC78:15	15DEC78:15	13DEC78:15	73	3.6	7.7	303	1093	146	92
73	369	16NOV77:24	18NOV77:21	18NOV77:12	46	3.6	7.7	307	606	203	167
74	401	24JAN79:24	25JAN79:24	25JAN79:09	25	3.6	7.7	333	458	98	74
75	355	13FEB77:06	15FEB77:06	13FEB77:18	49	3.6	7.7	313	598	239	191
76	242	17DEC71:12	18DEC71:09	17DEC71:24	22	3.6	7.7	307	402	62	50
77	145	27JAN66:15	28JAN66:21	27JAN66:21	31	3.6	7.7	314	542	128	98
78	286	03MAR74:18	04MAR74:03	03MAR74:21	10	3.6	7.1	236	228	104	71
79	316	16DEC75:21	19DEC75:03	18DEC75:09	55	3.6	7.7	319	782	113	89
80	473	22MAR84:09	22MAR84:24	22MAR84:21	16	3.6	7.7	320	328	281	269
81	71	06DEC62:15	07DEC62:18	06DEC62:24	28	3.6	7.7	316	731	1100	1082
82	328	05MAR76:15	07MAR76:24	05MAR76:18	58	3.6	7.7	260	758	356	299
83	429	18DEC80:03	19DEC80:15	19DEC80:09	37	3.6	7.7	333	467	146	113
84	300	25JAN75:21	26JAN75:21	26JAN75:15	25	3.6	7.7	313	540	194	185
85	415	09DEC79:18	11DEC79:18	09DEC79:24	49	3.5	7.7	311	572	155	107
86	485	19JAN85:15	23JAN85:24	20JAN85:03	106	3.5	7.7	310	1131	263	122
87	387	06OCT78:06	07OCT78:21	06OCT78:18	40	3.5	7.7	322	505	4541	4508
88	443	18OCT81:12	20OCT81:18	18OCT81:24	55	3.5	8.3	307	630	338	293
89	54	24JAN61:09	24JAN61:21	24JAN61:15	13	3.5	7.7	332	263	407	389
90	366	11OCT77:15	12OCT77:18	11OCT77:21	28	3.5	7.1	248	552	92	68
91	330	16MAR76:18	17MAR76:09	16MAR76:24	16	3.5	7.7	320	347	101	86
92	325	06FEB76:18	08FEB76:21	07FEB76:24	52	3.5	7.1	241	773	188	146
93	494	01DEC85:24	02DEC85:24	02DEC85:18	25	3.5	7.7	299	568	305	296
94	156	02NOV66:21	04NOV66:03	03NOV66:21	31	3.5	7.7	315	608	80	74
95	99	14MAR64:21	18MAR64:03	17MAR64:21	79	3.5	7.7	325	657	302	290
96	143	09JAN66:24	11JAN66:06	10JAN66:18	31	3.5	7.7	307	435	86	71
97	121	12FEB65:12	13FEB65:09	12FEB65:21	22	3.5	7.1	262	369	65	47
98	251	03FEB72:21	05FEB72:06	04FEB72:12	34	3.5	7.7	307	601	266	245
99	406	14MAR79:06	14MAR79:24	14MAR79:21	19	3.5	7.7	310	327	110	107
100	253	21FEB72:21	22FEB72:12	22FEB72:06	16	3.5	7.7	329	342	89	53
101	217	20NOV70:18	21NOV70:03	20NOV70:24	10	3.4	7.7	308	259	146	140
102	33	21JAN59:21	22JAN59:21	22JAN59:03	25	3.4	8.3	312	318	167	143
103	120	10FEB65:15	10FEB65:24	10FEB65:21	10	3.4	7.1	264	191	221	212
104	390	17NOV78:24	19NOV78:09	18NOV78:03	34	3.4	7.1	262	358	116	86
105	301	29JAN75:15	29JAN75:24	29JAN75:18	10	3.4	7.1	269	264	98	74
106	17	08NOV57:18	09NOV57:15	08NOV57:24	22	3.4	7.1	271	410	5741	5720
107	118	26JAN65:21	29JAN65:03	27JAN65:03	55	3.4	7.7	304	794	269	206
108	164	27JAN67:15	29JAN67:09	27JAN67:18	43	3.4	7.7	360	792	293	236
109	139	25DEC65:09	25DEC65:24	25DEC65:18	16	3.4	7.1	359	322	302	293
110	458	12NOV82:18	13NOV82:12	12NOV82:24	19	3.4	7.7	307	370	197	173
111	329	13MAR76:03	13MAR76:21	13MAR76:09	19	3.4	7.7	326	454	197	182
112	74	29DEC62:15	30DEC62:03	29DEC62:21	13	3.4	7.1	337	243	164	152
113	435	11FEB81:09	12FEB81:03	11FEB81:18	19	3.4	7.7	306	373	98	89
114	14	16FEB57:15	17FEB57:06	16FEB57:18	16	3.4	7.1	296	310	626	593
115	234	19MAR71:24	20MAR71:24	20MAR71:18	25	3.4	7.7	325	522	128	116
116	46	11FEB60:06	12FEB60:03	11FEB60:12	22	3.3	8.3	310	458	134	101
117	456	20OCT82:12	21OCT82:03	20OCT82:21	16	3.3	7.1	287	298	4811	4787
118	109	11NOV64:15	13NOV64:03	12NOV64:21	37	3.3	7.1	238	350	539	530
119	343	10DEC76:09	13DEC76:09	13DEC76:06	73	3.3	7.7	337	766	374	371
120	149	23MAR66:18	25MAR66:15	24MAR66:03	46	3.3	7.1	254	648	161	101
121	98	05MAR64:12	05MAR64:24	05MAR64:18	13	3.3	8.3	310	281	128	116
122	196	24JAN69:12	26JAN69:03	24JAN69:24	40	3.3	7.1	257	674	398	362
123	77	14FEB63:12	15FEB63:03	14FEB63:18	16	3.3	7.7	314	341	296	278
124	361	05APR77:15	05APR77:24	05APR77:21	10	3.3	7.7	311	236	140	128
125	344	14DEC76:12	15DEC76:03	14DEC76:15	16	3.3	7.1	220	287	113	32
126	331	21MAR76:09	21MAR76:24	21MAR76:18	16	3.3	7.7	329	253	125	113
127	308	29MAR75:18	30MAR75:24	30MAR75:21	31	3.3	7.1	285	414	146	140
128	181	17FEB68:03	18FEB68:21	17FEB68:12	43	3.3	9.1	303	704	221	182
129	441	01OCT81:15	02OCT81:15	01OCT81:24	25	3.3	7.7	314	462	113	95
130	285	27FEB74:18	01MAR74:03	28FEB74:21	34	3.3	6.7	252	379	152	140
131	489	05MAR85:03	05MAR85:21	05MAR85:06	19	3.3	7.1	267	397	407	371
132	32	15JAN59:21	17JAN59:03	16JAN59:03	31	3.3	7.7	312	575	308	272
133	270	28JAN73:21	29JAN73:12	28JAN73:24	16	3.3	7.1	359	362	236	221
134	67	14FEB62:06	14FEB62:21	14FEB62:09	16	3.3	7.1	299	273	227	206
135	445	20NOV81:09	21NOV81:18	20NOV81:18	34	3.3	8.3	340	481	371	338
136	418	25DEC79:03	25DEC79:18	25DEC79:09	16	3.3	9.1	1	415	167	155

Wave Height threshold = 2.00

max Dip Length = 24

min Storm Length = 10

Rank	Storm	Start	End	Peak	Dur	Hs	Ts	Dir	Energy	F->S	P->P
137	68	09APR62:15	09APR62:24	09APR62:21	10	3.3	7.7	272	192	1313	1307
138	507	23JAN87:03	23JAN87:21	23JAN87:12	19	3.3	7.7	317	339	398	386
139	245	30DEC71:18	31DEC71:06	30DEC71:21	13	3.3	7.1	264	233	74	62
140	430	24DEC80:15	24DEC80:24	24DEC80:21	10	3.2	7.7	351	233	164	131
141	472	11MAR84:06	11MAR84:21	11MAR84:15	16	3.2	7.1	317	293	293	278
142	117	17JAN65:21	19JAN65:24	18JAN65:12	52	3.2	7.7	347	530	146	107
143	465	16NOV83:12	17NOV83:06	16NOV83:21	19	3.2	7.7	349	382	152	119
144	119	01FEB65:18	04FEB65:09	01FEB65:24	64	3.2	7.1	282	543	203	140
145	454	30MAR82:21	31MAR82:24	31MAR82:21	28	3.2	7.1	287	277	137	122
146	371	26NOV77:03	26NOV77:21	26NOV77:12	19	3.2	7.1	338	351	137	122
147	239	19NOV71:09	22NOV71:03	21NOV71:03	67	3.2	7.1	308	829	371	341
148	185	03OCT68:15	04OCT68:21	03OCT68:21	31	3.2	7.7	310	364	3935	3908
149	480	22DEC84:03	22DEC84:18	22DEC84:18	16	3.2	7.7	313	232	386	380
150	452	13MAR82:09	13MAR82:24	13MAR82:21	16	3.2	7.1	288	252	1067	1058
151	194	07JAN69:03	07JAN69:21	07JAN69:09	19	3.2	7.7	310	332	176	149
152	189	13DEC68:12	15DEC68:06	13DEC68:15	43	3.2	7.1	254	510	239	188
153	377	25DEC77:03	26DEC77:06	25DEC77:06	46	3.2	7.1	300	614	101	44
154	219	01DEC70:21	02DEC70:06	01DEC70:21	10	3.2	6.7	240	173	227	203
155	420	11JAN80:18	12JAN80:15	12JAN80:09	22	3.2	7.1	304	381	125	116
156	5	11MAR56:09	11MAR56:18	11MAR56:12	10	3.2	7.1	296	224	80	62
157	327	22FEB76:03	22FEB76:12	22FEB76:06	10	3.2	7.1	355	223	260	248
158	152	10OCT66:18	11OCT66:21	11OCT66:21	28	3.2	7.1	303	359	170	167
159	114	02JAN65:18	03JAN65:06	02JAN65:24	13	3.2	7.1	339	243	419	389
160	461	28DEC82:15	29DEC82:03	28DEC82:24	13	3.2	7.1	256	284	548	545
161	148	18MAR66:21	19MAR66:24	19MAR66:21	28	3.2	7.1	297	328	317	311
162	110	20NOV64:06	21NOV64:24	21NOV64:06	43	3.2	7.7	302	485	248	200
163	146	16FEB66:21	17FEB66:21	17FEB66:03	25	3.2	7.1	301	356	509	485
164	115	08JAN65:18	09JAN65:21	09JAN65:03	28	3.2	7.1	306	495	170	146
165	4	08MAR56:09	08MAR56:24	08MAR56:21	16	3.2	7.1	295	225	296	290
166	273	21FEB73:15	22FEB73:03	21FEB73:18	13	3.2	7.1	319	263	158	140
167	104	09MAY64:03	09MAY64:18	09MAY64:09	16	3.1	7.1	262	214	623	611
168	65	30JAN62:09	30JAN62:24	30JAN62:12	16	3.1	7.1	332	255	1181	1163
169	235	23MAR71:03	23MAR71:24	23MAR71:18	22	3.1	7.1	329	321	95	71
170	230	12FEB71:24	13FEB71:18	13FEB71:06	19	3.1	7.1	6	278	113	95
171	27	09NOV58:09	10NOV58:09	10NOV58:06	13	3.1	7.1	310	233	737	728
172	338	07NOV76:15	08NOV76:03	07NOV76:21	13	3.1	7.1	332	222	248	230
173	112	13DEC64:18	15DEC64:06	14DEC64:18	37	3.1	7.1	310	416	395	374
174	426	20NOV80:24	21NOV80:18	21NOV80:12	19	3.1	7.1	309	272	989	977
175	105	23SEP64:15	24SEP64:12	23SEP64:21	22	3.1	7.1	270	318	3320	3299
176	477	15NOV84:21	16NOV84:21	16NOV84:03	25	3.1	6.7	276	397	134	113
177	53	07JAN61:21	08JAN61:18	08JAN61:09	22	3.1	7.1	318	440	974	938
178	421	22JAN80:21	23JAN80:12	23JAN80:03	16	3.1	7.1	318	260	281	257
179	50	24MAR60:18	25MAR60:03	24MAR60:21	10	3.1	7.1	331	195	74	59
180	3	25FEB56:15	25FEB56:24	25FEB56:18	10	3.1	7.1	297	210	1109	1082
181	241	15DEC71:18	16DEC71:06	15DEC71:21	13	3.1	6.7	238	225	128	113
182	197	03FEB69:15	04FEB69:24	03FEB69:21	34	3.1	7.1	302	338	275	236
183	393	04DEC78:09	05DEC78:18	04DEC78:18	34	3.1	7.1	255	462	143	104
184	451	28JAN82:12	28JAN82:24	28JAN82:18	13	3.1	7.1	313	239	131	113
185	191	23DEC68:06	24DEC68:21	23DEC68:12	40	3.1	6.7	247	722	119	77
186	23	03FEB58:12	03FEB58:21	03FEB58:18	10	3.1	7.1	327	171	680	653
187	370	21NOV77:03	22NOV77:06	21NOV77:09	28	3.1	7.1	265	436	125	68
188	62	05DEC61:03	05DEC61:18	05DEC61:09	16	3.1	7.1	288	261	200	185
189	356	24FEB77:24	25FEB77:24	25FEB77:12	25	3.1	7.1	272	498	305	281
190	173	18OCT67:21	19OCT67:06	18OCT67:24	10	3.1	7.1	334	189	4427	4418
191	170	28FEB67:03	28FEB67:24	28FEB67:09	22	3.1	7.1	326	346	104	83
192	403	04FEB79:09	05FEB79:09	04FEB79:24	25	3.1	7.1	312	365	173	164
193	335	15OCT76:06	16OCT76:03	15OCT76:21	22	3.1	7.1	306	368	3932	3923
194	320	14JAN76:06	15JAN76:06	14JAN76:18	25	3.1	7.1	305	364	176	137
195	38	21MAR59:15	21MAR59:24	21MAR59:18	10	3.1	7.1	328	217	149	140
196	45	06FEB60:12	08FEB60:21	07FEB60:06	58	3.1	7.7	305	638	1523	1478
197	240	10DEC71:21	11DEC71:09	11DEC71:03	13	3.1	7.1	257	221	527	479
198	283	10FEB74:18	11FEB74:21	10FEB74:24	28	3.1	7.1	313	303	290	245
199	89	18DEC63:12	19DEC63:21	18DEC63:18	34	3.1	7.1	324	374	146	116
200	183	08APR68:18	09APR68:21	08APR68:21	28	3.1	6.7	265	241	422	392
201	113	16DEC64:18	18DEC64:12	17DEC64:18	43	3.1	7.1	325	433	113	71
202	408	12OCT79:21	13OCT79:06	13OCT79:06	25	3.1	7.1	310	412	4577	4556
203	187	19NOV68:12	20NOV68:09	19NOV68:18	22	3	7.7	303	380	566	527
204	496	27DEC85:06	27DEC85:24	27DEC85:09	19	3	6.7	271	246	89	68

Wave Height threshold = 2.00

max Dip Length = 24

min Storm Length = 1

Rank	Storm	Start	End	Peak	Dur	Hs	Ts	Dir	Energy	F->S	P->P
1	29	10MAR92:05	11MAR92:12	10MAR92:14	32	4.00	9.00	352	2968	242	216
2	20	14JAN92:02	19JAN92:20	14JAN92:13	139	3.90	8.00	339	5342	646	518
3	22	23JAN92:20	24JAN92:20	24JAN92:11	25	3.50	8.00	322	1237	88	78
4	31	27MAR92:07	27MAR92:23	27MAR92:14	17	3.40	8.00	328	1110	129	116
5	13	04DEC91:04	04DEC91:22	04DEC91:11	19	3.30	8.00	302	1024	106	92
6	7	01NOV91:21	03NOV91:22	02NOV91:08	50	3.20	7.00	252	1978	97	54
7	10	23NOV91:23	25NOV91:09	24NOV91:02	35	3.10	7.00	222	1349	242	211
8	63	29DEC93:21	30DEC93:10	30DEC93:03	14	3.10	7.00	315	650	105	95
9	18	17DEC91:16	18DEC91:21	18DEC91:16	30	3.00	8.00	341	1204	102	95
10	49	13MAR93:20	14MAR93:05	14MAR93:02	10	3.00	8.00	348	530	606	603
11	40	12NOV92:23	13NOV92:10	13NOV92:04	12	2.90	7.00	309	537	662	654
12	17	14DEC91:14	16DEC91:02	14DEC91:16	37	2.90	7.00	288	1124	74	40
13	43	23DEC92:22	25DEC92:23	24DEC92:02	50	2.80	7.00	332	1280	502	452
14	51	01APR93:18	02APR93:06	01APR93:22	13	2.70	7.00	357	547	404	367
15	27	28FEB92:10	29FEB92:03	29FEB92:01	18	2.70	7.00	354	554	197	194
16	12	30NOV91:11	30NOV91:19	30NOV91:14	9	2.70	7.00	254	326	75	68
17	38	23MAY92:20	24MAY92:20	24MAY92:06	25	2.70	7.00	356	794	264	248
18	11	27NOV91:15	27NOV91:22	27NOV91:17	8	2.60	6.00	260	268	94	86
19	61	10DEC93:21	11DEC93:11	11DEC93:01	15	2.50	7.00	339	575	109	96
20	6	30OCT91:20	31OCT91:08	31OCT91:01	13	2.50	7.00	347	503	299	287
21	45	24JAN93:13	24JAN93:22	24JAN93:16	10	2.50	7.00	322	374	581	573
22	42	04DEC92:24	05DEC92:17	05DEC92:05	18	2.50	7.00	316	618	68	54
23	25	16FEB92:03	16FEB92:09	16FEB92:07	7	2.50	7.00	330	238	204	191
24	62	25DEC93:24	26DEC93:06	26DEC93:03	7	2.40	7.00	305	215	368	361
25	60	06DEC93:21	07DEC93:04	06DEC93:24	8	2.40	7.00	312	252	367	362
26	23	31JAN92:20	01FEB92:05	01FEB92:03	10	2.40	7.00	346	340	200	183
27	26	20FEB92:21	20FEB92:24	20FEB92:22	4	2.40	6.00	216	119	116	110
28	46	28JAN93:23	29JAN93:14	29JAN93:03	16	2.40	7.00	327	529	120	106
29	55	09OCT93:14	09OCT93:22	09OCT93:18	9	2.40	7.00	355	285	3595	3589
30	2	15APR91:16	15APR91:19	15APR91:17	4	2.40	6.00	291	133	127	122
31	28	01MAR92:09	01MAR92:17	01MAR92:13	9	2.30	6.00	235	248	54	35
32	50	16MAR93:09	17MAR93:17	17MAR93:14	33	2.30	7.00	345	586	92	83
33	24	07FEB92:20	08FEB92:23	08FEB92:07	28	2.30	7.00	328	833	194	171
34	47	30JAN93:21	01FEB93:04	31JAN93:05	32	2.30	6.00	264	744	76	49
35	5	18OCT91:20	19OCT91:02	19OCT91:01	7	2.30	7.00	354	195	318	317
36	39	16OCT92:19	17OCT92:03	16OCT92:21	9	2.30	7.00	310	281	3510	3494
37	37	13MAY92:19	13MAY92:22	13MAY92:21	4	2.30	7.00	358	123	195	193
38	14	06DEC91:03	07DEC91:10	06DEC91:06	32	2.30	7.00	307	382	77	42
39	57	05NOV93:23	06NOV93:05	06NOV93:03	7	2.20	6.00	327	194	124	122
40	54	13MAY93:02	13MAY93:05	13MAY93:04	4	2.20	6.00	353	110	439	437
41	53	24APR93:21	24APR93:24	24APR93:22	4	2.20	6.00	224	102	93	91
42	3	26SEP91:07	26SEP91:16	26SEP91:09	10	2.20	6.00	316	275	3935	3927
43	41	02DEC92:20	03DEC92:05	02DEC92:22	10	2.20	6.00	314	228	485	473
44	19	23DEC91:21	23DEC91:24	23DEC91:22	4	2.20	6.00	341	115	151	125
45	30	22MAR92:13	22MAR92:19	22MAR92:17	7	2.10	6.00	360	153	301	290
46	15	10DEC91:19	10DEC91:24	10DEC91:21	6	2.10	6.00	227	151	116	110
47	59	21NOV93:20	21NOV93:23	21NOV93:21	4	2.10	6.00	228	100	49	46
48	58	19NOV93:21	20NOV93:02	19NOV93:22	6	2.10	6.00	292	156	338	330
49	44	31DEC92:16	01JAN93:16	31DEC92:18	25	2.10	6.00	308	337	209	183
50	21	21JAN92:03	21JAN92:05	21JAN92:04	3	2.10	6.00	254	74	170	158
51	36	05MAY92:18	05MAY92:20	05MAY92:19	3	2.10	6.00	357	74	93	92
52	1	10APR91:11	10APR91:16	10APR91:14	6	2.10	6.00	309	148		
53	34	27APR92:06	27APR92:08	27APR92:07	3	2.10	6.00	352	78	350	348
54	8	06NOV91:04	07NOV91:10	06NOV91:04	31	2.10	6.00	222	512	132	91
55	33	12APR92:17	12APR92:20	12APR92:18	4	2.10	7.00	353	109	269	266
56	32	01APR92:14	01APR92:16	01APR92:15	3	2.10	6.00	334	81	128	120
57	16	12DEC91:23	13DEC91:01	12DEC91:23	3	2.10	5.00	217	74	53	49
58	56	31OCT93:24	01NOV93:01	31OCT93:24	2	2.00	6.00	335	52	538	533
59	52	21APR93:02	21APR93:02	21APR93:02	1	2.00	6.00	357	24	463	459
60	48	16FEB93:22	16FEB93:22	16FEB93:22	1	2.00	6.00	343	24	408	400
61	9	15NOV91:06	15NOV91:07	15NOV91:06	2	2.00	6.00	215	48	218	217
62	35	01MAY92:22	01MAY92:22	01MAY92:22	1	2.00	6.00	228	24	111	110
63	4	05OCT91:19	05OCT91:20	05OCT91:19	2	2.00	6.00	284	48	228	225

Wave Height threshold = 2.00 max Dip Length = 24 min Storm Length = 1

Rank	Storm	Start	End	Peak	Dur	Hs	Ts	Dir	Energy	F->S	P->P
29	1	10APR91:11	10APR91:16	10APR91:14	6	2.10	6.00	309	148		
20	2	15APR91:16	15APR91:19	15APR91:17	4	2.40	6.00	291	133	127	122
22	3	26SEP91:07	26SEP91:16	26SEP91:09	10	2.20	6.00	316	275	3935	3927
31	4	05OCT91:19	05OCT91:20	05OCT91:19	2	2.00	6.00	284	48	228	225
13	5	18OCT91:20	19OCT91:02	19OCT91:01	7	2.30	7.00	354	195	318	317
7	6	30OCT91:20	31OCT91:08	31OCT91:01	13	2.50	7.00	347	503	299	287
10	7	01NOV91:21	03NOV91:22	02NOV91:08	50	3.20	7.00	252	1978	97	54
63	8	06NOV91:04	07NOV91:10	06NOV91:04	31	2.10	6.00	222	512	132	91
18	9	15NOV91:06	15NOV91:07	15NOV91:06	2	2.00	6.00	215	48	218	217
49	10	23NOV91:23	25NOV91:09	24NOV91:02	35	3.10	7.00	222	1349	242	211
40	11	27NOV91:15	27NOV91:22	27NOV91:17	8	2.60	6.00	260	268	94	86
17	12	30NOV91:11	30NOV91:19	30NOV91:14	9	2.70	7.00	254	326	75	68
43	13	04DEC91:04	04DEC91:22	04DEC91:11	19	3.30	8.00	302	1024	106	92
51	14	06DEC91:03	07DEC91:10	06DEC91:06	32	2.30	7.00	307	382	77	42
27	15	10DEC91:19	10DEC91:24	10DEC91:21	6	2.10	6.00	227	151	116	110
12	16	12DEC91:23	13DEC91:01	12DEC91:23	3	2.10	5.00	217	74	53	49
38	17	14DEC91:14	16DEC91:02	14DEC91:16	37	2.90	7.00	288	1124	74	40
11	18	17DEC91:16	18DEC91:21	18DEC91:16	30	3.00	8.00	341	1204	102	95
61	19	23DEC91:21	23DEC91:24	23DEC91:22	4	2.20	6.00	341	115	151	125
6	20	14JAN92:02	19JAN92:20	14JAN92:13	139	3.90	8.00	339	5342	646	518
45	21	21JAN92:03	21JAN92:05	21JAN92:04	3	2.10	6.00	254	74	170	158
42	22	23JAN92:20	24JAN92:20	24JAN92:11	25	3.50	8.00	322	1237	88	78
25	23	31JAN92:20	01FEB92:05	01FEB92:03	10	2.40	7.00	346	340	200	183
62	24	07FEB92:20	08FEB92:23	08FEB92:07	28	2.30	7.00	328	833	194	171
60	25	16FEB92:03	16FEB92:09	16FEB92:07	7	2.50	7.00	330	238	204	191
23	26	20FEB92:21	20FEB92:24	20FEB92:22	4	2.40	6.00	216	119	116	110
26	27	28FEB92:10	29FEB92:03	29FEB92:01	18	2.70	7.00	354	554	197	194
46	28	01MAR92:09	01MAR92:17	01MAR92:13	9	2.30	6.00	235	248	54	35
55	29	10MAR92:05	11MAR92:12	10MAR92:14	32	4.00	9.00	352	2968	242	216
2	30	22MAR92:13	22MAR92:19	22MAR92:17	7	2.10	6.00	360	153	301	290
28	31	27MAR92:07	27MAR92:23	27MAR92:14	17	3.40	8.00	328	1110	129	116
50	32	01APR92:14	01APR92:16	01APR92:15	3	2.10	6.00	334	81	128	120
24	33	12APR92:17	12APR92:20	12APR92:18	4	2.10	7.00	353	109	269	266
47	34	27APR92:06	27APR92:08	27APR92:07	3	2.10	6.00	352	78	350	348
5	35	01MAY92:22	01MAY92:22	01MAY92:22	1	2.00	6.00	228	24	111	110
39	36	05MAY92:18	05MAY92:20	05MAY92:19	3	2.10	6.00	357	74	93	92
37	37	13MAY92:19	13MAY92:22	13MAY92:21	4	2.30	7.00	358	123	195	193
14	38	23MAY92:20	24MAY92:20	24MAY92:06	25	2.70	7.00	356	794	264	248
57	39	16OCT92:19	17OCT92:03	16OCT92:21	9	2.30	7.00	310	281	3510	3494
54	40	12NOV92:23	13NOV92:10	13NOV92:04	12	2.90	7.00	309	537	662	654
53	41	02DEC92:20	03DEC92:05	02DEC92:22	10	2.20	6.00	314	228	485	473
3	42	04DEC92:24	05DEC92:17	05DEC92:05	18	2.50	7.00	316	618	68	54
41	43	23DEC92:22	25DEC92:23	24DEC92:02	50	2.80	7.00	332	1280	502	452
19	44	31DEC92:16	01JAN93:16	31DEC92:18	25	2.10	6.00	308	337	209	183
30	45	24JAN93:13	24JAN93:22	24JAN93:16	10	2.50	7.00	322	374	581	573
15	46	28JAN93:23	29JAN93:14	29JAN93:03	16	2.40	7.00	327	529	120	106
59	47	30JAN93:21	01FEB93:04	31JAN93:05	32	2.30	6.00	264	744	76	49
58	48	16FEB93:22	16FEB93:22	16FEB93:22	1	2.00	6.00	343	24	408	400
44	49	13MAR93:20	14MAR93:05	14MAR93:02	10	3.00	8.00	348	530	606	603
21	50	16MAR93:09	17MAR93:17	17MAR93:14	33	2.30	7.00	345	586	92	83
36	51	01APR93:18	02APR93:06	01APR93:22	13	2.70	7.00	357	547	404	367
1	52	21APR93:02	21APR93:02	21APR93:02	1	2.00	6.00	357	24	463	459
34	53	24APR93:21	24APR93:24	24APR93:22	4	2.20	6.00	224	102	93	91
8	54	13MAY93:02	13MAY93:05	13MAY93:04	4	2.20	6.00	353	110	439	437
33	55	09OCT93:14	09OCT93:22	09OCT93:18	9	2.40	7.00	355	285	3595	3589
32	56	31OCT93:24	01NOV93:01	31OCT93:24	2	2.00	6.00	335	52	538	533
16	57	05NOV93:23	06NOV93:05	06NOV93:03	7	2.20	6.00	327	194	124	122
56	58	19NOV93:21	20NOV93:02	19NOV93:22	6	2.10	6.00	292	156	338	330
52	59	21NOV93:20	21NOV93:23	21NOV93:21	4	2.10	6.00	228	100	49	46
48	60	06DEC93:21	07DEC93:14	06DEC93:24	8	2.40	7.00	312	252	367	362
9	61	10DEC93:21	11DEC93:11	11DEC93:01	15	2.50	7.00	339	575	109	96
--	--	--	--	--	--	--	--	--	215	368	361

Selected Storms for Numerical Model Input

Wave Characteristics							
Storm Date	Type	Peak Hs (m)	Peak T (m)	Wave Energy (m ² s)*	Storm Dur. (hrs)	Offshore Wave Dirx.	W. L. Range (m > LWD)
2 Nov. '91	SW	3.2	7	1978	60	250 - 327	0.0 - 0.3
14 Jan. '92	NW	3.9	8	5340	139	150 - 270	0.4 - 0.8
24 Jan. '92	W	3.5	8	1237	26	318 - 360	0.3 - 0.6

Note: Wave Energy (m² s) is $H^2 \cdot T$ (Wave Height Squared * Wave Period)
Provides indication of relative wave energy

REPORT DOCUMENTATION PAGEForm Approved
OMB No. 0704-0188

Public reporting burden for this collection of information is estimated to average 1 hour per response, including the time for reviewing instructions, searching existing data sources, gathering and maintaining the data needed, and completing and reviewing the collection of information. Send comments regarding this burden estimate or any other aspect of this collection of information, including suggestions for reducing this burden, to Washington Headquarters Services, Directorate for Information Operations and Reports, 1215 Jefferson Davis Highway, Suite 1204, Arlington, VA 22202-4302, and to the Office of Management and Budget, Paperwork Reduction Project (0704-0188), Washington, DC 20503.

1. AGENCY USE ONLY (Leave blank)		2. REPORT DATE June 1996	3. REPORT TYPE AND DATES COVERED Final report	
4. TITLE AND SUBTITLE Geologic Effects on Behavior of Beach Fill and Shoreline Stability for Southeast Lake Michigan			5. FUNDING NUMBERS	
6. AUTHOR(S) Larry E. Parson, Robert B. Nairn, Andrew Morang				
7. PERFORMING ORGANIZATION NAME(S) AND ADDRESS(ES) U.S. Army Engineer Waterways Experiment Station, 3909 Halls Ferry Road, Vicksburg, MS 39180-6199 Baird & Associates, 221 Lakeshore Road East, Oakville, Ontario, Canada L6J 1H7			8. PERFORMING ORGANIZATION REPORT NUMBER Technical Report CERC-96-10	
9. SPONSORING/MONITORING AGENCY NAME(S) AND ADDRESS(ES) U.S. Army Corps of Engineers Washington, DC 20314-1000			10. SPONSORING/MONITORING AGENCY REPORT NUMBER	
11. SUPPLEMENTARY NOTES Available from National Technical Information Service, 5285 Port Royal Road, Springfield, VA 22161.				
12a. DISTRIBUTION/AVAILABILITY STATEMENT Approved for public release; distribution is unlimited.			12b. DISTRIBUTION CODE	
13. ABSTRACT (Maximum 200 words) A monitoring program to evaluate the effects of beach nourishment material placed on a cohesive shoreline in southeast Lake Michigan was conducted at St. Joseph, MI, by the U.S. Army Engineer Waterways Experiment Station. In conjunction with this monitoring program, this particular study focuses on a 6-km (3.7-mile) section of shoreline extending southward from the jetties of St. Joseph Harbor. Some of the geological variables that affect cohesive shores were investigated. The primary objective of the study was to develop an improved understanding of the relationship between the movement of the cohesionless sediment (both fine and coarse grain components) and the irreversible downcutting of the underlying glacial till at the St. Joseph project site. Data collected during the monitoring program were input into a 2-D numerical model to describe the cross-shore sediment process and to predict the profile response to storm conditions with the influence of the underlying glacial till represented as an erosion-resistant sublayer. The 2-D profile change tests were performed at 10 of the profile locations.				
14. SUBJECT TERMS Beach nourishment Glacial tilla St. Joseph Harbor, Michigan			15. NUMBER OF PAGES 104	
			16. PRICE CODE	
17. SECURITY CLASSIFICATION OF REPORT UNCLASSIFIED	18. SECURITY CLASSIFICATION OF THIS PAGE UNCLASSIFIED	19. SECURITY CLASSIFICATION OF ABSTRACT	20. LIMITATION OF ABSTRACT	